

INTERACTION NOTES

Note 191

15 September 1970

COMPUTER PROGRAMS FOR RADIATION AND SCATTERING BY  
ARBITRARY CONFIGURATIONS OF BENT WIRES

by

Hu H. Chao

Bradley J. Strait

Electrical Engineering Department  
Syracuse University  
Syracuse, New York

ABSTRACT

The problem of electromagnetic radiation and scattering from thin wires with arbitrary shape and with arbitrary excitation and loading is considered. This is treated as a boundary value problem which is formulated as an operator equation. Matrix methods along with the method of moments are used to solve the operator equation approximately. Computer programs suitable for handling radiation problems and plane-wave scattering problems are presented and described. For the former, current distributions, field patterns, and input impedances at the driving points are determined. For the latter, current distributions and bistatic radar cross section patterns are found. Examples are given to illustrate several applications of the programs. Numerical results are compared with experimental data and with results computed by other theoretical methods.

ACKNOWLEDGEMENTS

The authors wish to acknowledge the helpful suggestions of Dr. Roger F. Harrington, Dr. Joseph R. Mautz, and Mr. Kazuhiko Hirasawa of the Electrical Engineering Dept., Syracuse University.



## CONTENTS

	Page
ACKNOWLEDGEMENTS-----	1
CONTENTS-----	2
CHAPTER 1. INTRODUCTION-----	3
CHAPTER 2. THEORY-----	5
2-1. Introduction-----	5
2-2. Formulation of the Problem-----	5
2-3. Wire Configurations and Coordinate System-----	7
2-4. Derivation of the Matrix Equation-----	9
2-5. Evaluation of the Generalized Impedance Matrix-----	15
2-6. The Generalized Voltage Matrix-----	20
2-7. Radiation and Scattered Fields-----	21
2-8. Loaded Antennas and Scatterers-----	22
2-9. Boundary Condition at the Junction of Wires-----	24
2-10. Conclusion-----	27
CHAPTER 3. DESCRIPTION OF COMPUTER PROGRAMS-----	28
3-1. Introduction-----	28
3-2. Radiation Problem-----	28
3-3. Further Details-----	31
3-4. Scattering Problem-----	32
3-5. Conclusion-----	33
CHAPTER 4. EXAMPLES-----	34
4-1. Introduction-----	34
4-2. Radiation Problems-----	34
4-3. Scattering Problems-----	53
4-4. Conclusion-----	65
CHAPTER 5. CONCLUSION-----	66
REFERENCES-----	67
APPENDIX A-----	69
APPENDIX B-----	83
APPENDIX C-----	92
APPENDIX D-----	94

## Chapter 1

### INTRODUCTION

Computer programs are presented and described for analysis of arbitrarily bent wire antennas and scatterers. The problem configuration can involve more than one wire and it is not necessary that the wires all have the same shape. For example, a problem consisting of a wire loop antenna radiating in the presence of a linear wire radiator or scatterer could be handled with relative ease. The programs are very general and although they are limited here to problems involving a total of four different wires or less to conserve storage space there is no theoretical limitation on the number of wires that can be taken into account. The wires can be loaded continuously or discretely at arbitrary points and also, they can be excited or fed at any arbitrary point or points along their lengths. Finally, it is possible to include wire junctions in the problem geometry enabling treatment of special configurations such as wire crosses, supporting wires for long antennas, and so on.

For radiation problems the current distributions on the wires are computed along with appropriate field patterns and input impedances corresponding to the driving points. For scattering problems the current distributions are again calculated along with the magnitude and phase of the scattered field for each specified plane and appropriate bistatic radar cross-section patterns. The programs are presented in the Appendices of this report with the first (Appendix A) suitable for radiation problems and the second (Appendix B) applicable for scattering problems.

This report is a sequel to two earlier reports which presented computer programs for analysis and design of arrays of straight-wire antennas and scatterers [4,13]. The method of analysis used is due to Harrington [1,2] and is an application of the general "method of moments." The method was first applied to thin wire problems by Harrington and Mautz [3] and later by Strait and Hirasawa [4,13] in presenting the earlier programs mentioned above. Other important applications of the method include Cummins [7] treatment of circular arrays, studies of linear and planar arrays by Strait and

Hirasawa [5,6] and Kyle's [14] treatment of arrays of log-periodic antennas.

In this report all wires are assumed to be thin perfect conductors with wire losses treated as a special case of wire loading. Within the "method of moments" procedure a linear current approximation is used together with the "method of subsections." Hence, triangle current expansion functions are used where each function is non-zero only over a relatively small portion of a wire. Triangle functions are also used for testing functions (Galerkin's procedure). These choices were made because of the observation of Harrington and Mautz [3] that this solution converges about twice as fast as the solution resulting from use of pulses for current expansion functions and point matching (impulse testing functions) as used by Strait and Hirasawa [4-6,13] and also by Kyle [14].

This application of the method of moments is presented in Chapter 2. As mentioned earlier the computer programs are presented in the Appendices with the corresponding descriptions included in Chapter 3. Several applications and typical results from the programs are discussed in Chapter 4. Of particular interest is a novel wire cross scatterer which provides an interesting example of a wire junction problem. The computer programs are written in FORTRAN IV for use with an IBM 360/50 digital computer. Results presented in Chapter 4 are compared with those of other investigators wherever possible.

## Chapter 2

### THEORY

#### 2-1. Introduction

In this chapter the integro-differential equation for the current distribution of an array of thin wires is derived. Here, the term "thin wire" implies a wire of length  $L$  and radius  $a$ , where  $L/a \gg 1$  and  $a \ll \lambda$ , the wavelength. All wires are assumed to be perfect conductors, with wire losses treated as a special case of wire loading. Using the method of moments [1,2], this integro-differential equation is reduced to a matrix equation. The approximate current distributions on the wires are obtained by solving this matrix equation using standard techniques. Then, once the current distribution is known, other parameters of engineering interest can be easily derived.

In the first sections of this chapter, it is assumed that all wires are open wires, i.e., no loops and/or junctions. Also, it is assumed initially there is no loading on the wires. Effects of loading are discussed in Sec. 2-8. Then, in Sec. 2-9, the general method of solution is modified to handle loops and/or junctions.

#### 2-2. Formulation of the Problem

The problem of finding the current distributions on the wire antenna or scatterer elements is but a particular case of the general boundary value problem involving conducting bodies in a known impressed field,  $\vec{E}^i$ . The boundary condition at the surface of each perfect conductor is

$$\vec{n} \times \vec{E}^t = 0$$

where  $\vec{n}$  is a unit vector normal to the surface of the conductor and in the outward direction, and  $\vec{E}^t$  is the total electric field vector consisting of both incident and scattered fields. The scattered field  $\vec{E}^s$  is defined as the field produced by all currents and charges on the conductors. The equations that summarize this boundary value problem are

$$\bar{E}^S = -j\omega\bar{A} - \bar{\nabla}\phi \quad (2-1)$$

$$\bar{A} = \frac{\mu}{4\pi} \oint_S \bar{J} \frac{e^{-jkR}}{R} ds \quad (2-2)$$

$$\phi = \frac{1}{4\pi\epsilon} \oint_S \sigma \frac{e^{-jkR}}{R} ds \quad (2-3)$$

$$\sigma = -\frac{1}{j\omega} \bar{\nabla} \cdot \bar{J} \quad (2-4)$$

Finally, since  $\bar{E}^t = \bar{E}^i + \bar{E}^S$  the condition  $\bar{n} \times \bar{E}^t = 0$  results in

$$\bar{n} \times \bar{E}^S = -\bar{n} \times \bar{E}^i \quad (2-5)$$

on the surface of each conductor. Here,  $\bar{A}, \phi, \omega, \mu, \epsilon$  have the usual meanings [2],  $R$  is the distance from the source point to the point where the field is evaluated, and  $S$  is used to denote the surfaces of conductors.

For thin wires, the following approximations can be made:

1. The currents are assumed to flow only in the axial direction.
2. The current and charge densities are approximated by filaments of current  $I$  and charge  $\sigma$  on the wire axes.
3. The boundary condition (2-5) is applied to the axial component of  $\bar{E}$  on each wire surface.

Using these approximations, (2-1) through (2-5) reduce to

$$-\bar{E}_\ell^i = -j\omega\bar{A} - \frac{\partial\phi}{\partial\ell}\bar{u}_\ell \text{ on } S \quad (2-6)$$

$$\bar{A} = \frac{\mu}{4\pi} \int_{\text{axis}} \bar{I}(\ell) \frac{e^{-jkR}}{R} d\ell \quad (2-7)$$

$$\phi = \frac{1}{4\pi\epsilon} \int_{\text{axis}} \sigma(\ell) \frac{e^{-jkR}}{R} d\ell \quad (2-8)$$

$$\sigma = -\frac{1}{j\omega} \frac{dI(\ell)}{d\ell} \quad (2-9)$$

where  $l$  is the length variable along the wire axis. If a wire terminates, the additional boundary condition  $\bar{I} = 0$  at the ends of each wire must also be satisfied.

It is convenient to define an integro-differential operator  $L$  as

$$L(\bar{I}) = [j\omega\bar{A} + \bar{\nabla}\phi]_{\text{tan}} \quad (2-10)$$

where the subscript "tan" refers to the tangential component. Then,

$$L(\bar{I}) = \bar{E}_{\text{tan}}^i \quad \text{on } S \quad (2-11)$$

$$\bar{I} = 0 \quad \text{at the ends of the wires} \quad (2-12)$$

It is evident that  $L$  is a linear operator. The domain of the operator  $L$  is the space of those functions  $\bar{I}$  which satisfy the boundary condition (2-12) and have first order derivatives. The range of the operator  $L$  is the space of all possible functions  $\bar{E}_{\text{tan}}^i$  on the surfaces of the wires.

Using the method of moments<sup>\*</sup>, this functional equation can be reduced to a matrix equation of finite order, which can be solved using standard techniques.

### 2-3. Wire Configurations and Coordinate System

Figure 2-1 shows a typical configuration and coordinate system for the wires. The origin of the coordinate system should be placed as near the wires as possible. Point  $P_{i,j}$  is a typical point on the axis of a wire which is used to define the wire geometry and where the subscript  $i$  denotes the number of the wire and subscript  $j$  denotes the number of the defining point of the wire. As in Fig. 2-2, each wire of a given problem configuration is approximated by a piecewise linear wire. Each short straight wire piece from point  $P_{i,j}$  to point  $P_{i,j+1}$  is called a segment  $\Delta\bar{l}_{i,j}$  and the length of the segment  $\Delta l_{i,j}$  is simply the distance between

---

\*References [1] and [2] contain detailed descriptions of the general "method of moments" procedure.

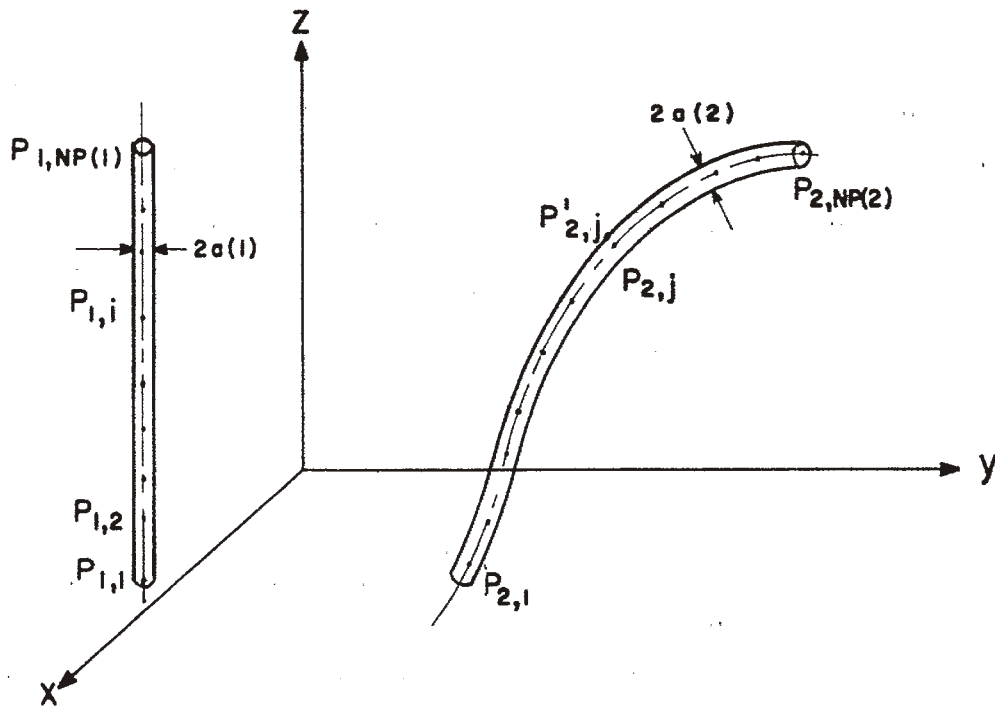


Fig. 2-1. Typical configuration and coordinate system.

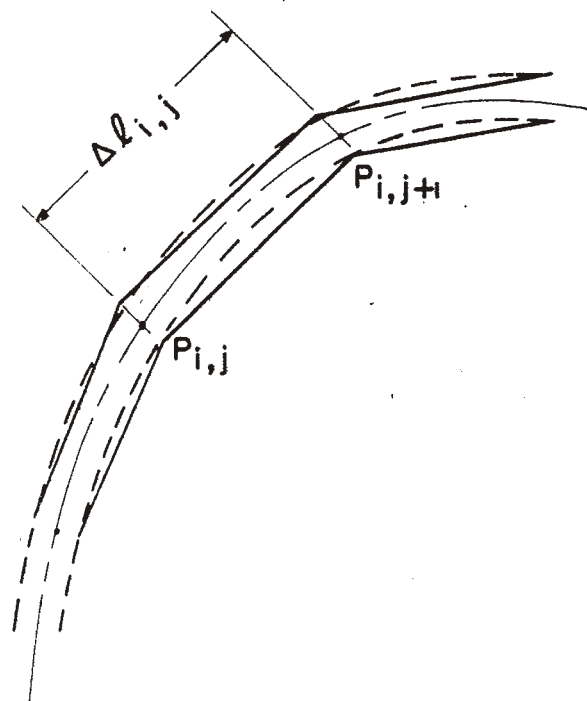


Fig. 2-2. Approximation to the wire.



these two defining points. For the programs described in this report the number of segments for each wire must be even. Also, as pointed out previously, the wire configurations to be considered are restricted to thin wires.

#### 2-4. Derivation of the Matrix Equation

In order to apply the method of moments, it is convenient to define the inner product for this problem as

$$\langle \bar{W}, \bar{F} \rangle = \oint_S \bar{W} \cdot \bar{F} \, ds \quad (2-13)$$

The next step is to choose a set of expansion or basis functions  $\bar{F}_n$  and a set of weighting or testing functions  $\bar{W}_n$ . The expansion functions should be in the domain of the operator  $L$  since it is this set that will form an approximation to the current. These functions should be linearly independent and should be chosen so that a reasonably good approximation to  $\bar{I}$  can be obtained by a finite series expansion of the form

$$\bar{I} = \sum_i \sum_n I_{i,n} \bar{F}_{i,n} \quad (2-14)$$

where  $I_{i,n}$  are the complex coefficients to be determined. The weighting functions should be in the range of the operator  $L$ . These functions should be linearly independent and should be chosen so that the product  $\langle \bar{W}_{j,m}, \bar{E}^i \rangle$  depends on relatively independent properties of  $\bar{E}^i$ .

Substituting (2-14) into (2-11) (noting the linearity of the operator  $L$ ), (2-11) reduces to

$$\sum_i \sum_n I_{i,n} L \bar{F}_{i,n} = \bar{E}_{\text{tan}}^i \quad (2-15)$$

Taking the inner product of (2-15) with each testing function  $\bar{W}_{j,m}$  results in

$$\sum_i \sum_n I_{i,n} \langle \bar{W}_{j,m}, L \bar{F}_{i,n} \rangle = \langle \bar{W}_{j,m}, \bar{E}_{\text{tan}}^i \rangle \quad (2-16)$$

$j=1, \dots, NW, m=1, \dots, NE(j)$ , where  $NW$  is the number of wires, and  $NE(j)$  is the number of expansion functions on the  $j$ th wire. Now, define the generalized network matrices as

$$[Z_{j,m,i,n}] = \begin{bmatrix} \langle \bar{W}_{1,1}, L\bar{F}_{1,1} \rangle & \dots & \langle \bar{W}_{1,1}, L\bar{F}_{1,NE(1)} \rangle & \langle \bar{W}_{1,1}, L\bar{F}_{2,1} \rangle & \dots & \langle \bar{W}_{1,1}, L\bar{F}_{NW,NE(NW)} \rangle \\ \langle \bar{W}_{1,2}, L\bar{F}_{1,1} \rangle & \dots & \langle \bar{W}_{1,2}, L\bar{F}_{1,NE(1)} \rangle & \langle \bar{W}_{1,2}, L\bar{F}_{2,1} \rangle & \dots & \langle \bar{W}_{1,2}, L\bar{F}_{NW,NE(NW)} \rangle \\ \vdots & & & & & \\ \langle \bar{W}_{1,NE(1)}, L\bar{F}_{1,1} \rangle & \dots & & & & \\ \langle \bar{W}_{2,1}, L\bar{F}_{1,1} \rangle & \dots & & & & \\ \vdots & & & & & \\ \langle \bar{W}_{NW,NE(NW)}, L\bar{F}_{1,1} \rangle & \dots & & & & \end{bmatrix} \quad (2-17)$$

$$[V_{j,m}] = \begin{bmatrix} \bar{W}_{1,1}, \bar{E}_{\tan}^i \\ \bar{W}_{1,2}, \bar{E}_{\tan}^i \\ \vdots \\ \bar{W}_{1,NE(1)}, \bar{E}_{\tan}^i \\ \bar{W}_{2,1}, \bar{E}_{\tan}^i \\ \vdots \\ \bar{W}_{NW,NE(NW)}, \bar{E}_{\tan}^i \end{bmatrix} \quad (2-18)$$

$$[I_{j,m}] = \begin{bmatrix} I_{1,1} \\ I_{1,2} \\ \vdots \\ I_{1,NE(1)} \\ I_{2,1} \\ \vdots \\ I_{NW,NE(NW)} \end{bmatrix} \quad (2-19)$$

Equation (2-16) can be written as a matrix equation

$$[Z][I] = [V] \quad (2-20)$$

where  $[Z]$  is the generalized impedance matrix of dimension equal to  $M \times M$  ( $M$  is the number of expansion functions),  $[V]$  is the generalized voltage matrix of dimension  $M \times 1$ , and  $[I]$  is the generalized current matrix, also of dimension  $M \times 1$ .

The desired solution for  $[I]$  is obtained by inverting the matrix  $[Z]$

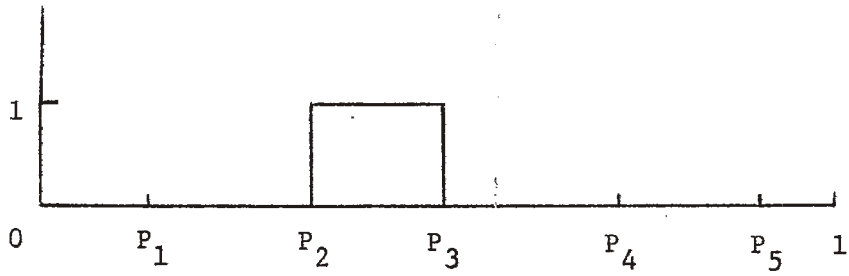
$$[I] = [Z]^{-1}[V] = [Y][V] \quad (2-21)$$

where  $[Y] = [Z]^{-1}$  is called the generalized admittance matrix. The admittance matrix  $[Y]$  and the impedance matrix  $[Z]$  are basically functions only of the geometry of the problem, completely independent of any excitations.

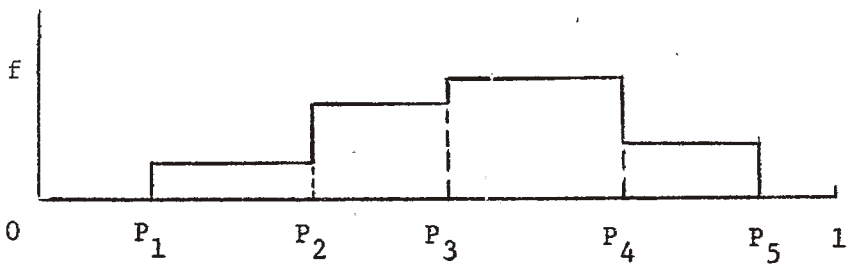
So far, the impressed field is considered arbitrary and hence, both radiation and scattering problems can be included.

There are many possibilities for both expansion functions and testing functions. Two typical types of current expansion functions are triangle functions and pulse functions. A piecewise linear approximation is obtained by using triangle functions where each function is non-zero only over a portion of one wire (usually two or four segments). A step approximation is obtained by using pulse functions where each function is again non-zero only over a portion of one wire (usually one segment). (These two types of expansion functions refer to the method of subsections discussed by Harrington [1,2].) When impulse testing functions (usually located at the center of a segment) are used, this is referred to as the "point matching method" [1,2]. For "Galerkin's Method" [8] testing functions and expansion functions are the same set of functions.

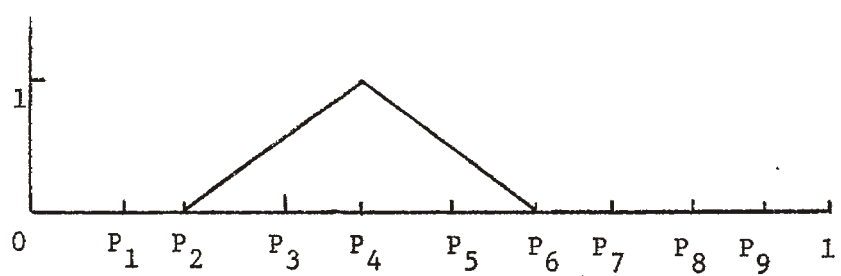
In choosing various sets of possible expansion and testing functions, it is necessary to consider the ease of evaluating the matrix elements and the realization of a well-conditioned matrix  $[Z]$ . It is known that for the



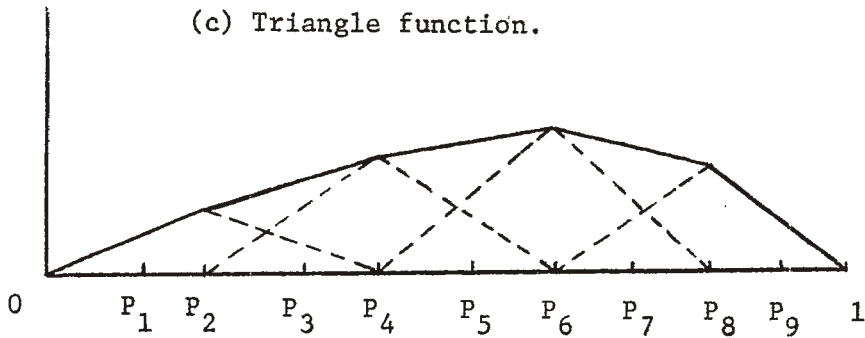
(a) Pulse function.



(b) Step approximation.



(c) Triangle function.



(d) Piecewise linear approximation.

Fig. 2-3. Subsectional bases and functional approximation.

point matching method or Galerkin's method, subsectional expansions, using pulse or triangle functions, give well-conditioned matrices [1].

Harrington and Mautz [3] have solved the single straight-wire problem using three different procedures. These include point-matching with pulses as basis functions, point-matching with triangle expansion functions, and Galerkin's procedure with triangle expansion functions. They found with segments less than  $\lambda/10$  in length, no significant difference in results is observed between the last two methods and also that the last two methods converge about twice as fast as the first.

It appears the second method mentioned above should involve less computation than the last. However, this is not true in the problem treated here. It turns out that the second method requires calculation

of the Green's function  $\int_{\Delta \ell} \frac{e^{-jkR}}{R} d\ell$  more times than the last. Hence, the

programs and descriptions of this report use Galerkin's method with triangle (piecewise linear) current expansion functions.

The triangle expansion function is simply a triangle function of unit height with peak at the point  $P_{i,2n+1}$  as shown in Fig. 2-4. The direction of  $\bar{T}_{i,n}$  is coincident with the axis of the piecewise linear (approximate) wire and in the direction as shown in Fig. 2-4. Each triangle function  $\bar{T}_{i,n}$  is non-zero only over four consecutive segments. Successive triangles overlap every two segments except at the ends of open wires. The overlapping is illustrated in Fig. 2-3d. Boundary condition (2-12) is automatically satisfied, since the current is indeed zero at each open end. Note that the triangle function extends over four segments rather than just two. This is to improve curve-fitting by the piecewise linear wire.

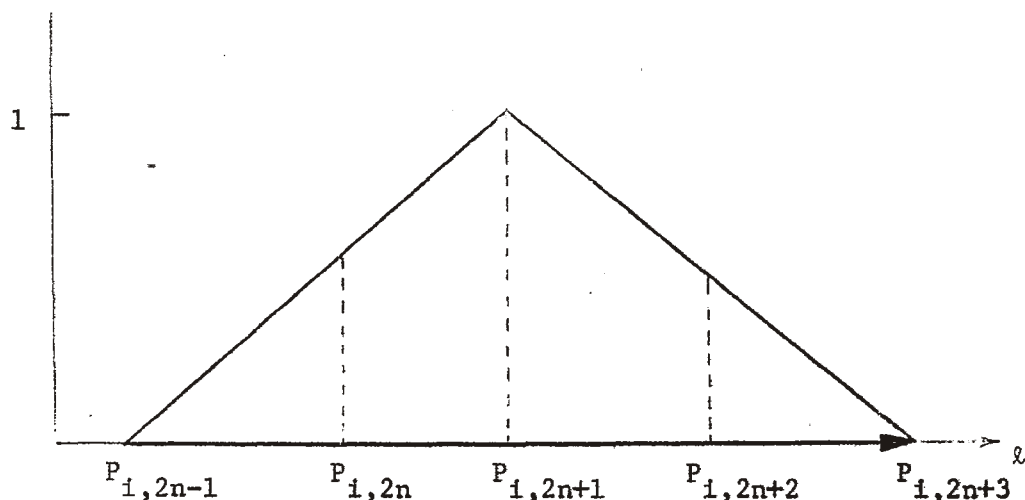


Fig. 2-4. Triangle function  $\bar{T}_{i,n}$ .

The only difficulty with using triangle functions as expansion functions is that the first order derivatives  $\frac{d T_{i,n}}{d l}$  do not exist at the isolated points  $P_{i,2n-1}$ ,  $P_{i,2n}$ ,  $P_{i,2n+1}$ ,  $P_{i,2n+2}$ ,  $P_{i,2n+3}$ . Hence, the triangle function is not actually in the domain of the operator  $L$ . This difficulty can be avoided by using an extended operator [1,2]. By defining

$$\frac{d f}{d l} (l) = \frac{\frac{d f}{d l} (l+) + \frac{d f}{d l} (l-)}{2} \quad (2-22)$$

the original domain can be extended to the space of those functions which are continuous. The triangle function is a continuous function, and hence there is no difficulty in using triangle functions as expansion functions for the problems discussed here.

When the impressed field is well behaved, as in the case of plane-wave excitation, the solution is apparently quite accurate using as few as 10 expansion functions per wavelength. When the impressed field is singular, as in the case of a lumped voltage source, convergence of the current near the source is slower and more difficult to interpret. However, Harrington and

Mautz [3] point out that the current at a voltage source changed at most by four percent as the number of expansion functions per wavelength changed from 32 to 64, and usually much less than this amount.

Hence, triangle functions are chosen as expansion functions so that

$$\bar{F}_{i,n} = \bar{T}_{i,n}$$

where  $\bar{T}_{i,n}$  is as in Fig. 2-4. Also, the testing functions  $\bar{W}_{i,n}$  are

$$\bar{W}_{i,n} = \bar{T}'_{i,n}$$

where  $\bar{T}'_{i,n}$  is exactly the same as  $\bar{T}_{i,n}$  except these are located on the surfaces of the wires instead of the axes of the wires.

### 2-5. Evaluation of the Generalized Impedance Matrix

The elements of the generalized impedance matrix (2-17) are explicitly expressed as

$$Z_{j,m,i,n} = \oint_S \bar{W}_{j,m} \cdot (j\omega\bar{A}_{i,n} + \bar{\nabla}\phi_{i,n}) \tan ds \quad (2-23)$$

where  $\bar{A}_{i,n}$  and  $\phi_{i,n}$  are calculated using (2-7) through (2-9) where  $\bar{I} = \bar{F}_{i,n}$ .  $\bar{A}_{i,n}$  and  $\phi_{i,n}$  are simply the vector and scalar potentials due to the current  $\bar{I} = \bar{F}_{i,n}$  and charge  $\sigma = -\frac{1}{j\omega} \frac{d\bar{I}}{d\ell}$  on the wires. Since  $\bar{W}_{j,m}$  has a non-zero value only on a line C, (2-23) reduces to

$$Z_{j,m,i,n} = \int_C \bar{W}_{j,m} \cdot (j\omega\bar{A}_{i,n} + \bar{\nabla}\phi_{i,n}) \tan d\ell' \quad (2-24)$$

where C is a line on the surface of the wire parallel to the axis of the wire. Equation (2-24) can be reduced to

$$Z_{j,m,i,n} = \int_C W_{j,m} (j\omega\bar{A}_{i,n} + \bar{\nabla}\phi_{i,n}) \cdot d\bar{\ell}' \quad (2-25)$$

since the direction of  $\bar{W}_{j,m}$  is coincident with the direction of the line C. From

$$\frac{d}{d\ell'} (W_{j,m} \phi_{i,n}) = W_{j,m} \frac{d\phi_{i,n}}{d\ell'} + \phi_{i,n} \frac{dW_{j,m}}{d\ell'}$$

it follows that

$$\int_C d(W_{j,m} \phi_{i,n}) = \int_C W_{j,m} d\phi_{i,n} + \int_C \phi_{i,n} dW_{j,m} \quad (2-26)$$

The left hand side of (2-26) is zero, since  $W_{j,m}$  is zero at the ends of open wires. Hence (2-24) can be reduced to

$$Z_{j,m,i,n} = j\omega \int_C W_{j,m} \bar{A}_{i,n} \cdot d\bar{\ell}' - \int_C \phi_{i,n} dW_{j,m} \quad (2-27)$$

Equation (2-27) is more convenient for computation than Eq. (2-24) because the gradient operator on  $\phi$  has been eliminated.

Substituting (2-7) through (2-9) into (2-27) results in

$$Z_{j,m,i,n} = \int_{\text{axis}} d\ell \int_C d\ell' [j\omega \mu \bar{W}_{j,m} \cdot \bar{F}_{i,n} + \frac{1}{j\omega \epsilon} \frac{dW_{j,m}}{d\ell'} \frac{dF_{i,n}}{d\ell}] \frac{e^{-jkR}}{4\pi R} \quad (2-28)$$

where  $R$  is the distance from the source point to the field point.

In evaluating the integral of (2-28),  $F_{i,n}$  is conveniently approximated by four pulses as shown in Fig. 2-5,  $\frac{dF_{i,n}}{d\ell}$  is also represented by four pulses as shown in Fig. 2-5, and  $W_{j,m}$  and  $\frac{dW_{j,m}}{d\ell'}$  are approximated by four impulses as shown in Fig. 2-6. The pulse amplitudes are

$$C_{i,n}(1) = \frac{\frac{1}{2} \Delta\ell_{i,2n-1}}{\Delta\ell_{i,2n-1} + \Delta\ell_{i,2n}} \quad (2-29)$$

$$C_{i,n}(2) = \frac{\Delta\ell_{i,2n-1} + \frac{1}{2}\Delta\ell_{i,2n}}{\Delta\ell_{i,2n-1} + \Delta\ell_{i,2n}} \quad (2-30)$$

$$C_{i,n}(3) = \frac{\frac{1}{2} \Delta\ell_{i,2n+1} + \Delta\ell_{i,2n+2}}{\Delta\ell_{i,2n+1} + \Delta\ell_{i,2n+2}} \quad (2-31)$$



$$C_{i,n}^{(4)} = \frac{\frac{1}{2} \Delta \ell_{i,2n+2}}{\Delta \ell_{i,2n+1} + \Delta \ell_{i,2n+2}} \quad (2-32)$$

$$D_{i,n}^{(1)} = D_{i,n}^{(2)} = \frac{1}{\Delta \ell_{i,2n-1} + \Delta \ell_{i,2n}} \quad (2-33)$$

$$D_{i,n}^{(3)} = D_{i,n}^{(4)} = \frac{-1}{\Delta \ell_{i,2n+1} + \Delta \ell_{i,2n+2}} \quad (2-34)$$

The impulse amplitudes are  $\Delta \ell_{j,2m-1} C_{j,m}^{(1)}$ ,  $\Delta \ell_{j,2m} C_{j,m}^{(2)}$ ,  $\Delta \ell_{j,2m+1} C_{j,m}^{(3)}$ ,  $\Delta \ell_{j,2m+2} C_{j,m}^{(4)}$ ,  $\Delta \ell_{j,2m-1} D_{j,m}^{(1)}$ ,  $\Delta \ell_{j,2m} D_{j,m}^{(2)}$ ,  $\Delta \ell_{j,2m+1} D_{j,m}^{(3)}$ , and  $\Delta \ell_{j,2m+2} D_{j,m}^{(4)}$ . Also, it is convenient to define

$$\psi(Q_{j,m}, Q_{i,n}) = \frac{1}{4\pi\Delta \ell_{i,n}} \int_{P_{i,n}}^{P_{i,n+1}} \frac{e^{-jkR}}{R} dl \quad (2-35)$$

where the point  $Q_{i,n}$  is at the center of the  $n$ th segment of the  $i$ th wire and  $R$  is the distance from the point  $Q_{j,m}$  to  $dl$ . Equation (2-28) can be written as

$$Z_{j,m,i,n} = j\omega\mu Z_1 + \frac{1}{j\omega\epsilon} Z_2 \quad (2-36)$$

where

$$Z_1 = \sum_{A=1}^4 \sum_{B=1}^4 C_{j,m}^{(A)} C_{i,n}^{(B)} \Delta \bar{\ell}_{j,2m-2+A} \cdot \Delta \bar{\ell}_{i,2n-2+B} \psi(Q_{j,2m-2+A}, Q_{i,2n-2+B}) \quad (2-37)$$

$$Z_2 = \sum_{A=1}^4 \sum_{B=1}^4 D_{j,m}^{(A)} D_{i,n}^{(B)} \Delta \ell_{j,2m-2+A} \Delta \ell_{i,2n-2+B} \psi(Q_{j,2m-2+A}, Q_{i,2n-2+B}) \quad (2-38)$$

Finally, the Green's function  $\psi$  is evaluated as described by Harrington [1].

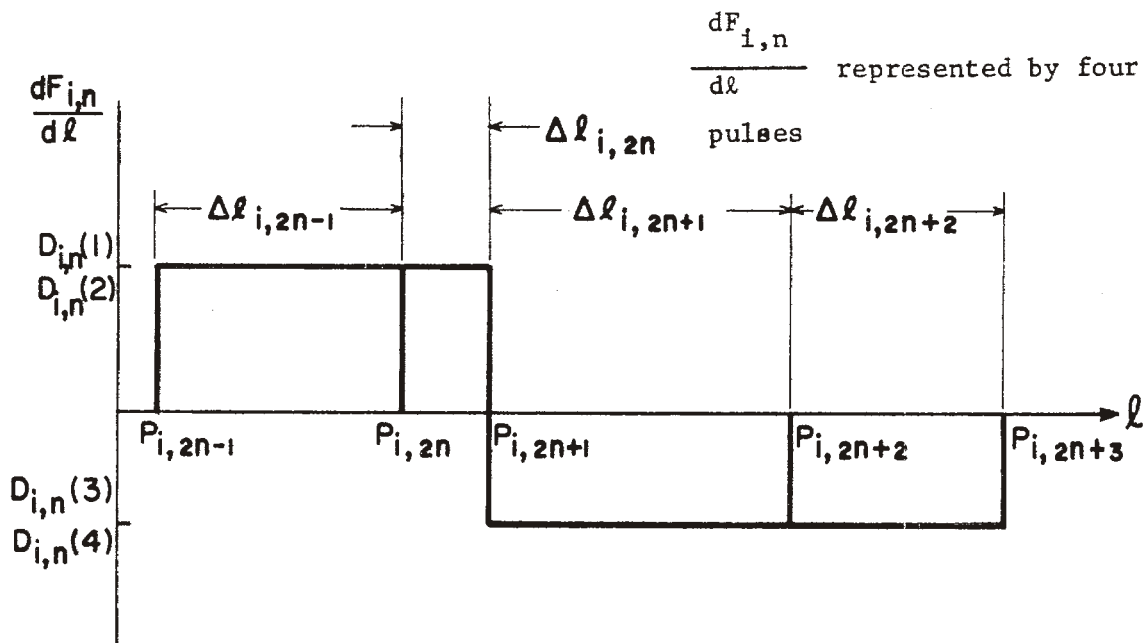
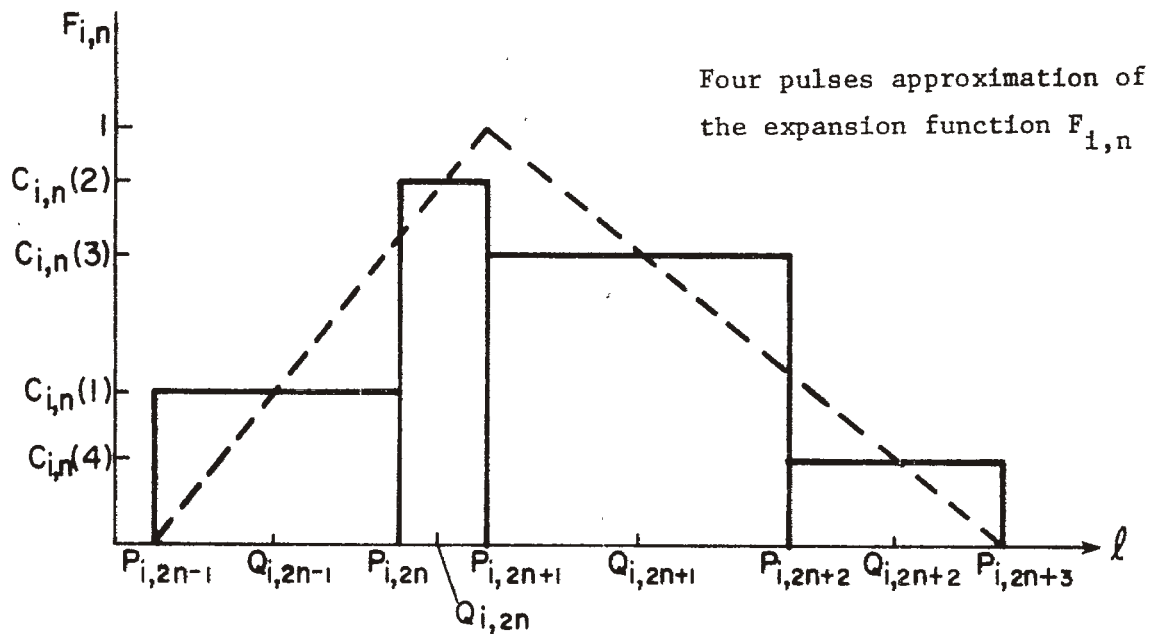


Fig. 2-5. Approximations to the expansion function  $F_{i,n}$  and its derivative  $\frac{dF_{i,n}}{dl}$  for performing the integrations of (2-28).

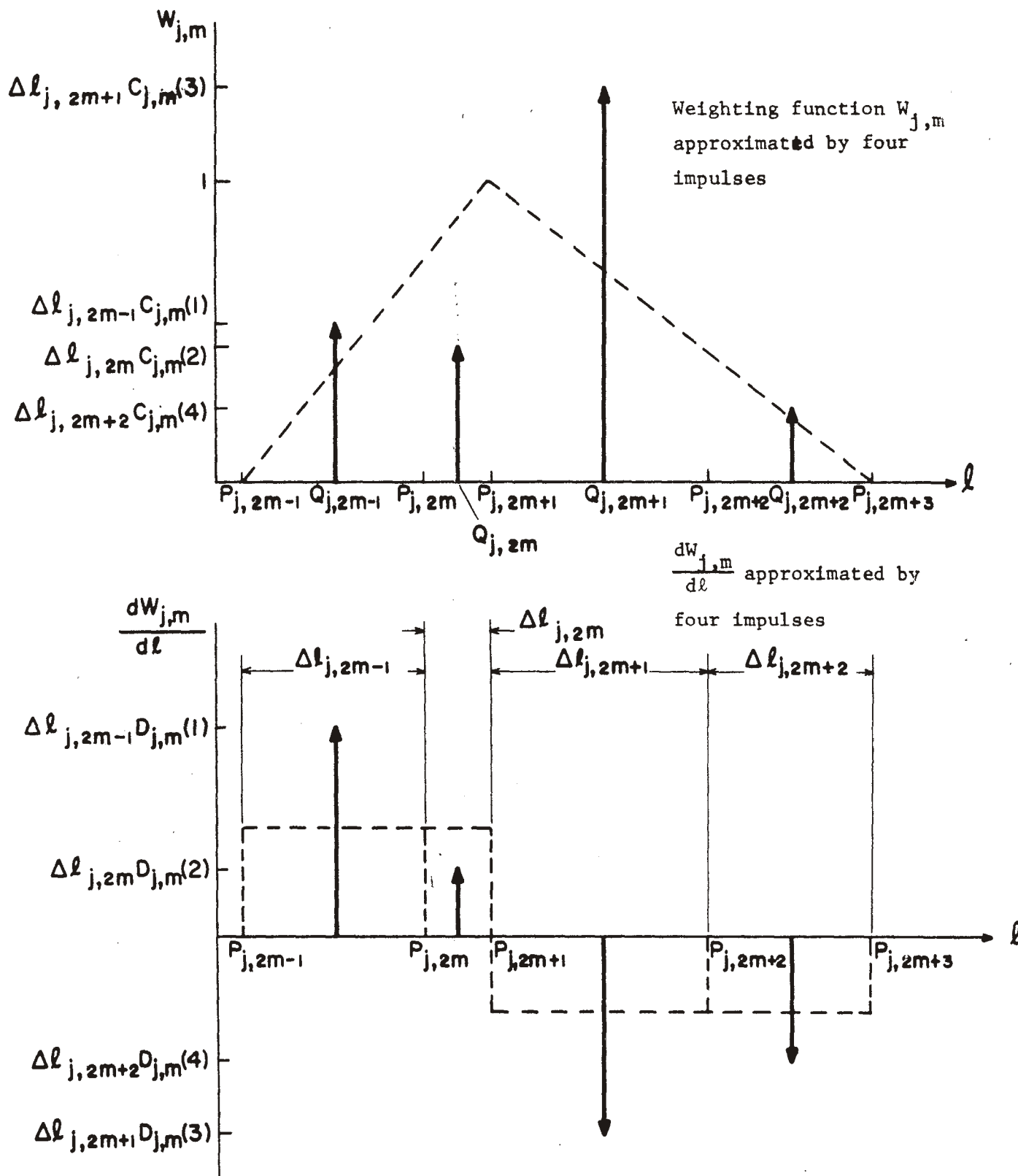


Fig. 2-6. Approximations to the testing function  $W_{j,m}$  and its derivative  $\frac{dW_{j,m}}{dl}$  for performing the integrations of (2-28)

## 2-6. The Generalized Voltage Matrix

In this report antenna excitation can be treated either for lumped sources or for distributed sources. The lumped source corresponding to the  $m$ th triangle function of the  $j$ th wire is represented by a delta-function at the top of the triangle. In this case the elements of the generalized voltage matrix can be evaluated as

$$V_{j,m} = \langle \bar{W}_{j,m}, \bar{E}^i \rangle = U_{j,m} \quad (2-39)$$

where  $U_{j,m}$  is the voltage of the source at the peak of the  $m$ th triangle function on the  $j$ th wire. The distributed source at the  $m$ th segment on the  $j$ th wire is defined as a source corresponding to an impressed field represented by a pulse function on the  $m$ th segment of the  $j$ th wire as shown in Fig. 2-7. In this case the elements of the generalized voltage matrix can be evaluated as (approximate the weighting function  $\bar{W}_{j,m}$  by four pulses as shown in Fig. 2-5)

$$V_{j,m} = \langle \bar{W}_{j,m}, \bar{E}^i \rangle = \sum_{A=1}^4 C_{j,m}(A) U_{j,2m-2+A} \quad (2-40)$$

where  $U_{j,2m-2+A}$  is the voltage of the source on the  $2m-2+A$  segment of the  $j$ th wire.

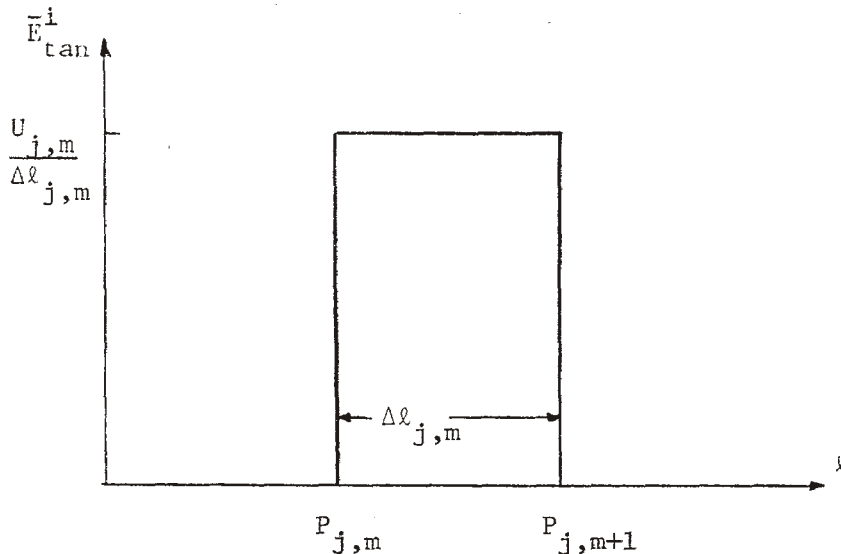


Fig. 2-7. The tangential component of the impressed field which is used to represent a distributed voltage source with voltage  $U_{j,m}$  on the  $m$ th segment of the  $j$ th wire.

For scattering problems the elements of the generalized voltage matrix are given by (approximate the weighting function by four impulses as shown in Fig. 2-6)

$$V_{j,m} = \langle \bar{W}_{j,m}, \bar{E}^i \rangle = \sum_{A=1}^4 C_{j,m}^{(A)} \Delta \ell_{j,2m-2+A} E_{j,2m-2+A}^i \quad (2-41)$$

where  $E_{j,2m-2+A}^i$  is the tangential component of the impressed field at the center of the  $2m-2+A$  segment of the  $j$ th wire.

## 2-7. Radiation and Scattered Fields

It has been shown [2] that the radiation field corresponding to the generalized current matrix [I] is given by

$$\bar{E}^s \cdot \bar{u} = - \frac{j\omega\mu}{4\pi r_o} e^{-jk r_o} [R][I] \quad (2-42)$$

when a moment solution is used. Here  $r_o$  is the distance to the field point in question and [R] is a measurement row matrix defined by

$$[R] = [\langle \bar{F}_{1,1}, \bar{E}^r \rangle, \langle \bar{F}_{1,2}, \bar{E}^r \rangle, \dots, \langle \bar{F}_{NW,NE(NW)}, \bar{E}^r \rangle] \quad (2-43)$$

Where

$$\bar{E}^r = \bar{u} e^{-j\bar{k}_r \cdot \bar{r}_n} \quad (2-44)$$

is the unit plane wave produced by a current element ( $I\bar{\ell}_r$  in Fig. 2-8) at the field point in question,  $\bar{u}$  is a unit vector specifying the polarization of the wave,  $\bar{k}_r$  is a wave number vector pointing in the direction of propagation of the wave, and  $\bar{r}_n$  is the radius vector to a point  $n$  on the antenna. It is convenient to consider two orthogonal components of  $\bar{E}^s$ , say  $\bar{E}_\theta^s$  and  $\bar{E}_\phi^s$ , determined by letting  $\bar{u} = \bar{u}_\theta$  and  $\bar{u} = \bar{u}_\phi$ . From these, other scattered field properties of interest can be easily calculated.

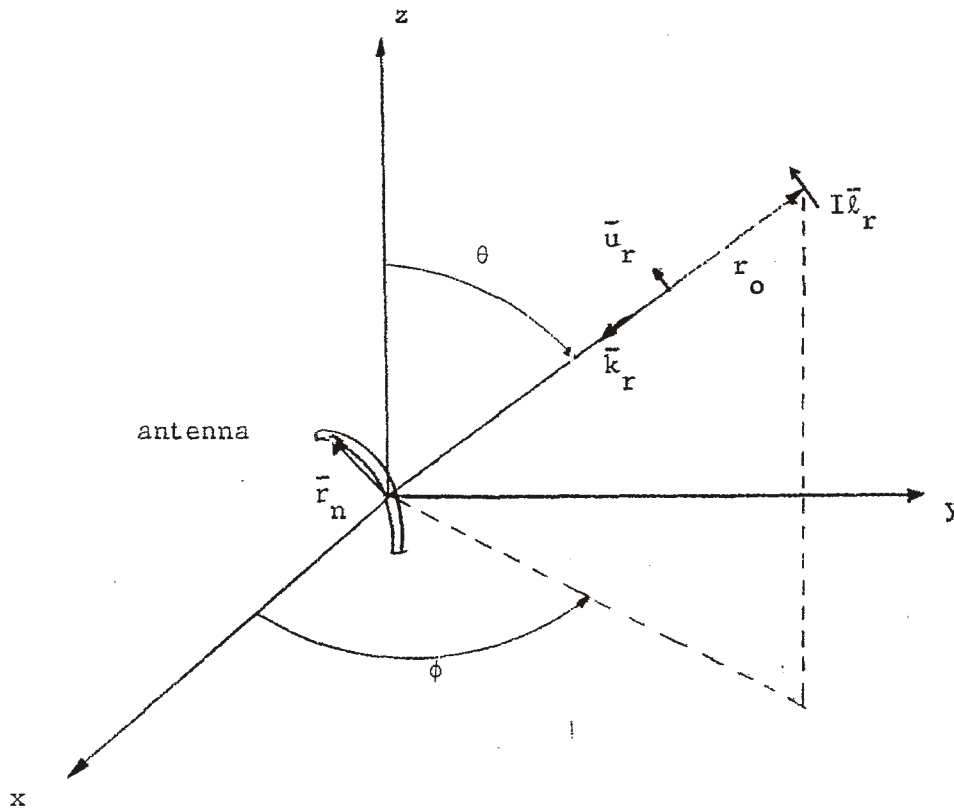


Fig. 2-8. Wire antenna and distant dipole.

2-8. Loaded Antennas and Scatterers

A continuously loaded wire is one for which the tangential electric field is related to the current  $\bar{I}$  on the wire by an impedance function of position  $\eta$  according to

$$\bar{E}_{\text{tan}}^t = \bar{E}_{\text{tan}}^s + \bar{E}_{\text{tan}}^i = \eta \bar{I} \quad (2-45)$$

Now  $\bar{E}_{\text{tan}}^s$  is related to the current  $\bar{I}$  by

$$\bar{E}_{\text{tan}}^s = -L(\bar{I}) \quad (2-46)$$

where the operator  $L$  is given by (2-10). Combining (2-45) and (2-46) results in

$$L(\bar{I}) = \bar{E}_{\text{tan}}^i - \eta \bar{I} \quad (2-47)$$

Reducing (2-47) to a matrix equation by the method of moments yields

$$[Z][I] = [V] - [ZL][I] \quad (2-48)$$

where  $[Z]$ ,  $[I]$ ,  $[V]$  have the usual meanings and

$$[ZL] = [\langle \bar{w}_{j,m}, \eta \bar{F}_{i,n} \rangle] \quad (2-49)$$

The solution of (2-48) for the generalized current matrix is

$$[I] = [Z + ZL]^{-1}[V] \quad (2-50)$$

In this report loads can be treated either as lumped loads or as distributed loads. A lumped load at the  $m$ th triangle function on the  $j$ th wire is defined as a load with the  $\eta$  function represented by an impulse at the peak of the triangle. In this case  $[ZL]$  is a diagonal matrix. The elements on the diagonal can be evaluated as

$$ZL_{j,m,j,m} = ZLL_{j,m} \quad (2-51)$$

where  $ZLL_{j,m}$  is the impedance of the load at the peak of the  $m$ th triangle function on the  $j$ th wire. The distributed load of the  $m$ th segment of the  $j$ th wire is defined as a load with the  $\eta$  function represented by a pulse function over the segment. In this case  $[ZL]$  is a tri-diagonal matrix. The elements on the tri-diagonal can be evaluated as (approximate the weighting function by four pulses shown in Fig. 2-5)

$$ZL_{j,m,j,m} = \sum_{A=1}^4 C_{j,m}^{(A)} C_{j,m}^{(A)} ZLL_{j,2m-2+A} \quad (2-52)$$

$$ZL_{j,m,j,m+1} = \sum_{A=3}^4 C_{j,m}^{(A)} C_{j,m+1}^{(A-2)} ZLL_{j,2m-2+A} \quad \text{if } m+1 \leq NE(j) \quad (2-53)$$

$$ZL_{j,m,j,m-1} = \sum_{A=1}^2 C_{j,m}^{(A)} C_{j,m-1}^{(A+2)} ZLL_{j,2m-2+A} \quad \text{if } m-1 \geq 1 \quad (2-54)$$

where  $ZLL_{j,2m-2+A}$  is the impedance of the load of the  $2m-2+A$  segment of the  $j$ th wire.

## 2-9. Boundary Condition at the Junction of Wires

Consider the antenna as shown in Fig. 2-9 the current on each arm is assumed to be positive when it flows into the junction. Requiring that there be no charge build-up at the junction of the wires yields the boundary condition

$$I_1 + I_2 + I_3 = 0 \quad (2-55)$$

at the junction P.

It is shown in Fig. 2-10 that any kind of current on the antenna can be approximated linearly by using triangle functions  $\bar{F}_{1,1}, \dots, \bar{F}_{1,N1}, \bar{F}_{2,1}, \dots, \bar{F}_{2,N2}, \bar{F}_{3,1}, \dots, \bar{F}_{3,N3}$  as basis functions. Here  $\bar{F}_{1,1}, \dots, \bar{F}_{1,N1-1}, \bar{F}_{2,1}, \dots, \bar{F}_{2,N2-1}, \bar{F}_{3,1}, \dots, \bar{F}_{3,N3-1}$  are ordinary triangle functions as defined in previous sections and  $\bar{F}_{1,N1}, \bar{F}_{2,N2}, \bar{F}_{3,N3}$  are "right-angle" functions that exist only over two segments. Because L is a linear operator, the triangle functions  $I_{1,N1} \bar{F}_{1,N1}, I_{2,N2} \bar{F}_{2,N2}, I_{3,N3} \bar{F}_{3,N3}$  can be divided into six triangle functions  $I'_{1,N1} \bar{F}_{1,N1}, I''_{1,N1} \bar{F}_{1,N1}, I'_{2,N2} \bar{F}_{2,N2}, I''_{2,N2} \bar{F}_{2,N2}, I'_{3,N3} \bar{F}_{3,N3}, I''_{3,N3} \bar{F}_{3,N3}$  such that

$$I_{1,N1} = I'_{1,N1} + I''_{1,N1} \quad (2-56)$$

$$I_{2,N2} = I'_{2,N2} + I''_{2,N2} \quad (2-57)$$

$$I_{3,N3} = I'_{3,N3} + I''_{3,N3} \quad (2-58)$$

By assuming

$$I''_{1,N1} = -I'_{3,N3} \quad (2-59)$$

$$I''_{2,N2} = -I'_{1,N1} \quad (2-60)$$

$$I''_{3,N3} = -I'_{2,N2} \quad (2-61)$$

equations (2-56) - (2-61) reduce to



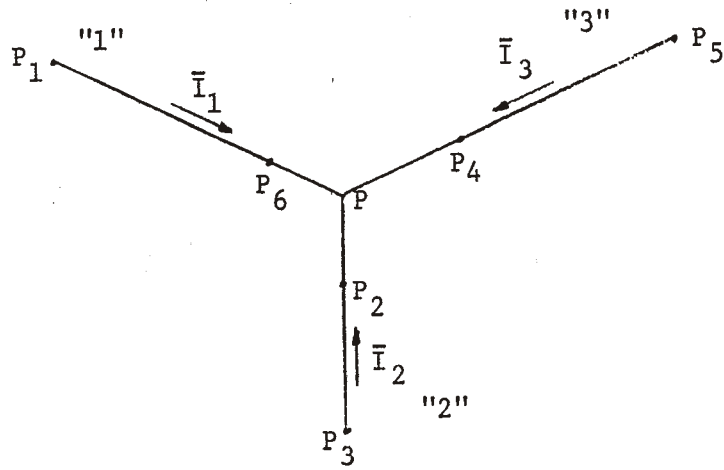


Fig. 2-9. Antenna with three arms

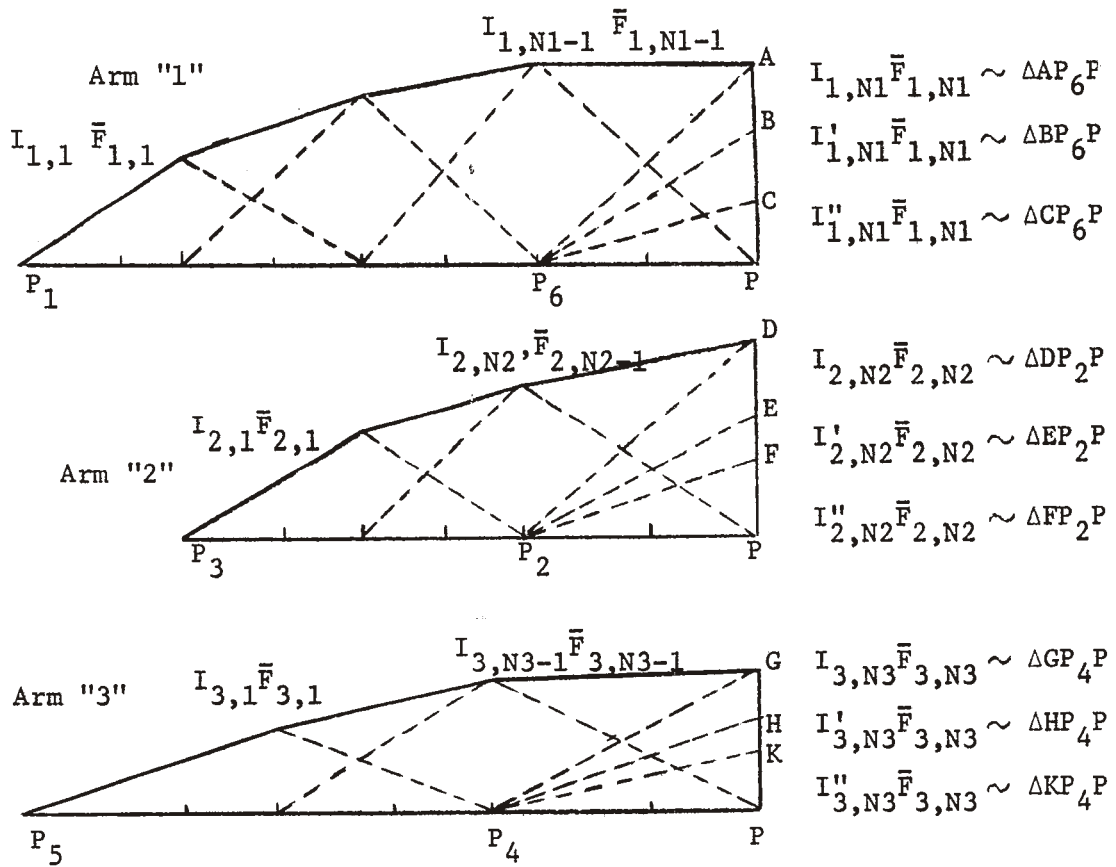


Fig. 2-10. Piecewise linear approximation of current distribution on the arms of the antenna.

$$I_{1,N1} = I'_{1,N1} - I'_{3,N3} \quad (2-62)$$

$$I_{2,N2} = I'_{2,N2} - I'_{1,N1} \quad (2-63)$$

$$I_{3,N3} = I'_{3,N3} - I'_{2,N2} \quad (2-64)$$

In this problem  $I_{1,N1}$ ,  $I_{2,N2}$ ,  $I_{3,N3}$  can be any values which satisfy

$$I_{1,N1} + I_{2,N2} + I_{3,N3} = 0 \quad (2-65)$$

Equations (2-62) - (2-64) form a set of linear equations with  $I'_{1,N1}$ ,  $I'_{2,N2}$ ,  $I'_{3,N3}$  as unknowns. For this set of linear equations the ranks of the coefficient matrix

$$\begin{pmatrix} 1 & 0 & -1 \\ -1 & 1 & 0 \\ 0 & -1 & 1 \end{pmatrix}$$

and the augmented matrix

$$\begin{pmatrix} 1 & 0 & -1 & I_{1,N1} \\ -1 & 1 & 0 & I_{2,N2} \\ 0 & -1 & 1 & I_{3,N3} \end{pmatrix}$$

are the same when (2-65) is satisfied. Hence, this set of linear equations possesses a solution.

Since the rank of the coefficient matrix is one less than the order of the coefficient matrix, one unknown can be chosen arbitrarily and the other two unknowns will be expressed in terms of this one. Now, set  $I'_{3,N3} = 0$ , so that there exists only one solution of (2-62) - (2-64). Hence triangle functions  $\bar{F}_{1,1}, \dots, \bar{F}_{1,N1-1}$ ,  $\bar{F}'_{1,N1}$ ,  $\bar{F}_{2,1}, \dots, \bar{F}_{2,N2-1}$ ,  $\bar{F}'_{2,N2}$ ,  $\bar{F}_{3,1}, \dots, \bar{F}_{3,N3-1}$ , are a suitable set of expansion functions. Where

$$\bar{F}'_{1,N1} = \bar{F}_{1,N1} - \bar{F}_{2,N2} \quad (2-66)$$

$$\bar{F}'_{2,N2} = \bar{F}_{2,N2} - \bar{F}_{3,N3}$$

are ordinary triangle functions over  $P_6PP_2$ ,  $P_2PP_4$ , respectively. Hence this problem can be solved using the method described in the previous sections by treating it as a problem which consists of three open wires, say  $P_1PP_2$ ,  $P_3PP_4$ ,  $P_5P$  as shown in Fig. 2-9. It should be noted, however, that  $PP_2$ ,  $PP_4$ , must each be exactly two segments.

It is very easy to extend this method to problems having more complex geometrical configurations. Of course, the loop can be treated as an open wire with its ends overlapping by two segments. Examples involving wire junctions are included in Chapter 4 of this report.

#### 2-10. Conclusion

In this chapter, problems of radiation and scattering from thin wires with arbitrary shapes, excitations, and loadings were considered. Using arbitrary impressed fields, radiation problems and scattering problems were included in the same discussion. Using the method of moments the functional equation of the problem was reduced to a matrix equation. Reasons for choosing triangle functions for both expansion functions and weighting functions were pointed out. Formulas for numerical evaluation of the generalized impedance matrix [Z], generalized voltage matrix [V], and generalized load impedance matrix [ZL] were derived. A method for handling wire junctions was also included.

## Chapter 3

### DESCRIPTION OF COMPUTER PROGRAMS

#### 3-1. Introduction

Computer programs for radiation problems or plane-wave scattering problems for thin wires with arbitrary excitation and loading are presented in the Appendices. The programs are written in Fortran IV for use with an IBM 360/50 digital computer. A description of these programs is given in this chapter. Particular emphasis is given to data input to aid the reader in applying the programs to a specific problem of interest. Complex variables are used since many variables in electromagnetic theory are indeed complex. Use of common region is made to save memory space. Comment cards are included to aid the reader in understanding the programs. Program listing along with sample input and output data are given in the Appendices.

#### 3-2. Radiation Problem

A program suitable for solving radiation problems is presented in Appendix A. This program is appropriate for thin wire antennas with lumped sources and/or lumped loads located at the peaks of the triangle functions. The restrictions on the types and positions of the sources and loads can be removed by some minor program modifications as discussed at the end of the next section. The maximum number of wires that can be handled here is four. The maximum number of expansion functions for any wire is fifteen. For antennas having more wires or longer wires requiring additional expansion functions to obtain a good current approximation, the dimension statements should be changed. All input data are provided for in the main program, as there are no read statements in the subroutines. All FORMAT statements are placed at the end of the main program.

The first data statement reads in the wavelength in meters, denoted by WAVE in the computer program.

The second data statement reads in the total number of wires in the problem geometry. This is denoted by NWIRE in the program.

The remaining read statements are included in DO Loop 550. This loop iterates a total of NWIRE times. Hence the set of read statements included also executes NWIRE times. Therefore, these five read statements correspond to NWIRE sets of data cards, with each set corresponding to one wire of the total in the problem geometry.

The third read statement reads in  $BA(NW)$ ,  $NS(NW)$ ,  $NF(NW)$ , and  $NL(NW)$ , where NW is the index of DO LOOP 550.  $BA(NW)$  is the wire radius in wavelengths of the NWth wire.  $NS(NW)$  is the number of segments making up the NWth wire. (NS should be an even number.)  $NF(NW)$  is the number of feed points on the NWth wire; i.e., the number of segments to which excitation voltages are applied. (If no excitation is applied on the wire,  $NF(NW) = 1$  and the source is specified as a source with zero voltage.)  $NL(NW)$  is the number of loads on the NWth wire. (If no loads are used on the wire then  $NL(NW)=1$  and the load is specified as  $ZL(1,1) = (0.0, 0.0)$ , a load with zero impedance.)

The fourth read statement reads in the positions of the feed points on the NWth wire. For example, if excitation voltages are applied to the peaks of the third and eighth triangle functions on the NWth wire then  $IF(NW,1) = 3$  and  $IF(NW,2) = 8$ .

The fifth read statement reads in the applied excitation voltages at the feed points which are specified by the fourth data statement as discussed above.

The sixth read statement provides the positions of the loads along the NWth wire. Thus if the first load on the NWth wire is applied at the peak of the fifth triangle function, the second to the eighth, etc., then  $LP(NW,1) = 5$ ,  $LP(NW,2) = 8$ , and so on.

The seventh read statement reads in the load impedances to be applied on the NWth wire at the points specified by the sixth data statement. These are written as complex numbers, in ohms.

As mentioned in Section 2-9, all problems are treated as antennas involving open wires. Hence, the number of expansion functions on the NWth wire can be evaluated as

$$NE(NW) = NS(NW)/2 - 1$$

and the number of points on the axis of the wire which should be specified can be evaluated as

$$NP(NW) = NS(NW) + 1$$

[X(1,NW,I),X(2,NW,I),X(3,NW,I)] corresponds to the Cartesian coordinates of the point  $P_{NW,I}$  as shown in Fig. 2-2. These points can either be specified by reading in the coordinates or by calculating them with a generating function.

DO LOOP 560 obtains XX, XD, and TLEN, where the numbers XX are the coordinates of the center points of the segments, XD are the direction numbers of the segments, and TLEN are the lengths of the segments.

The generalized impedance matrix [Z] is computed using subroutine CALZ. Modification of the matrix [Z] to include the effects of loads on the wires is performed by subroutine CALZL. The generalized admittance matrix [Y] is obtained by inverting the matrix [Z] using subroutine LINEQ. (Because we store [Y] and [Z] in the same locations, the admittance matrix is still named [Z] in the program.) The generalized voltage matrix [V] (denoted by [U] in the program) is evaluated using subroutine BIGV. Once the matrices [Z]<sup>-1</sup> and [V] are available, the generalized current matrix [I] can be obtained by performing the matrix product in subroutine CRNT. DO LOOP 30 computes the magnitude and phase of the current and prints them out along with the real and imaginary parts. The input impedances at the feed points and the total input power are calculated in DO LOOP 55. These also printed out as parts of the data output.

The far-zone field is computed as described in Sec. 2-7. The polar and azimuthal components of the electric field,  $E_{\theta}$  and  $E_{\phi}$ , are computed using subroutines ROW and PATT to evaluate (2-43) and (2-42) respectively.  $E_{\theta}$  and  $E_{\phi}$  are labeled E(1) and E(2) respectively in the program. After

computing the magnitude and phase of the electric field, the polar coordinates of the point where the field is calculated, the real and imaginary parts of the field, and its magnitude and phase are printed out. Finally, the power gain GATHE and GAPHI are calculated for the two field components  $E_\theta$  and  $E_\phi$  respectively.

### 3-3. Further Details

The generalized impedance matrix [Z] is computed using formulas derived in Sec. 2-5. Elements of [Z] are calculated in order by column. DO LOOP 60 computes the Green's function  $\psi$  (denoted by PSI in the program), which is defined by (2-35), using the formulas provided by Harrington [1]. DO LOOP 70 corresponds to (2-36) - (2-38), where C(K), P(I), D(K), Q(I) and XDD in the program correspond to  $C_{j,m}(K)$ ,  $C_{i,n}(I)$ ,  $D_{j,m}(K)$ ,  $D_{i,n}(I)$  and  $\Delta \bar{l}_{j,2m-2+K} \cdot \Delta \bar{l}_{i,2n-2+I}$  in (2-37) and (2-38) respectively. Finally, the "four subscript" array (denoted by [Z4] in the program) is changed to the "two subscript" array [Z] in DO LOOP 90.

Subroutine CALZL in Appendix A is developed from (2-51). It is correct only when all loads are lumped loads located at the peaks of the triangle functions since (2-51) is only valid for this type of loading.

Subroutine LINEQ inverts a complex matrix by the Gauss-Jordan method with pivot selection. The input and output matrices are stored in the same locations.

Subroutine BIGV in Appendix A is developed from Eq. (2-39) which is suitable for the case of lumped sources at the peaks of the triangle functions.

In subroutine ROW,  $U(1,I)$  is the direction cosine of  $\bar{u}_\theta$  and  $U(2,I)$  is the direction cosine of  $\bar{u}_\phi$ . Hence  $R(1,I)$  or  $R(2,I)$  is the matrix [R] defined by (2-43) whenever  $\bar{u}$  is equal to  $\bar{u}_\theta$  or  $\bar{u}_\phi$  respectively.

So far, the wire radius must be constant for any one wire. (It can be different for different wires.) This restriction can be relaxed by specifying the radius of the wire in wavelengths at the center of each segment as  $BA(NW,I)$ , defining  $A(NW,I) = BA(NW,I) \cdot WAVE$  in the main program, and substituting  $A(NWF,NSF)$  in place of  $A(NWF)$  in subroutine CALZ.

When excitation along the wire is represented by other than impulsive sources, subroutine BIGV must be changed. For example, when distributed sources as described in Sec. 2-6 are used then (2-40) should be used to evaluate the generalized voltage matrix. Appendix C presents the modifications which should be applied to Appendix A when distributed sources are used.

When loading along the wire is represented by other than impulsive loads subroutine CALZL must be changed. For example, when distributed loads as described in Sec. 2-8 are used then (2-52) - (2-54) should be used to develop subroutine CALZL. Appendix D provides the subroutine which is suitable for use when loading is represented as distributed loads.

### 3-4. Scattering Problem

Earlier it was pointed out that when the wires are acting as scatterers in an incident field  $\vec{E}^i$  then the elements of the generalized voltage matrix are evaluated using (2-41). Once the generalized voltage matrix is known the analysis procedures can be carried out as before. The computer program presented in Appendix B is suitable for determining the current distributions and bistatic radar cross-section patterns for loaded wires that are irradiated by a plane incident wave. All loads along the wires should be lumped loads at the peaks of the triangle functions. This restriction to the types and positions of the loads can be removed using some minor modifications as described at the end of the last section. All subroutines, except BIGV, in Appendix B are the same as those in Appendix A.

The main program before the instruction CALL LINEQ in Appendix B can be made from the program in Appendix A by dropping NF(NW) in the third read statement and dropping the fourth and fifth read statements entirely.

Sometimes there is interest in the behavior of the scatterer for several angles and polarizations of the incident wave. If the number of different incident waves is NOSET, the DO LOOP 794 will execute NOSET times. There are two read statements in DO LOOP 794 to specify



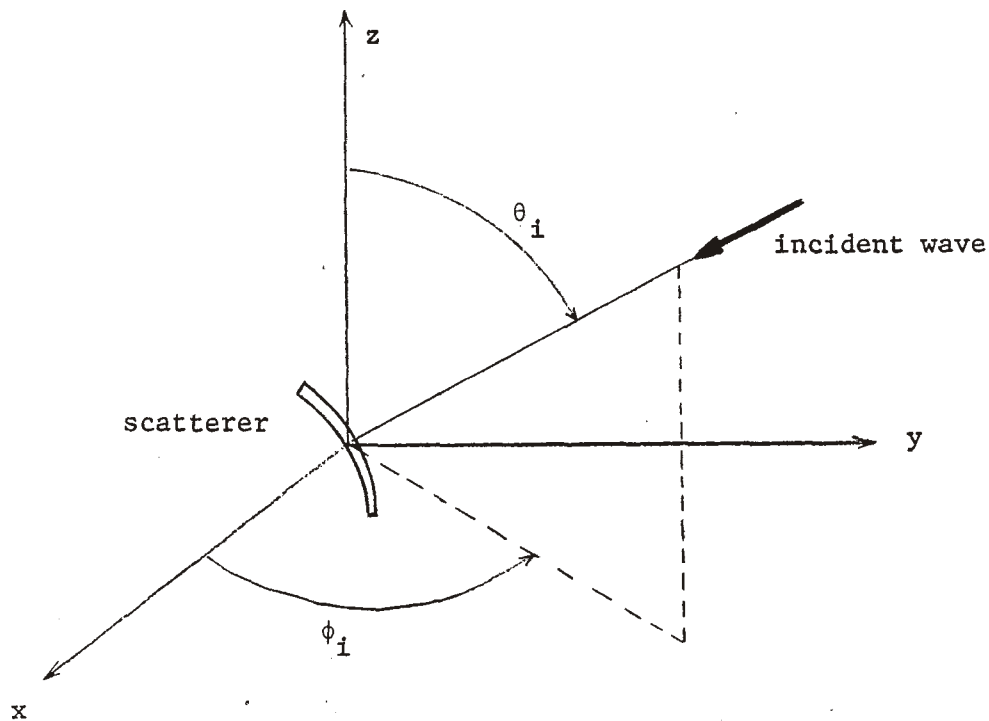


Fig. 3-1. Thin wire irradiated by a plane incident wave.

the incident wave. The first reads in angle  $\theta_i$  and  $\phi_i$  designating the direction of propagation of the incident wave. These are indicated in Fig. 3-1. The second data statement reads in the  $\theta$  and  $\phi$  components of the incident electric field where phase is with respect to the origin of the coordinate system. ( $E_\theta$  is denoted by EI(1) and  $E_\phi$  is denoted by EI(2) in the program.)

The generalized voltage matrix [V] (denoted by [U] in the program) is computed using subroutine BIGV. Once this matrix is known, the analysis procedures are carried out as before.

### 3-5. Conclusion

In this chapter computer programs suitable for handling radiation and scattering problems involving thin wires of arbitrary shape are described. In the next chapter these programs are applied for analysis of electromagnetic properties of several frequently encountered wire configurations.

4-1. Introduction

In this chapter several examples are presented to illustrate certain applications of the programs described in the previous chapter, and numerical results are compared with experimental data and/or results obtained by other theoretical methods.

4-2. Radiation Problems

As a first example consider a half-wave straight wire antenna that is centered with a unit voltage. The wire configuration and coordinate system are shown in Fig. 4-1, where the antenna length  $L = \lambda/2$  and the wire radius  $a = 0.00702\lambda$ . It is evident that in the input data  $NWIRE = 1$  and  $BA = 0.00702$ . The wavelength is given as 1.0 meter so that  $WAVE = 1.0$ . The analysis is carried out using 28 equal-length segments with the computer program as presented in Appendix A. (Hence,  $NS(NW) = 28$  in the program.) DO LOOP 1510 in the main program is used in this case to generate the coordinates of the points on the axis of the wire. This is in lieu of specifying the points individually as data input. These points are specified in order from the lowest point to the highest point on the wire. Hence, the positive current reference is the positive direction of the z-axis. The excitation is represented by a lumped voltage source at the peak of the seventh triangle function. (Since the peak of the seventh triangle function is located at the center of the wire.) Therefore,  $NF(1) = 1$  and  $IF(1,1) = 7$  in the program. There is no loading on the wire, so that the data input provides one lumped load at the peak of the first triangle function with impedance equal to zero. Thus,  $NL(1) = 1$ ,  $LP(1,1) = 1$ , and  $ZL(1,1) = (0.0,0.0)$  in the program. Numerical results for current are plotted in Fig. 4-2 with the solid line. The field and the power gain are calculated in the plane  $\phi = 0$  at intervals  $\Delta\theta = 20^\circ$ , and the gain pattern is plotted in Fig. 4-3. These results compare very favorably with the experimental data measured

by Mack [9] and with the results computed by Strait and Hirasawa [4] using pulses for expansion functions and point-matching.

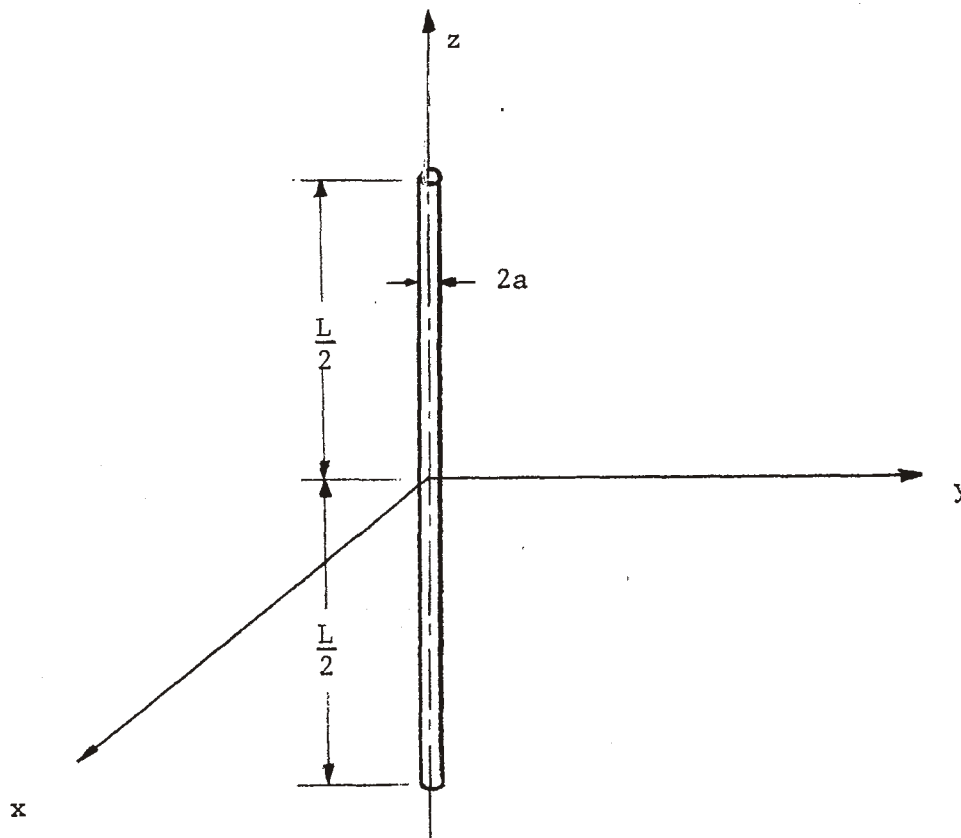


Fig. 4-1. Straight wire and coordinate system.

Next consider the same problem with the excitation represented as a distributed source with gap length  $\lambda/14$  (the length of two segments), i.e., the unit voltage source is thought of as two half voltage sources over the fourteenth and fifteenth segments. Here  $NF(1) = 2$ ,  $IF(1,1) = 14$ ,  $IF(1,2) = 15$ ,  $V(1,1) = (0.5, 0, 0)$ , and  $V(1,2) = (0.5, 0, 0)$ . Numerical results of current are plotted in Fig. 4-7 with the dashed line. There is no difference in the real part of the current but a little difference in the imaginary part is noted near the source. This difference is expected since the singularity of the source is treated differently in the two methods.

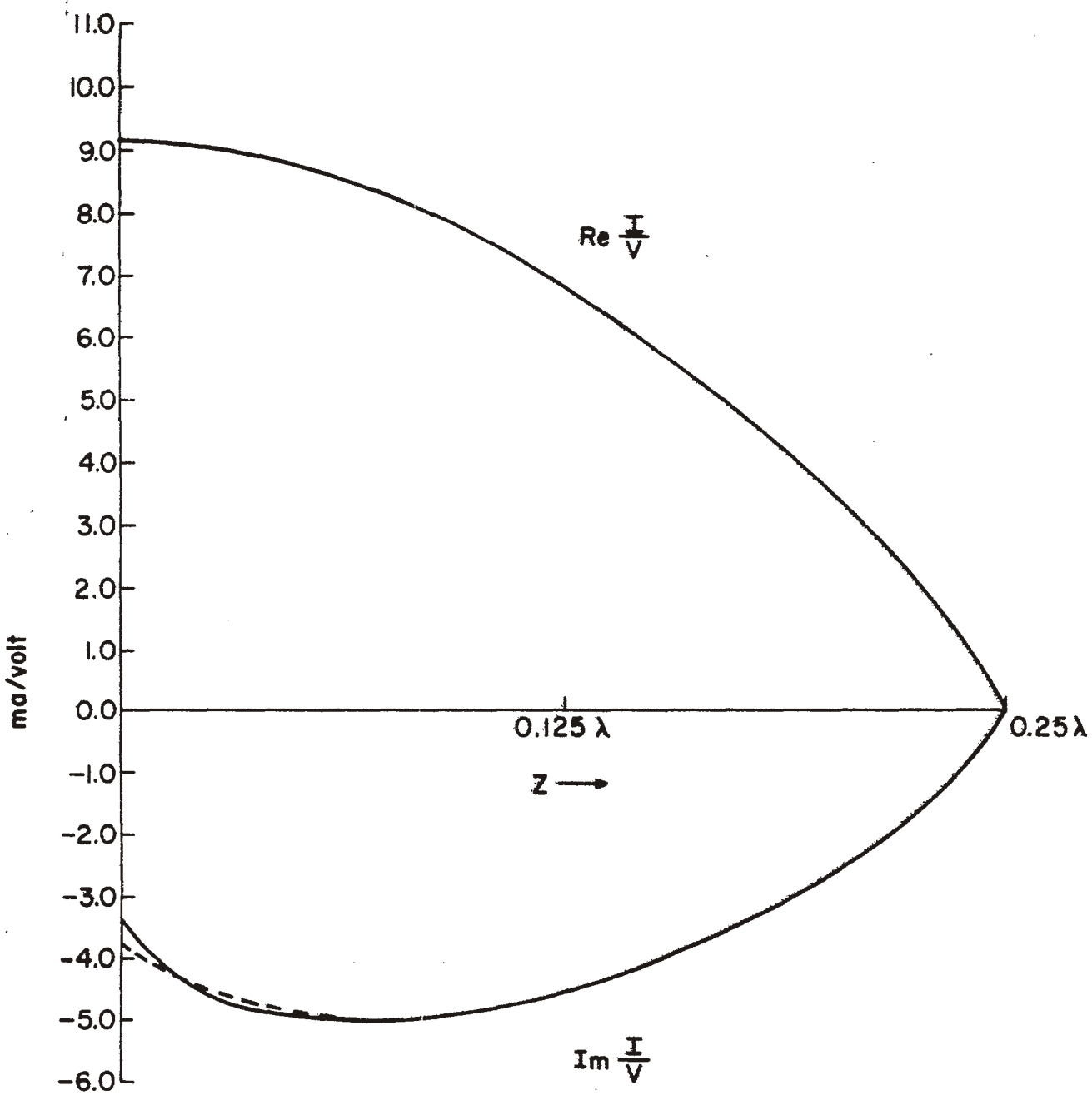


Fig. 4-2. Current on a half-wave straight wire antenna that is centered with a unit voltage. (example 1, see page 32).

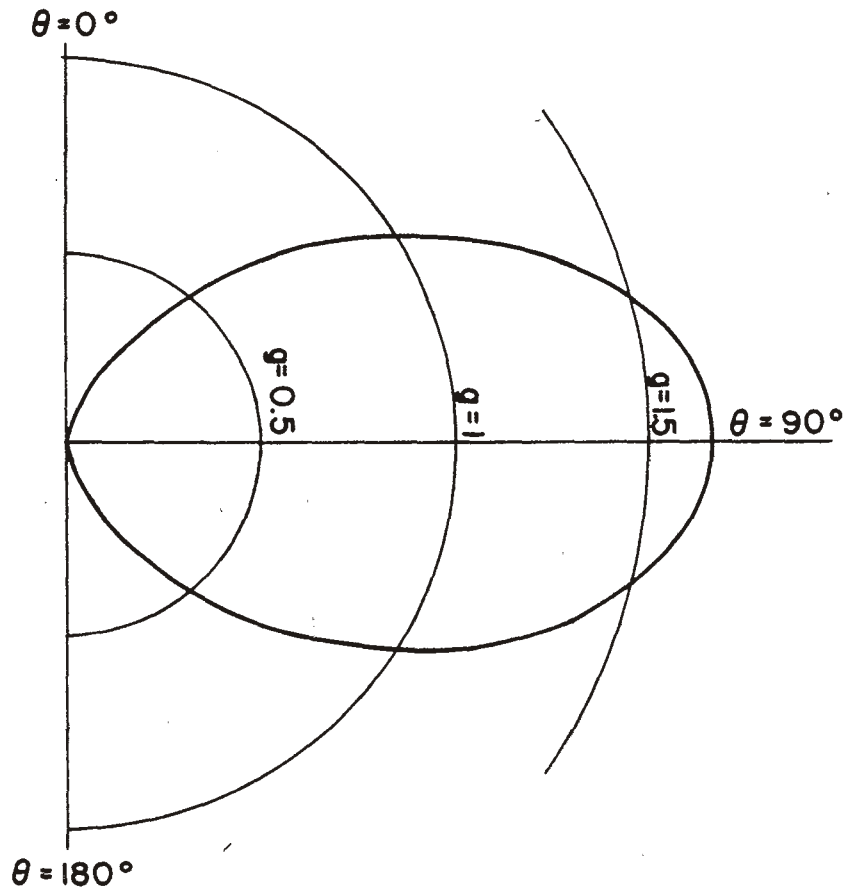


Fig. 4-3. Gain pattern for a centered half-wave straight wire antenna. (example 1, see page 32).

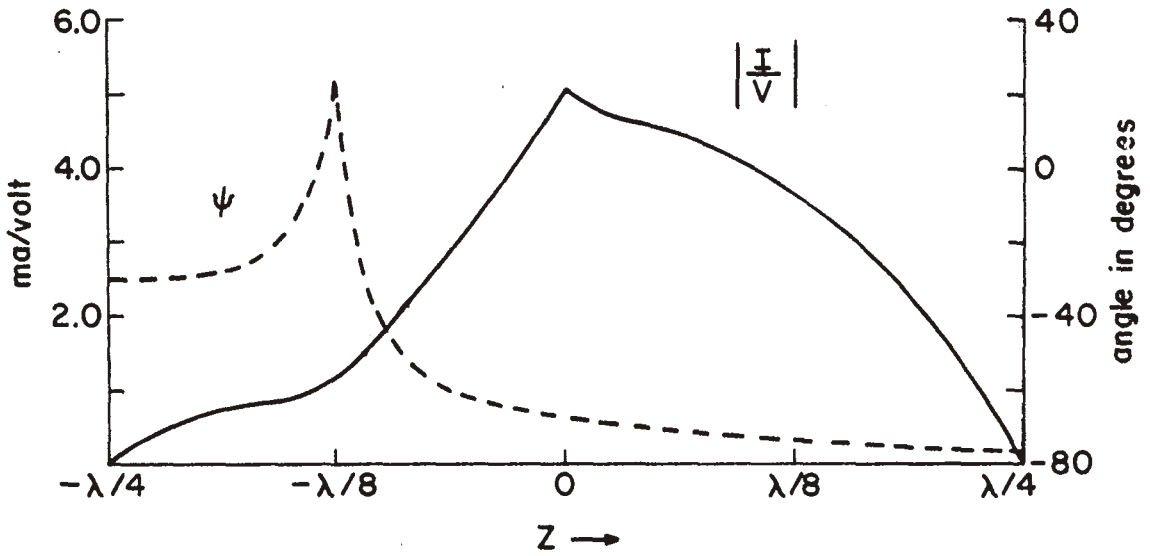


Fig. 4-4. Current on a loaded half-wave straight wire antenna. (example 2, see page 36).

The next example (example 2) considers a half-wave straight-wire antenna that is excited with a unit voltage one quarter wavelength from the end of the wire and loaded at the center point with  $Z_L = j 100$  ohms. The configuration and coordinate system are shown in Fig. 4-1, when  $L = \lambda/2$  and  $a = 0.00674\lambda$ . Excitation is at  $z = -\frac{\lambda}{8}$  and the wavelength is given as 1 meter. The analysis is carried out using 24 equal-length segments with the computer program as presented in Appendix A. The points on the axis are specified by the same method used in the first example. Hence, the current reference is the same as before (positive in +z direction). The excitation is represented by a lumped voltage source at the peak of the third triangle function. The load is treated as a lumped load at the peak of the sixth triangle function. (NL(1) = 1, LP(1,1) = 6, ZL(1,1) = (0.0, 100.0) in the program.) Numerical results for current are plotted in Fig. 4-5. This compares favorably with results computed by Strait and Hirasawa [4] and earlier by Harrington and Mautz [3].

The third example is a five-wavelength wire antenna that is centered with a unit voltage. The configuration and coordinate system are again shown in Fig. 4-1 where  $L = 5\lambda$  and  $a = 0.00639\lambda$ . The wavelength is given as one meter. One hundred equal-length segments are used along with the computer program of Appendix A. The dimension statements were changed, however, in order to permit use of large number of expansion functions. The generating function which was used to evaluate the coordinates of the points on the axis of the wire in the first example is again used after changing the statement

$$HH = 0.25 * WAVE$$

to

$$HH = 2.5 * WAVE$$

The excitation is represented by a lumped voltage source at the peak of the 25th triangle function. Current is plotted in Fig. 4-5 and this compares favorably with the results computed by Strait and Hirasawa [4] using pulses and point-matching.

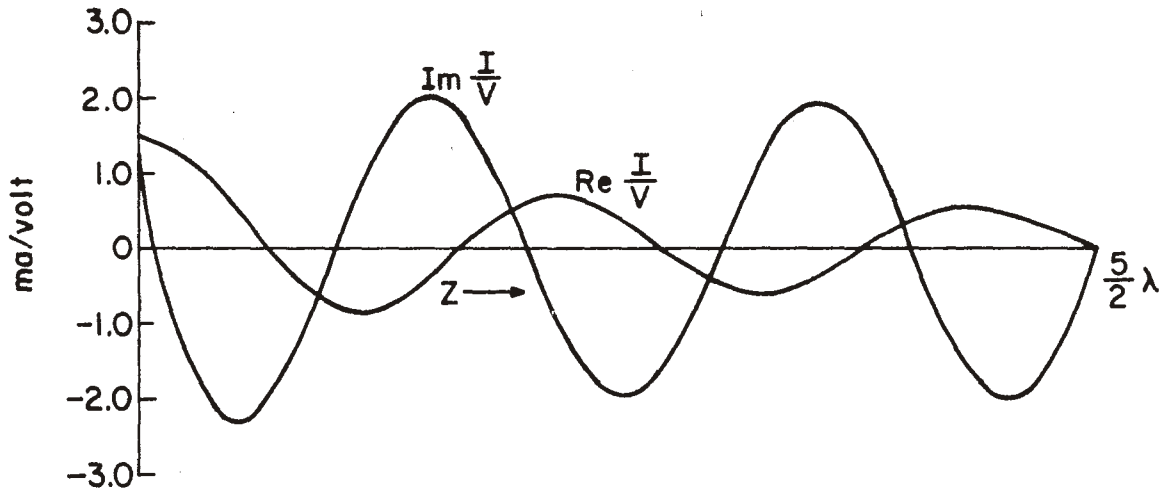


Fig. 4-5. Current on a five-wave length straight wire antenna that is centered with a unit voltage. (example 3, see page 36).

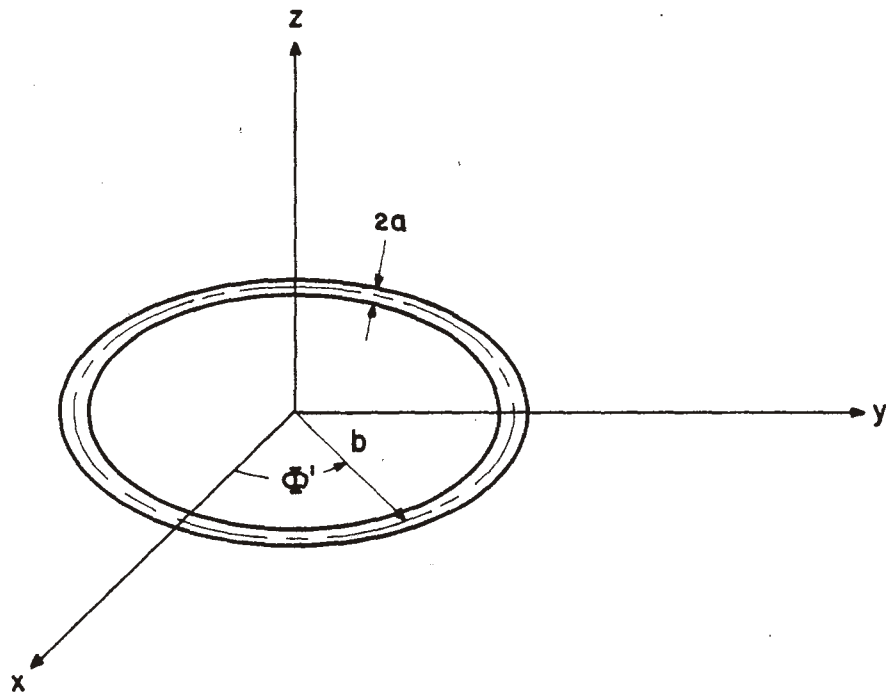


Fig. 4-6. Circular-loop and coordinate system.

As a fourth example consider a circular loop antenna with wire radius  $a = 0.00106\lambda$  and circular radius  $b = \lambda/2\pi$  as shown in Fig. 4-6. The wavelength is given as 1 meter. Excitation is a unit voltage at  $\phi' = 0$ . This problem is treated as an open wire with two segments overlapping at the ends of the wire as shown in Fig. 4-7. The analysis is carried out using 34 segments for the

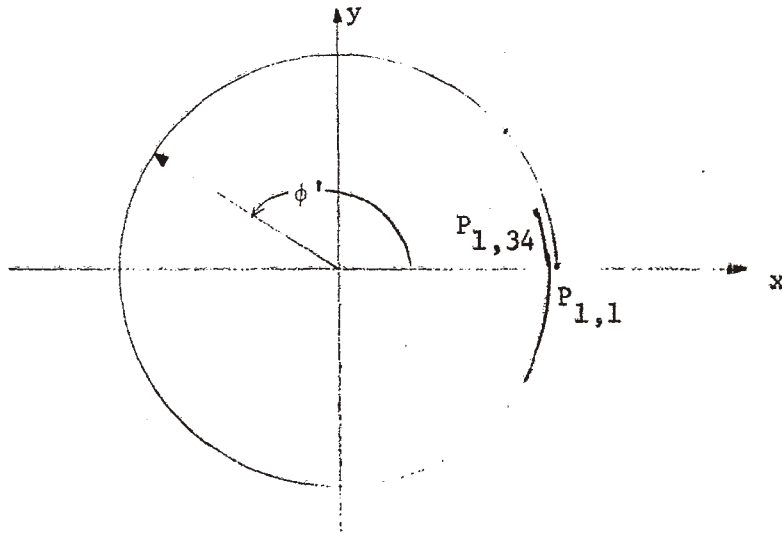


Fig. 4-7. Circular loop antenna.

open wire. The coordinates of the points on the axis of the wire are determined in the program using the following generating function:

```

RID = WAVE/(2. * PI)
DPHI = 2. * PI/(NS(NW) - 2)
NPNW = NP(NW) - 3
DO 1510 I = 1,NPNW
X(1, NW, I) = RID * COS ((I-1) * DPHI)
X(2, NW, I) = RID * SIN ((I-1) * DPHI)
1510 X(3,NW,I) = 0.
DO 1511 J = 1,3
X(J, NW, NPNW) = X(J, NW, 3)
X(J, NW, NPNW-1) = X(J, NW, 2)
1511 X(J, NW, NPNW - 2) = X(J, NW, 1)

```



where DO LOOP 1511 is used to provide the overlap of the two segments at the ends of the wire. Positive current reference is in the direction of increasing  $\phi$ . The excitation is represented by a lumped voltage source of unit voltage at the peak of the 16th triangle function. Numerical results for current are plotted in Fig. 4-8 and those compare reasonably well with results evaluated by Iizuka [10]. Radiation field and power gain are calculated in the plane  $\phi = 0.180^\circ$  and the plane  $\theta = 90^\circ$ . These results are plotted in Fig. 4-10. As expected, the  $\theta$ -component of the radiation field is zero.

The fifth example to be considered is the same as that above except there is a load  $Z_L = 100$  ohms at  $\phi' = 180^\circ$ . This load is represented as a lumped load at the peak of the eighth triangle function. Numerical results of current are plotted in Fig. 4-9 and again, these can be compared with those evaluated by Iizuka [10]. Gain patterns in the plane  $\phi = 0, 180^\circ$  and the plane  $\theta = 90^\circ$  are plotted in Fig. 4-11.

Next, consider an example involving a parasitic element. The wire configuration and coordinate system are shown in Fig. 4-12 where  $L = 0.5\lambda$ ,  $a = 0.00702\lambda$ , and  $d = 0.5\lambda$ . (Here, NWIRE = 2 in the computer program.) Wire "1" is centered with a unit voltage and wire "2" is a parasitic element. The wavelength is given as one meter. Thirty-two segments are used in the driven antenna with twenty-four segments on the parasitic antenna. (NS(1) = 32 and NS(2) = 24 in the program.) In the computer program the points on the axes of the wires can be evaluated using the following generating function:

```

DWAVE = 0.5 * WAVE
  HH = 0.25 * WAVE
  NPNW = NP(NW)
  DO 1510 I = 1, NPNW
    X(1,NW,I) = DWAVE * (3./2. - NW)
    X(2,NW,I) = 0
1510    X(3,NW,I) = 2*HH/NS(NW) * (I - 1) - HH

```

Current is assumed to be positive in the +z direction. Excitation is represented by a lumped unit voltage source at the peak of the 8th triangle function on the first wire. Currents on the wires are plotted in Fig. 4-14.

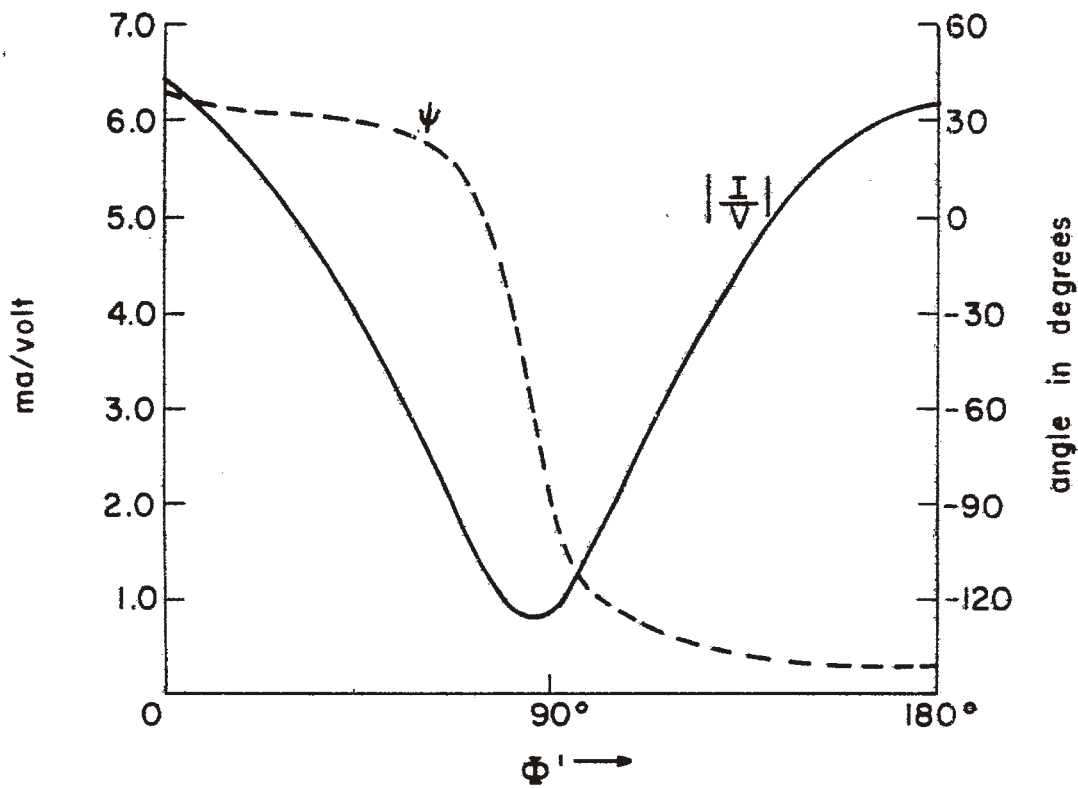


Fig. 4-8. Current on a circular loop antenna with circumference  $2\pi b = \lambda$ . (example 4, see page 38).

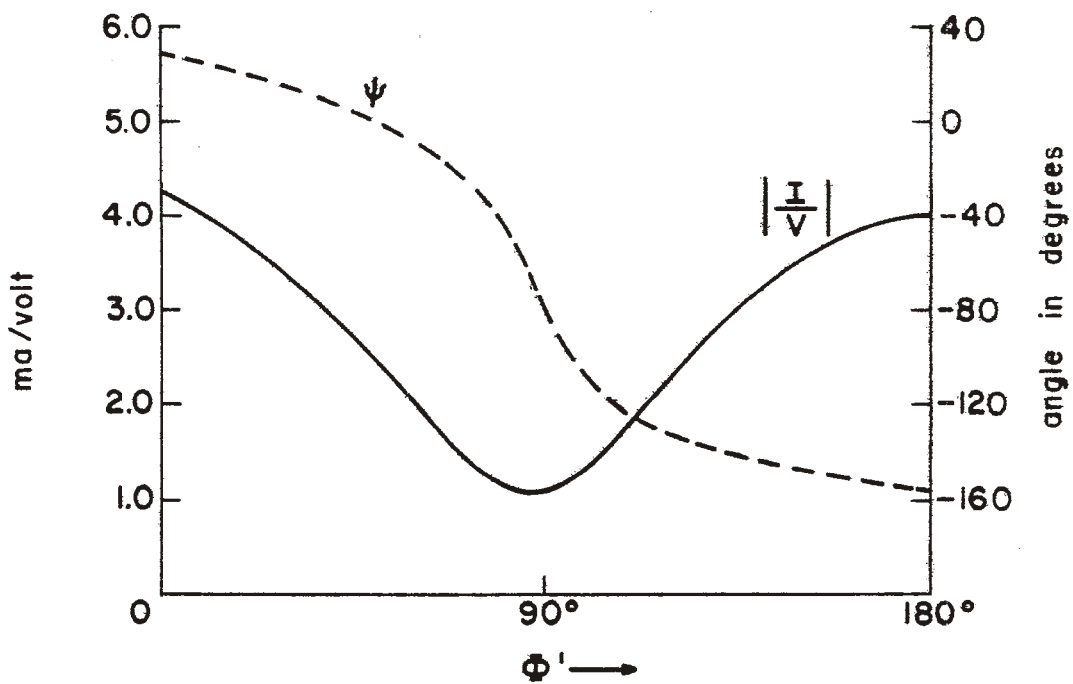


Fig. 4-9. Current on a loaded circular loop antenna with circumference  $2\pi b = \lambda$ . (example 5, see page 39).

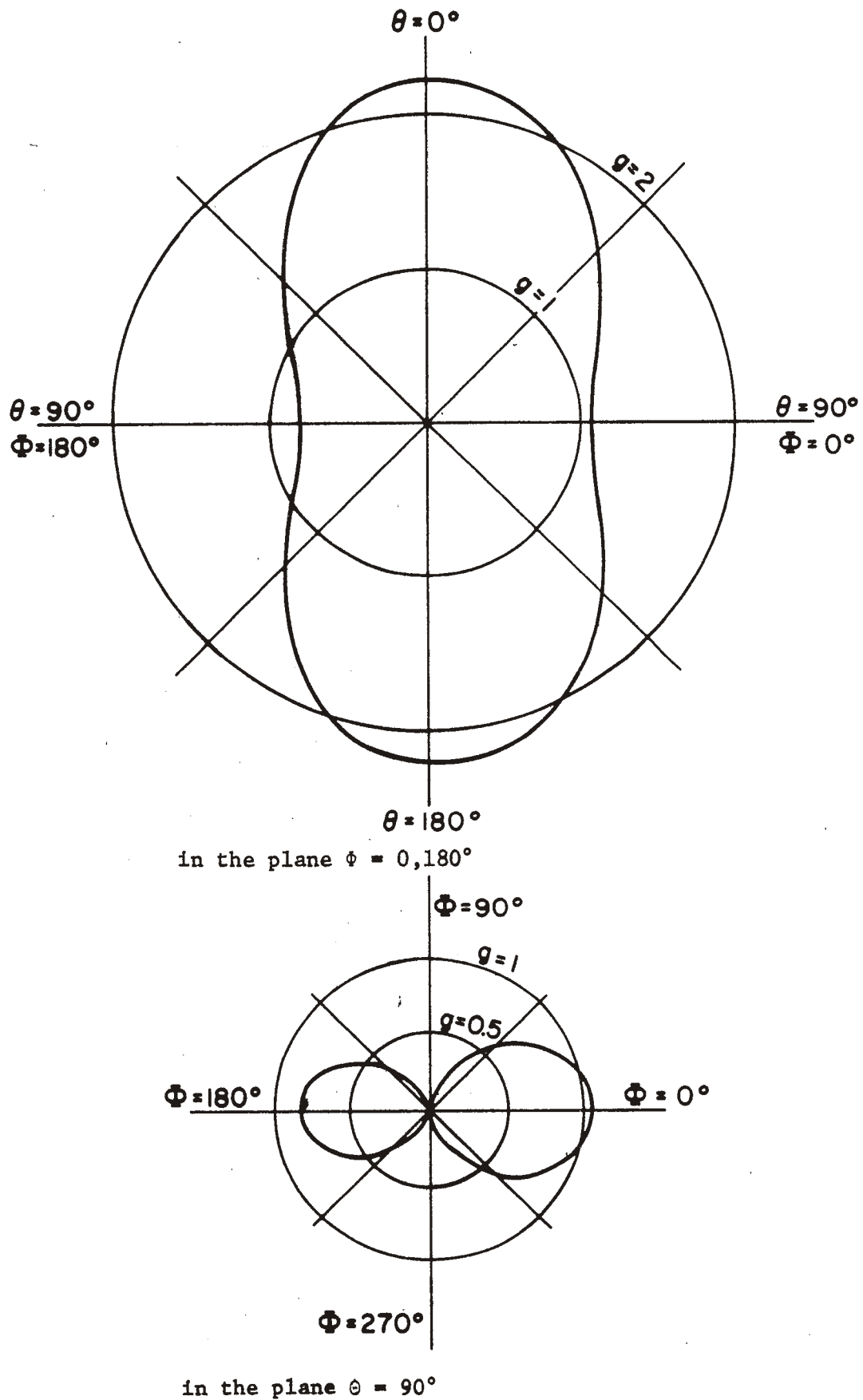


Fig. 4-10. Gain pattern of the circular loop antenna.  
 (example 4, see page 38)

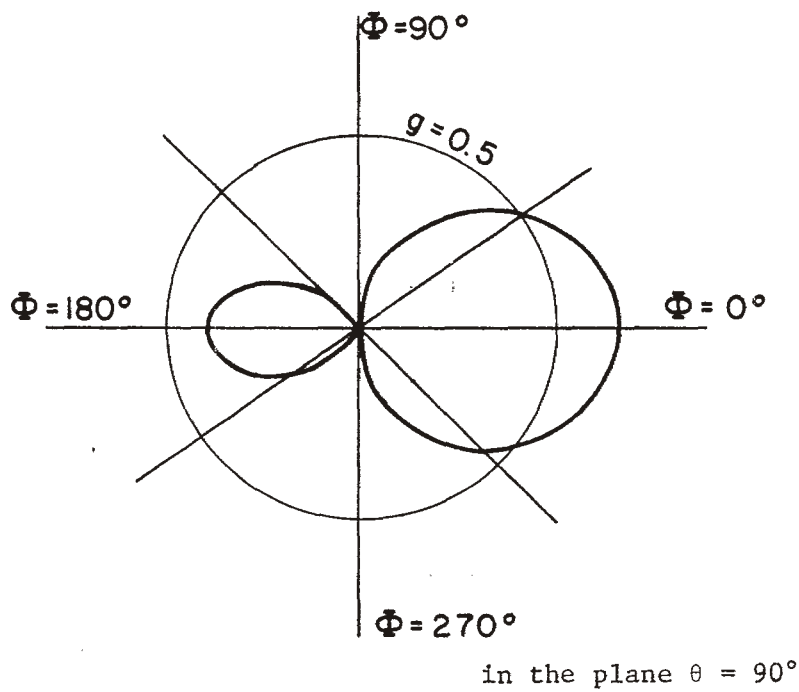
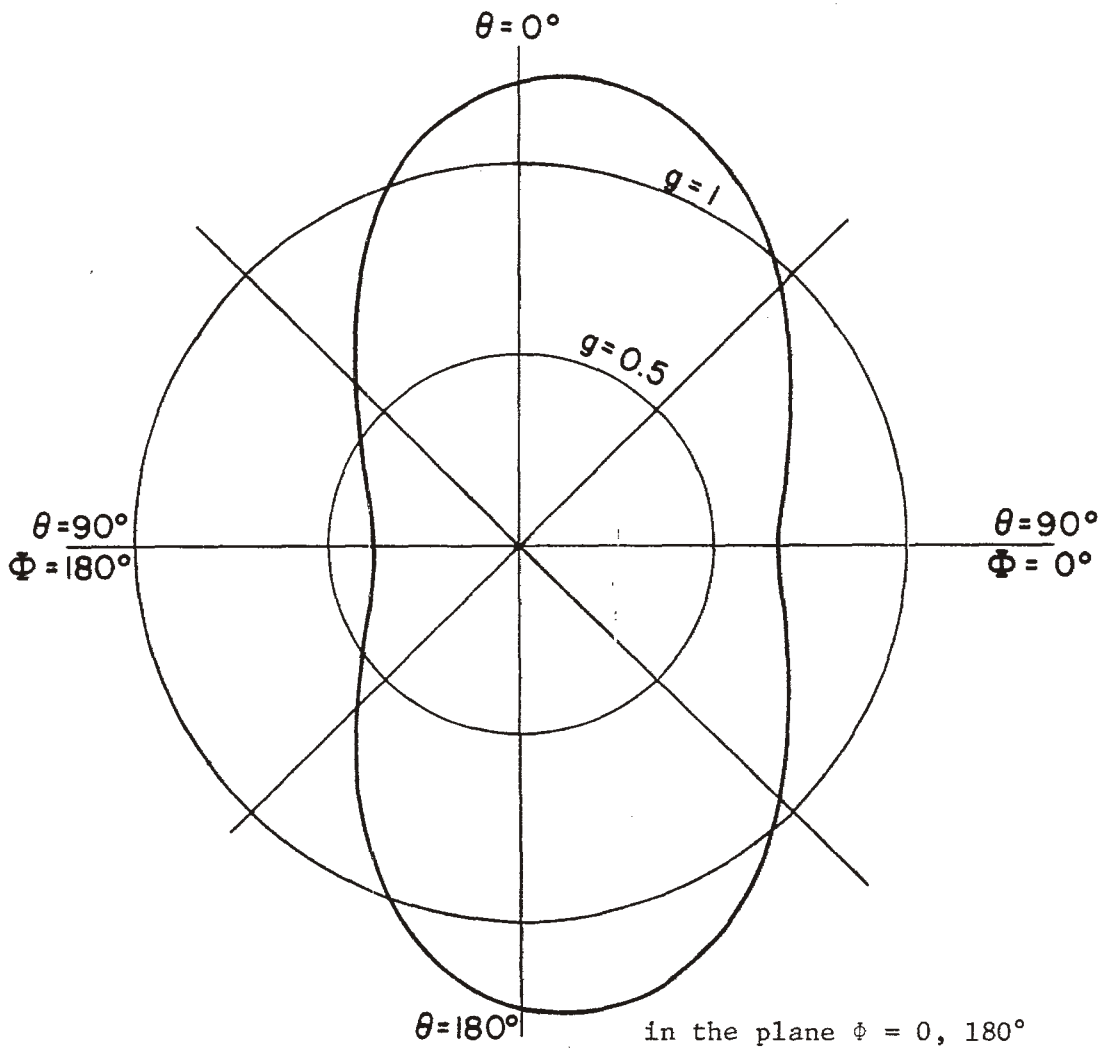


Fig. 4-11. Gain pattern of the loaded circular loop antenna. (example 5, see page 39).

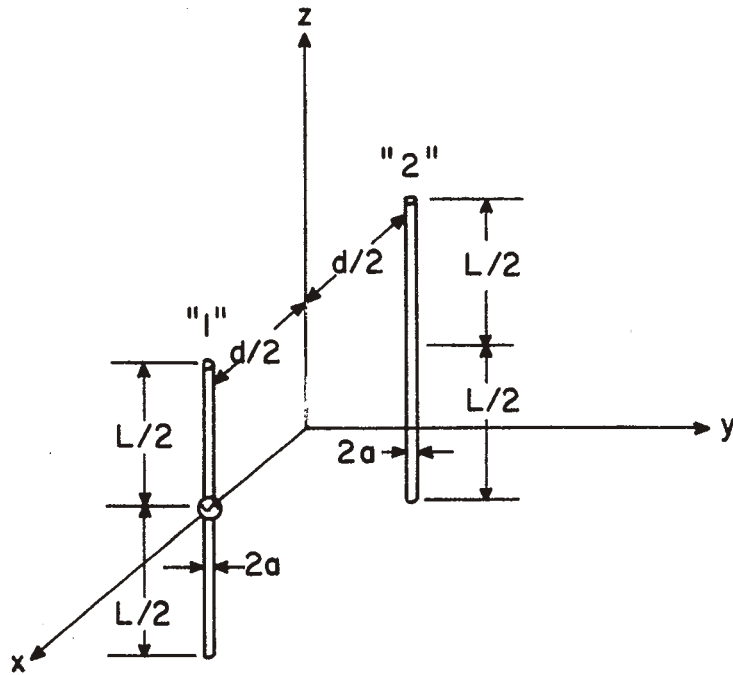


Fig. 4-12. A centered wire with a parasitic element.

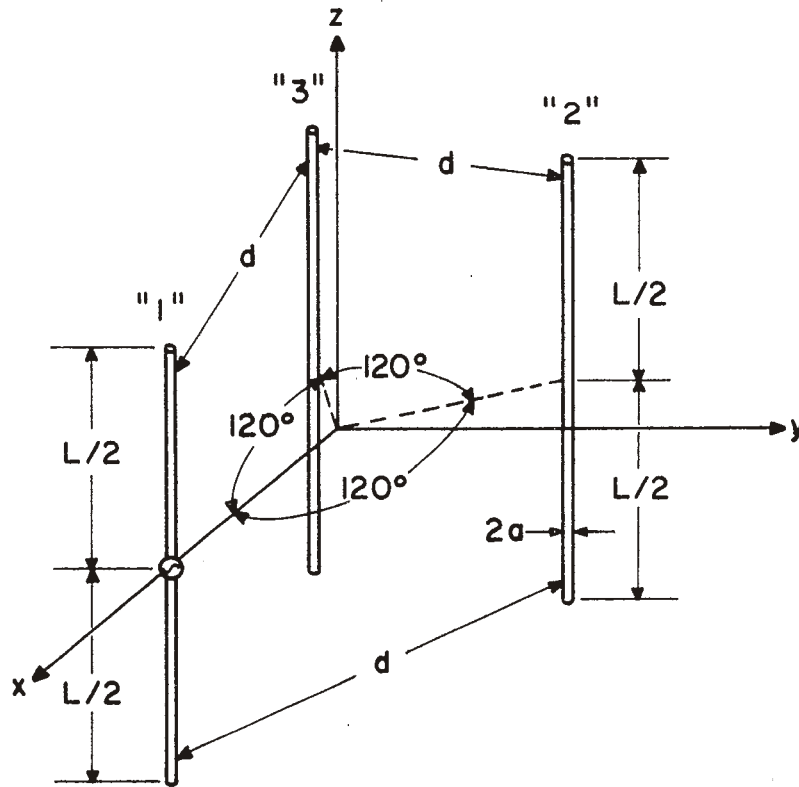


Fig. 4-13. A centered wire with two parasitic elements.

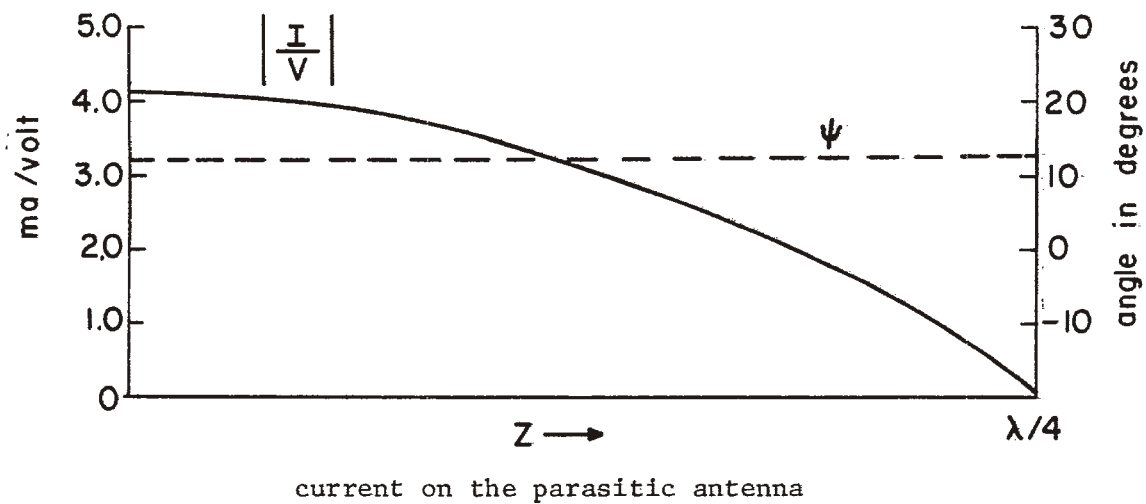
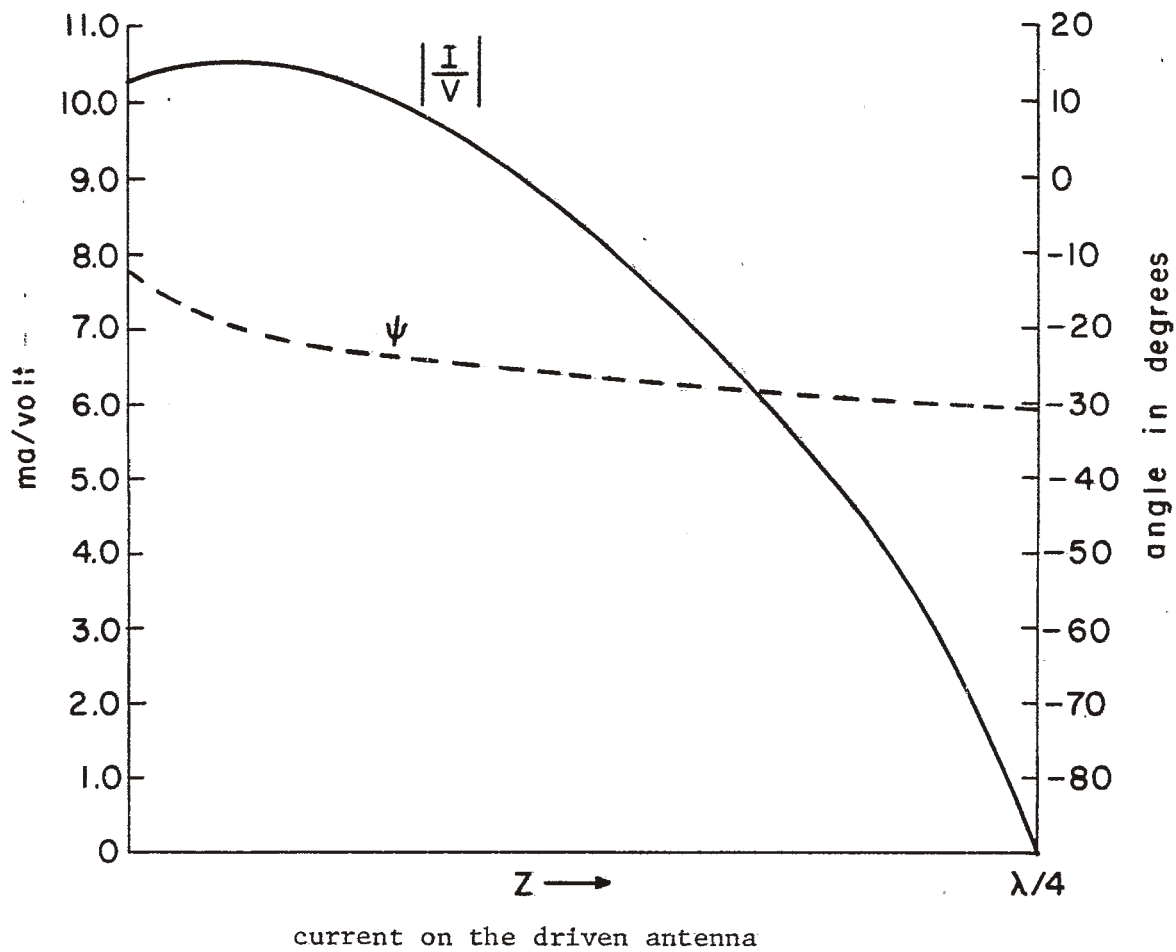


Fig. 4-14. Current on the parasitic array of two elements.  
(example 6, see page 39).

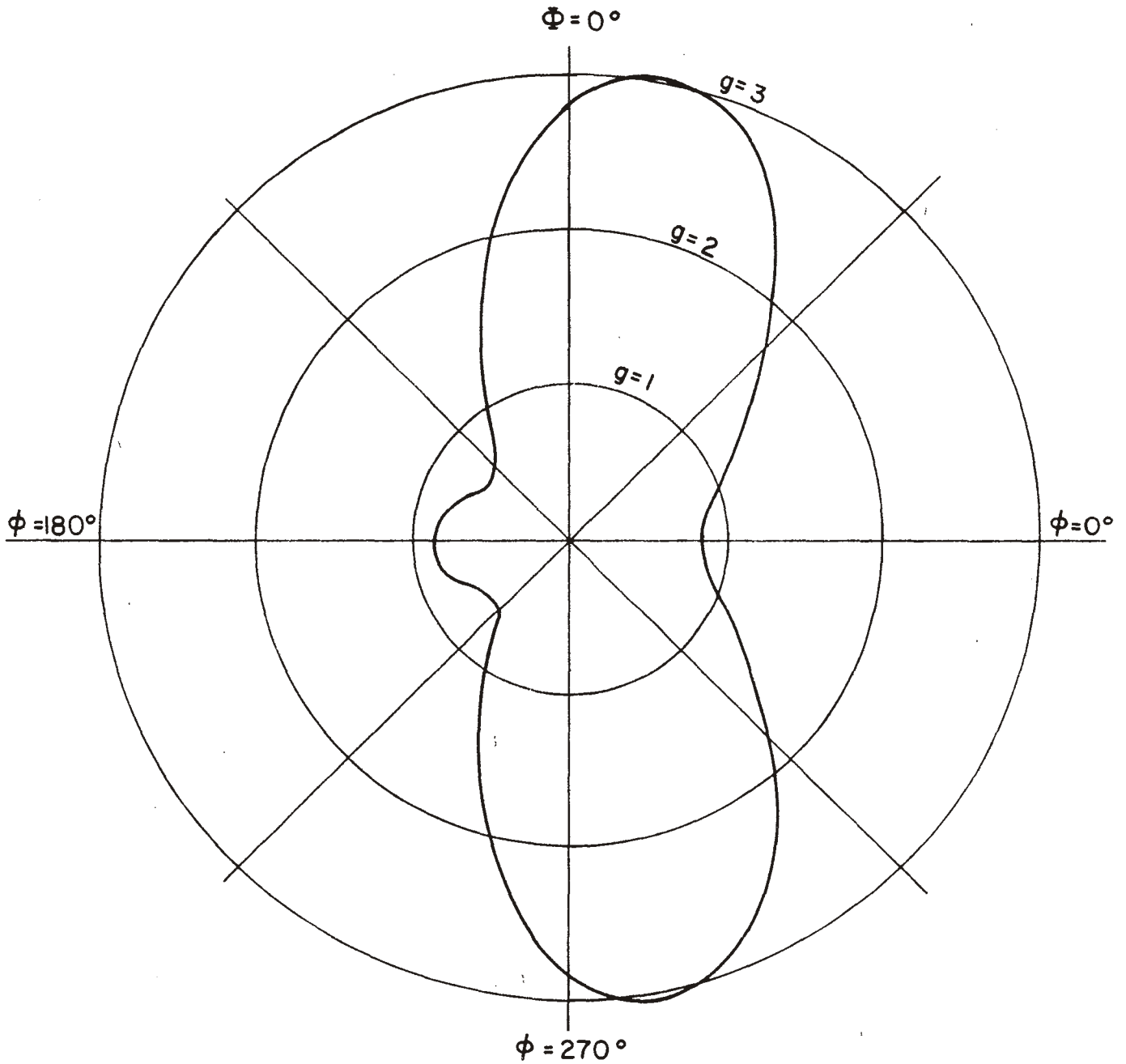


Fig. 4-15. Gain pattern of the parasitic array of two elements in the plane  $\theta = 90^\circ$ . (example 6, see page 39).

Power gain for the plane  $\theta = 90^\circ$  is plotted in Fig. 4-15. These results compare with the experimental values measured by Mack [9] and show excellent agreement.

Next consider a parasitic array with three elements as shown in Fig. 4-13, where  $L = 0.75\lambda$ ,  $a = 0.00702\lambda$ , and  $d = 0.5\lambda$ . Wire "1" is centered with a unit voltage. Wires "2" and "3" are parasitic wire elements. The wavelength is given as 1 meter. The analysis is carried out using 20 segments on each antenna. Current is assumed to be positive for the +z direction. In the computer program the points on the axes of the wires can be determined as follows:

```

          DWAVE = 0.5 * WAVE/SQRT(3.)
          HH = 0.375 * WAVE
          NPNW = NP(NW)
          DO 1510 I = 1, NPNW
            X(1,NW,I) = DWAVE * COS ((NW-1) * PI * 2./3.)
            X(2,NW,I) = DWAVE * SIN ((NW-1) * PI * 2./3.)
1510      X(3,NW,I) = 2*HH/NS(NW) * (I-1) - HH

```

Excitation is represented by a lumped unit voltage source at the peak of the fifth triangle function on the first wire. Numerical results for current are plotted in Fig. 4-16. The radiation pattern in the plane  $\theta = 90^\circ$  is plotted in Fig. 4-17. Once again, the agreement of this solution with the experimental values measured by Mack [9] is excellent.

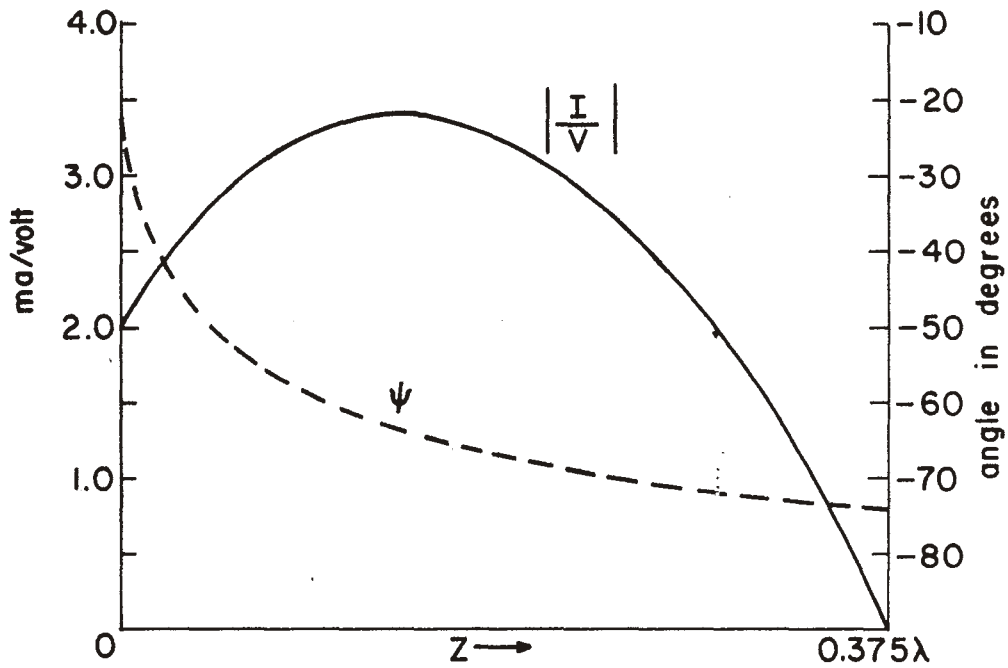
The next example (example 8) considers a folded dipole antenna. The wire configuration and coordinate system are shown in Fig. 4-18, where  $H = 0.5\lambda$ ,  $d = 0.01\lambda$ , and  $a = 0.001\lambda$ . The wavelength is given as one meter. This problem is treated as an open wire with two segments overlapping at the ends of the wire as shown in Fig. 4-19. The analysis is carried out using 46 segments for the open wire. Points on the axis of the wire are specified for this example by a read statement in DO LOOP 550

```

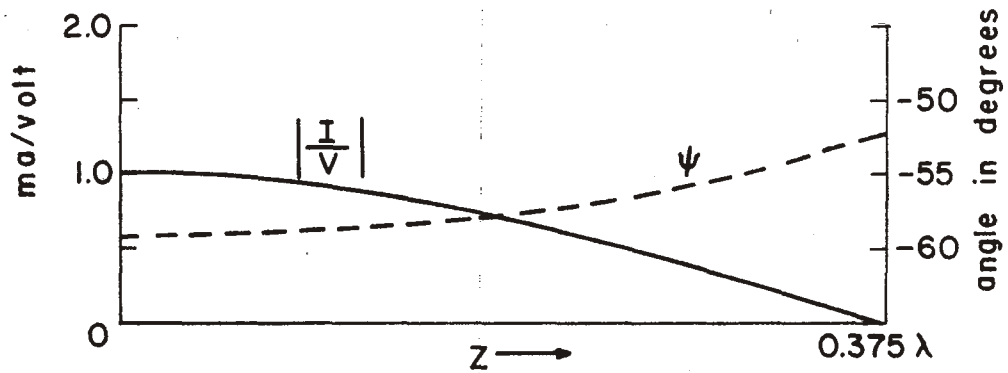
          NPNW = NP(NW)
          READ (1,2) (X(J,NW,I), J=1,3), I=1, NPNW)

```





current on the driven antenna



current on the parasitic antenna

Fig. 4-16. Current on the parasitic array of three elements. (example 7, see page 46).

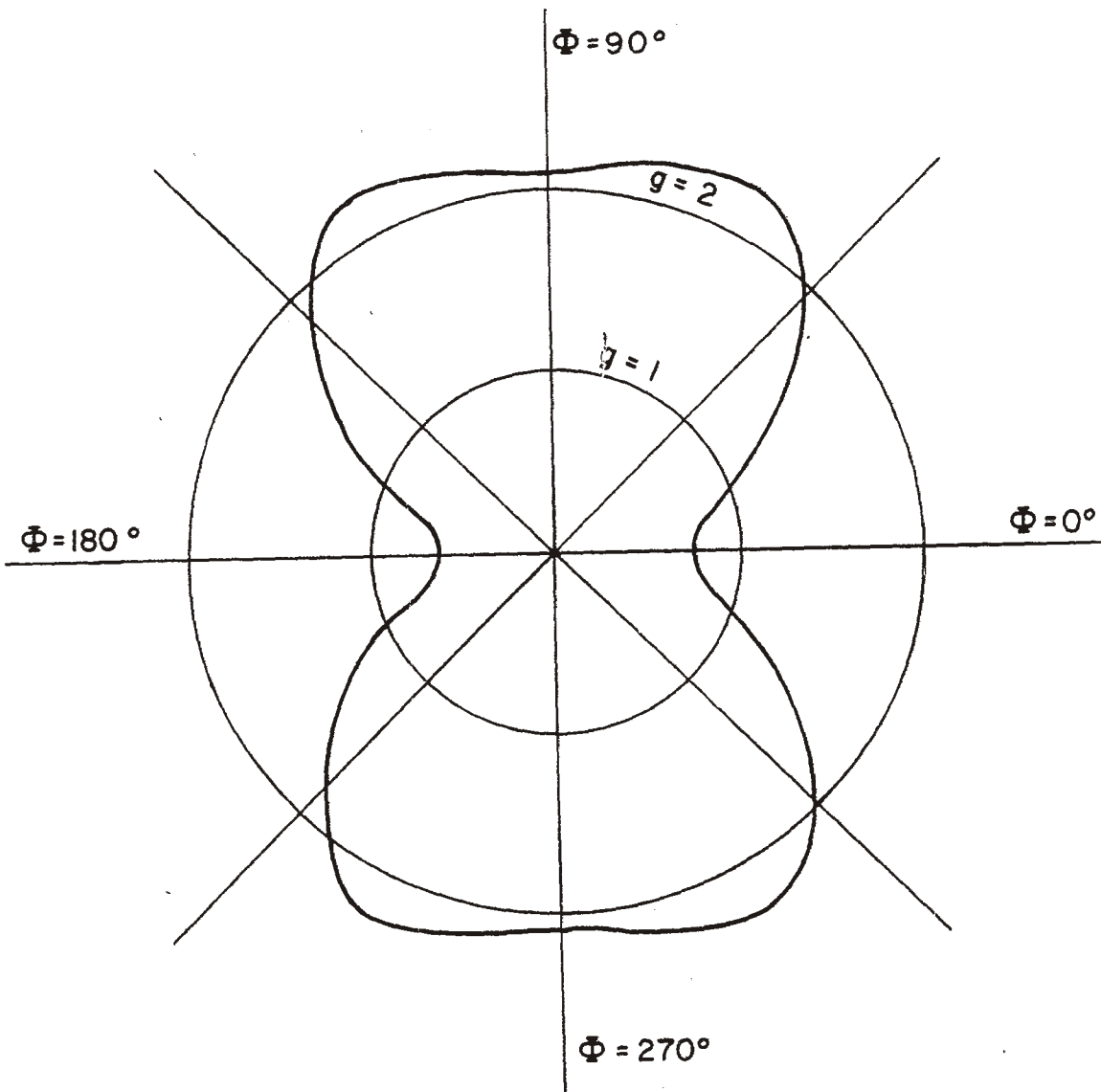


Fig. 4-17. Gain pattern of the parasitic array of three elements in the plane  $\theta = 90^\circ$ . (example 7, see page 46)

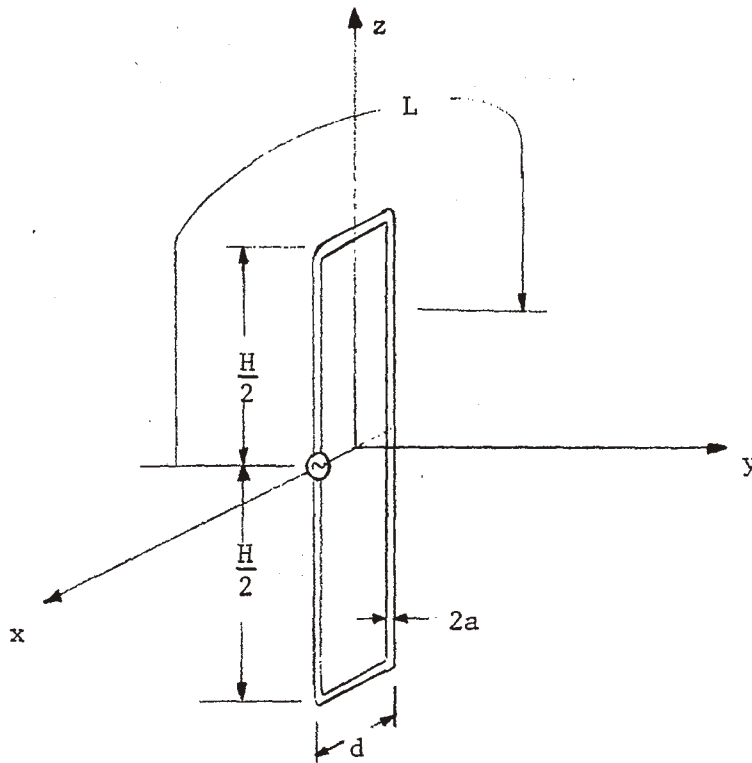


Fig. 4-18. The folded dipole antenna.

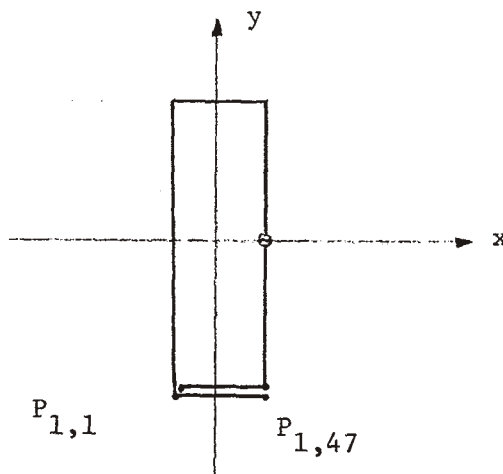


Fig. 4-19. The folded dipole antenna.

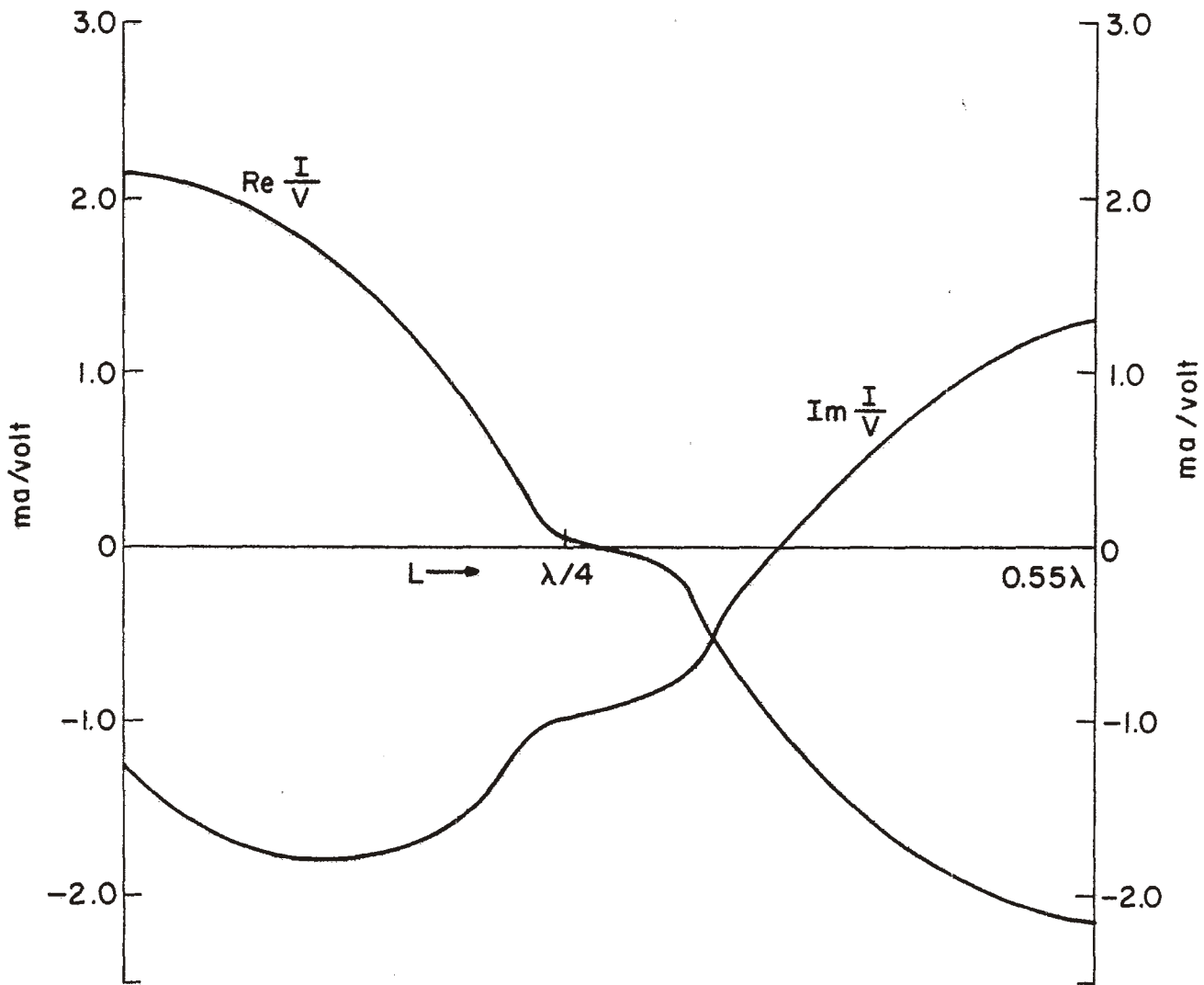


Fig. 4-20. Current distribution on the folded dipole antenna.  
 (example 8, see page 46)

Forty-seven data cards correspond to this read statement. This number, of course, points out the advantage of using a generating function whenever possible. Current for the folded dipole is plotted in Fig. 4-20.

#### 4-3. Scattering Problems

Now, consider a full-wave, center-loaded ( $Z_\ell = 75$  ohms), straight wire that is irradiated by a plane wave of unit amplitude with angle of incidence  $\theta_i = 90^\circ$ ,  $\phi_i = 0^\circ$ . (Hence, THEI = 90.0 and PHII = 0.0 in the program.) The polarization of the wave is the  $\bar{u}_\theta$  direction, so that  $E(1) = (-1.0, 0.0)$  and  $E(2) = (0.0, 0.0)$ . Note, here phase is with respect to the coordinate origin. The wire configuration and coordinate system are shown in Fig. 4-1 where  $L = \lambda$  and  $a = 0.00674\lambda$ . The wavelength is given as 1 meter. The analysis is carried out using twenty segments. Points on the axis are determined in the computer program in the same manner as in the first example discussed earlier. Current is assumed to be positive for the +z direction. Numerical results for current are plotted in Fig. 4-21 and the bistatic radar cross-section pattern is shown in Fig. 4-22. These results can be compared with those of Strait and Hirasawa [4].

The next example considers a circular loop that is loaded with a resonant load and irradiated by a plane incident wave of unit amplitude with angle of incidence  $\phi_i = 0$ ,  $\theta_i = 90^\circ$ . The polarization of the wave is the  $\bar{u}_\phi$  direction so that  $E(1) = (0.0, 0.0)$  and  $E(2) = (1.0, 0.0)$  in the program. The wavelength is given as one meter. The wire configuration and coordinate system are shown in Fig. 4-6 where  $a = 0.00159\lambda$ ,  $2\pi b = x$  and the load is located at  $\phi' = 0$ . A resonant load is defined as one for which  $Y_L$  has a susceptance equal to the negative of the input susceptance of the loop. In this problem the resonant load is  $Z_L = j 232.558$  ohms. The loop is treated as an open wire overlapping two segments at the ends of the wire (Fig. 4-7). The points on the axis of the wire can be specified as discussed in example 4. Positive current reference is in the direction of increasing  $\phi$ . The analysis is carried out using 34 segments for the open

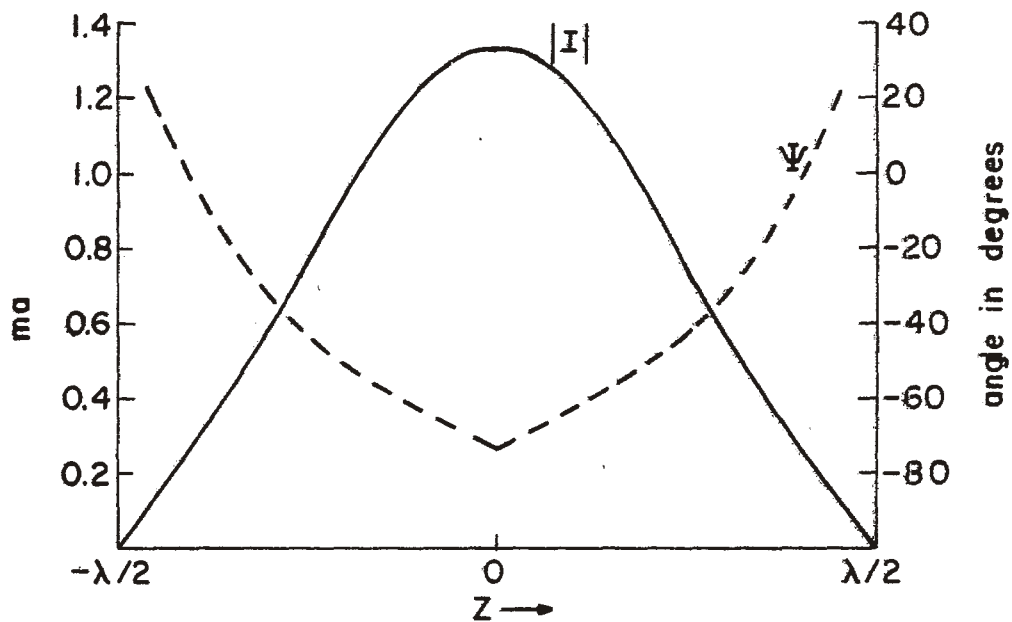


Fig. 4-21. Current on a one-wavelength, center-loaded, linear scatterer. (example 9, see page 51)

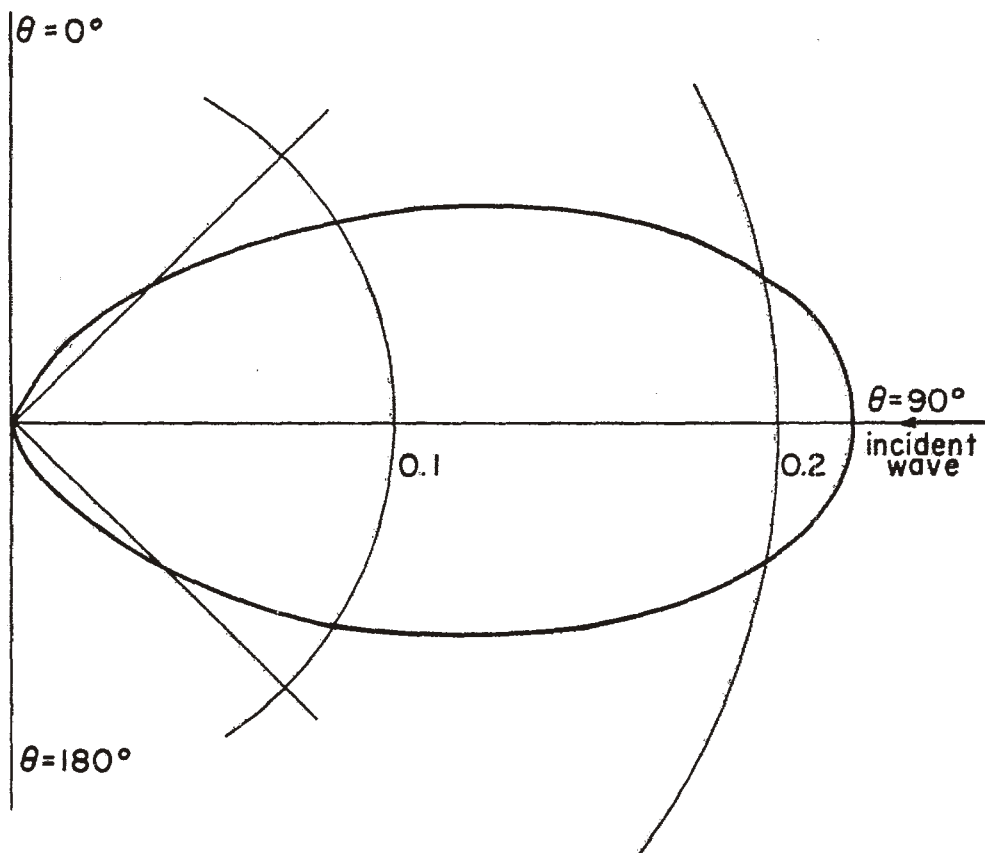


Fig. 4-22. Bistatic radar cross-section  $\sigma/\lambda^2$  pattern for the full-wave, center-loaded, linear scatterer. (example 9, see page 51)

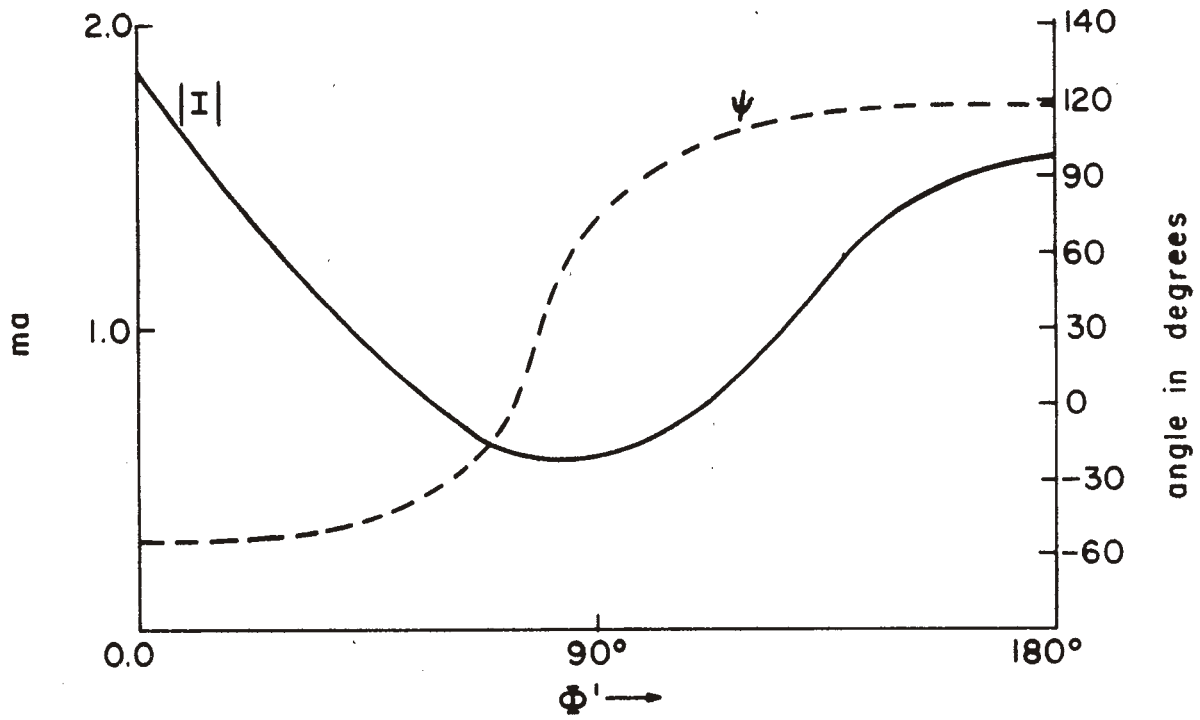


Fig. 4-23. Current on a loaded circular loop scatterer.  
(example 10, see page 51)

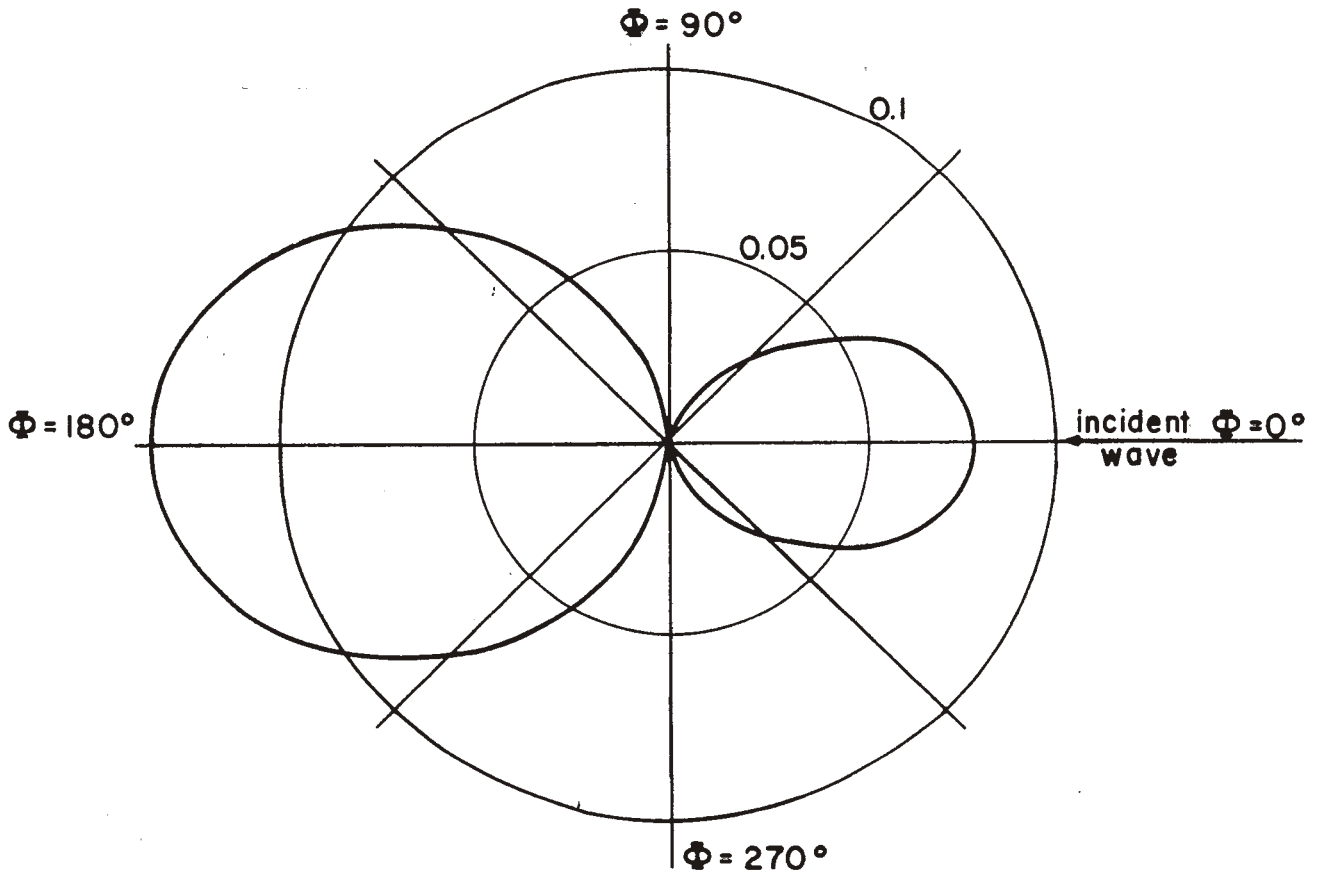


Fig. 4-24. Bistatic radar cross-section  $\sigma_{\phi\phi}/\lambda^2$  pattern in the plane  $\theta = 90^\circ$  of a loaded circular loop scatterer.  
(example 10, see page 51) 55

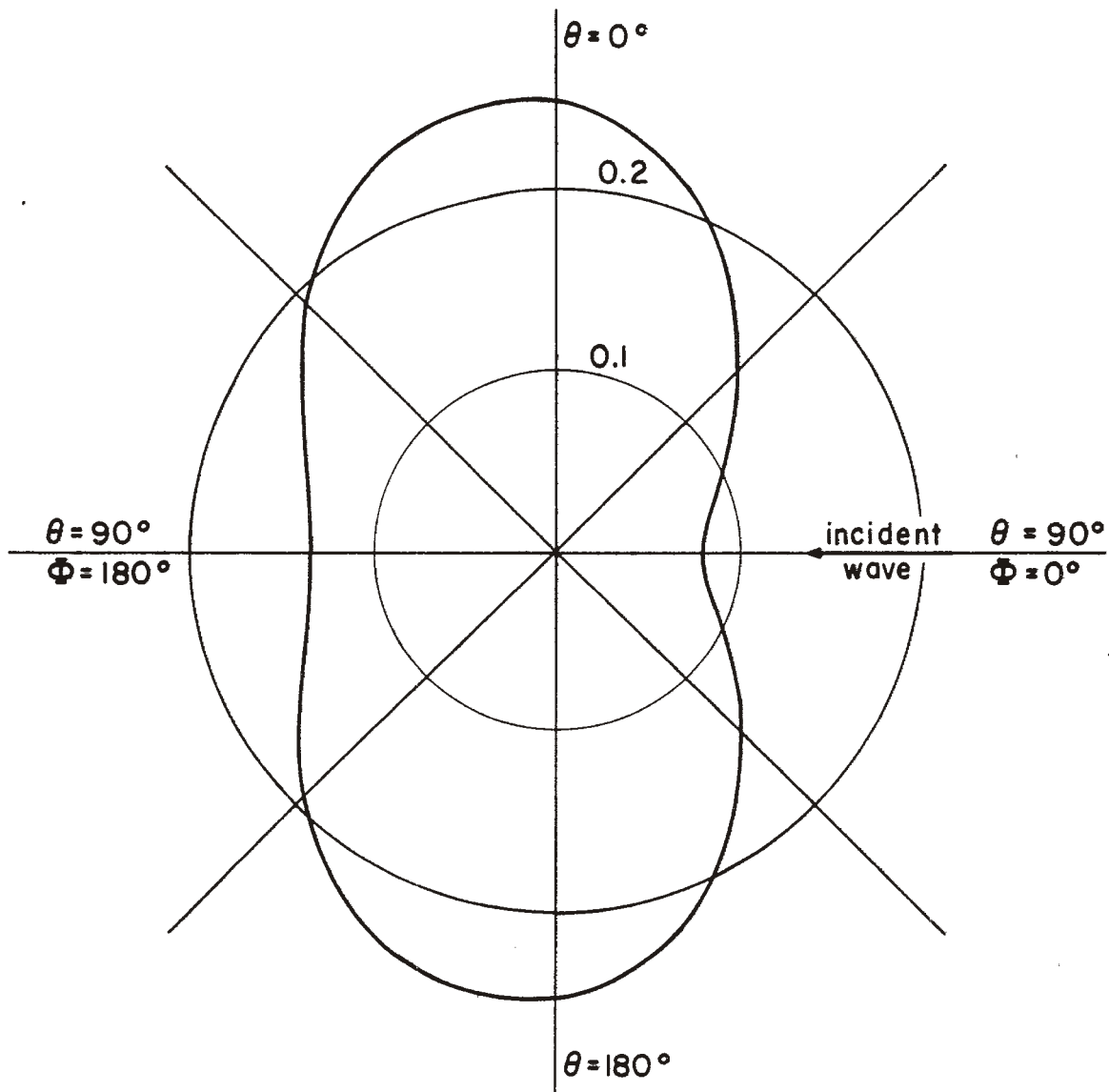


Fig. 4-25. Bistatic radar cross-section  $\sigma_{\phi\phi}/\lambda^2$  pattern in the plane  $\phi = 0^\circ, 180^\circ$  of a loaded circular loop scatterer. (example 10, see page 51)



wire. Current distribution is plotted in Fig. 4-23. Bistatic radar cross section  $\sigma_{\phi\phi}/\lambda^2$  pattern\* in the plane  $\theta = 90^\circ$  is plotted in Fig. 4-24 and  $\sigma_{\phi\phi}/\lambda^2$  pattern in the plane  $\phi = 0, 180^\circ$  is plotted in Fig. 4-25. The results can be compared with those of Harrington and Mautz [11].

The eleventh example considers a wire cross that is irradiated by a plane wave of unit amplitude with angle of incidence  $\theta_i = 90^\circ$ ,  $\phi_i = 90^\circ$ . The polarization of the wave is the  $\bar{u}_\theta$  direction. The configuration and coordinate system are shown in Fig. 4-26 where  $L_1 = L_3 = L_4 = 0.11\lambda$ ,  $L_2 = 0.22\lambda$ ,  $a = 0.00222\lambda$ . The wavelength is given as one meter. This problem is treated

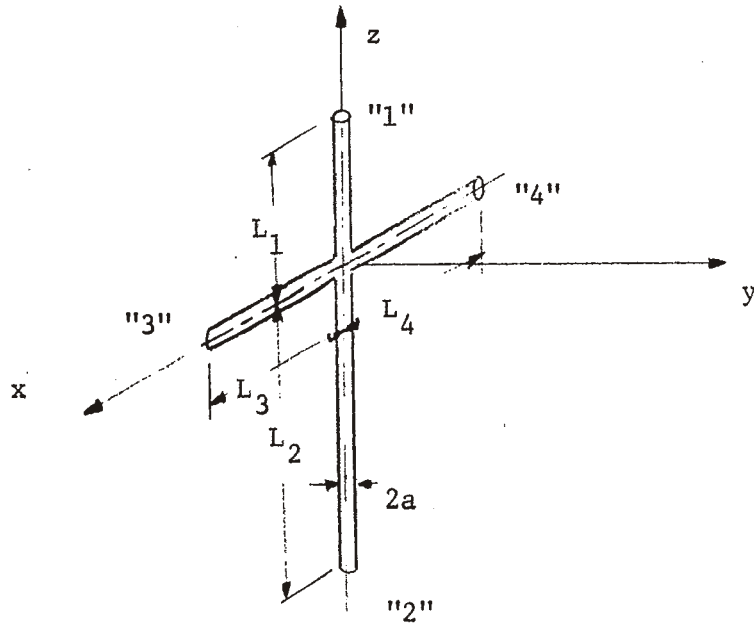


Fig. 4-26. Wire cross scatterer.

\*The bistatic radar cross-sections are denoted by  $\sigma_{\phi\phi}/\lambda^2$ ,  $\sigma_{\theta\phi}/\lambda^2$ ,  $\sigma_{\phi\theta}/\lambda^2$ , and  $\sigma_{\theta\theta}/\lambda^2$ . Here, the first subscript denotes the polarization of the scattered field and the second subscript denotes the polarization of the incident wave. For example, in this problem  $\sigma_{\phi\phi} = \lim_{r \rightarrow \infty} (4\pi r^2 \left| \frac{E_\theta^s}{E_\phi^i} \right|^2)$  and  $\sigma_{\theta\phi} = \lim_{r \rightarrow \infty} (4\pi r^2 \left| \frac{E_\theta^s}{E_\phi^i} \right|^2)$ .

as a problem with four open wires as in Fig. 4-27. The analysis is carried out using 14 segments for wires "1", "3", 12 segments for wire "4" and 28 for wire "2", where all segments are of equal length. The computer program for this problem is presented in Appendix B. DO LOOP 1512 and DO LOOP 1517 in the main program are used to generate the coordinates of the points on the axes of the wires. Current references in the computer program are shown in Fig. 4-27. Current distributions are plotted in Fig. 4-29. The current reference in Fig. 4-29 is different from that used in the program. Current is positive in the  $-x$  direction for the horizontal wire and the  $+z$  direction for the vertical wire. As expected the current on the horizontal wire has odd symmetry. Bistatic radar cross-section  $\sigma_{\theta\theta}/\lambda^2$  pattern in the plane  $\phi = 90^\circ, 270^\circ$  is plotted in Fig. 4-30 and  $\sigma_{\phi\theta}/\lambda^2$  pattern in the plane  $\theta = 90^\circ$ , is plotted in Fig. 4-31.  $\sigma_{\phi\theta}/\lambda^2$  in the plane  $\phi = 90^\circ, 270^\circ$  and  $\sigma_{\theta\theta}/\lambda^2$  in the plane  $\theta = 90^\circ$  is circular.

The twelfth example is the same as example 11 except the horizontal wire crosses the vertical wire at its center ( $L_1 = L_2 = 0.165\lambda$  in Fig. 4-26.) This problem is solved in the same manner as the previous example. Current distributions on the wires are plotted in Fig. 4-32. As expected there is no current on the horizontal wire.

The last example (example 13) again involves the wire cross except the horizontal wire is located at the top of the vertical wires, i.e.,  $L_1 = 0$  and  $L_2 = 0.33\lambda$  in Fig. 4-26. This problem is treated as one with three open wires as shown in Fig. 4-28. The analysis is carried out using the same segment length as in the above two examples. Points on the axes of these wires can be specified in the program as follows

```

AENOS = 0.22*WAVE/24.
NPNW = NP(NW)
DO 1518 I=1,NPNW
IF (NW.LE.1) X(1,NW,I) = 0
IF (NW.EQ.2) X(1,NW,I) = 0.11*WAVE-AENOS*(I-1)
IF (NW.EQ.3) X(1,NW,I) = -X(1,3,I)
X(2,NW,I) = 0
IF (NW.GE.2) X(3,NW,I) = 0
IF (NW.EQ.1) X(3,NW,I) = AENOS*(I-1) - 0.33*WAVE
1518 CONTINUE

```

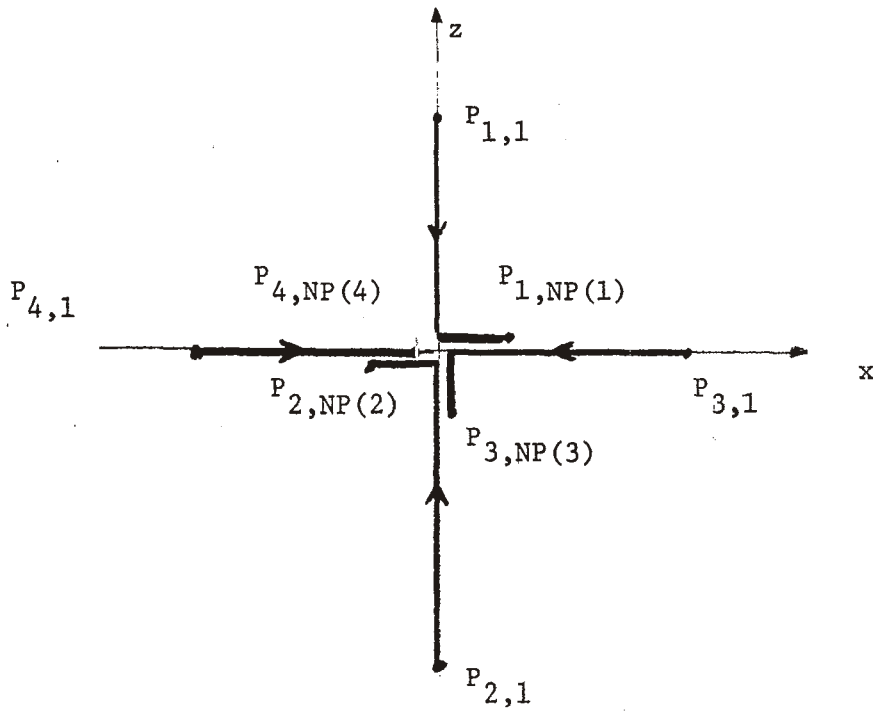


Fig. 4-27. Wire cross of examples eleven and twelve.

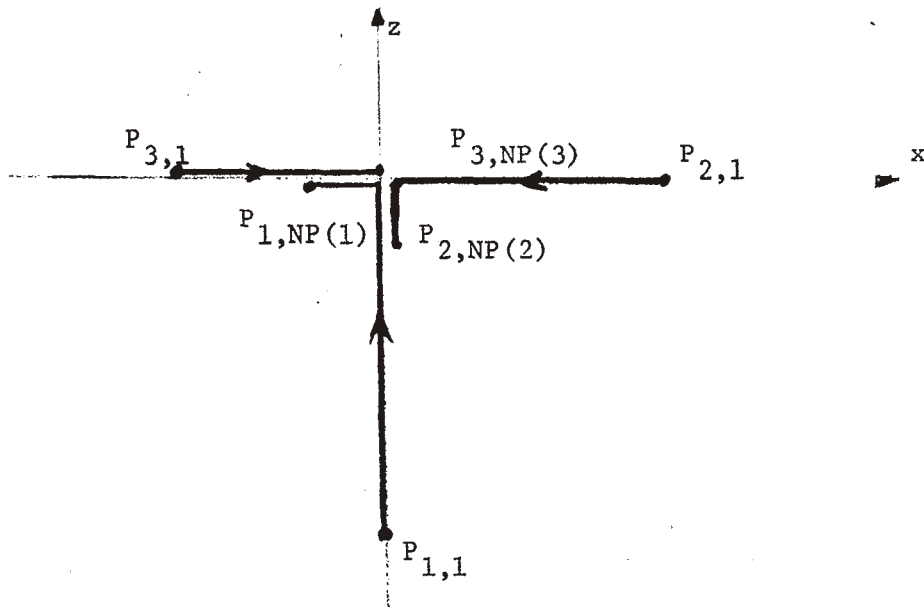


Fig. 4-28. Wire cross of example thirteen.

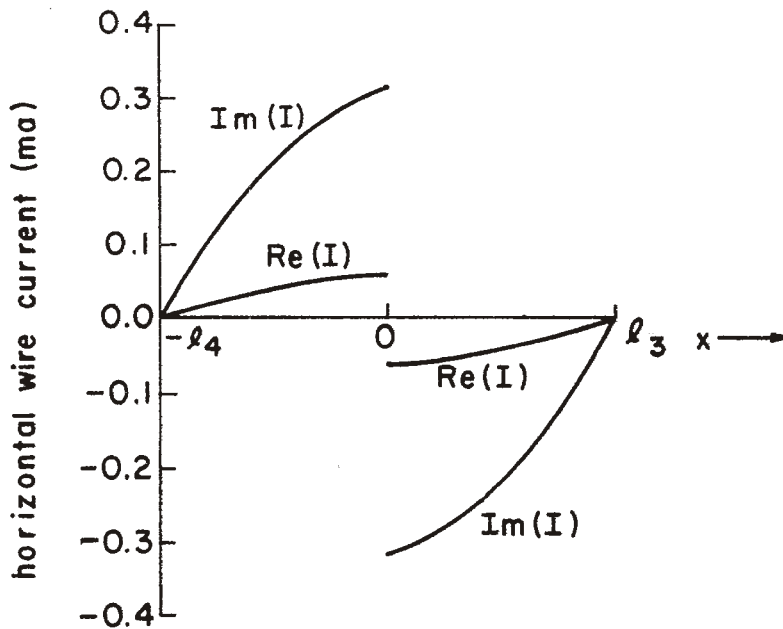
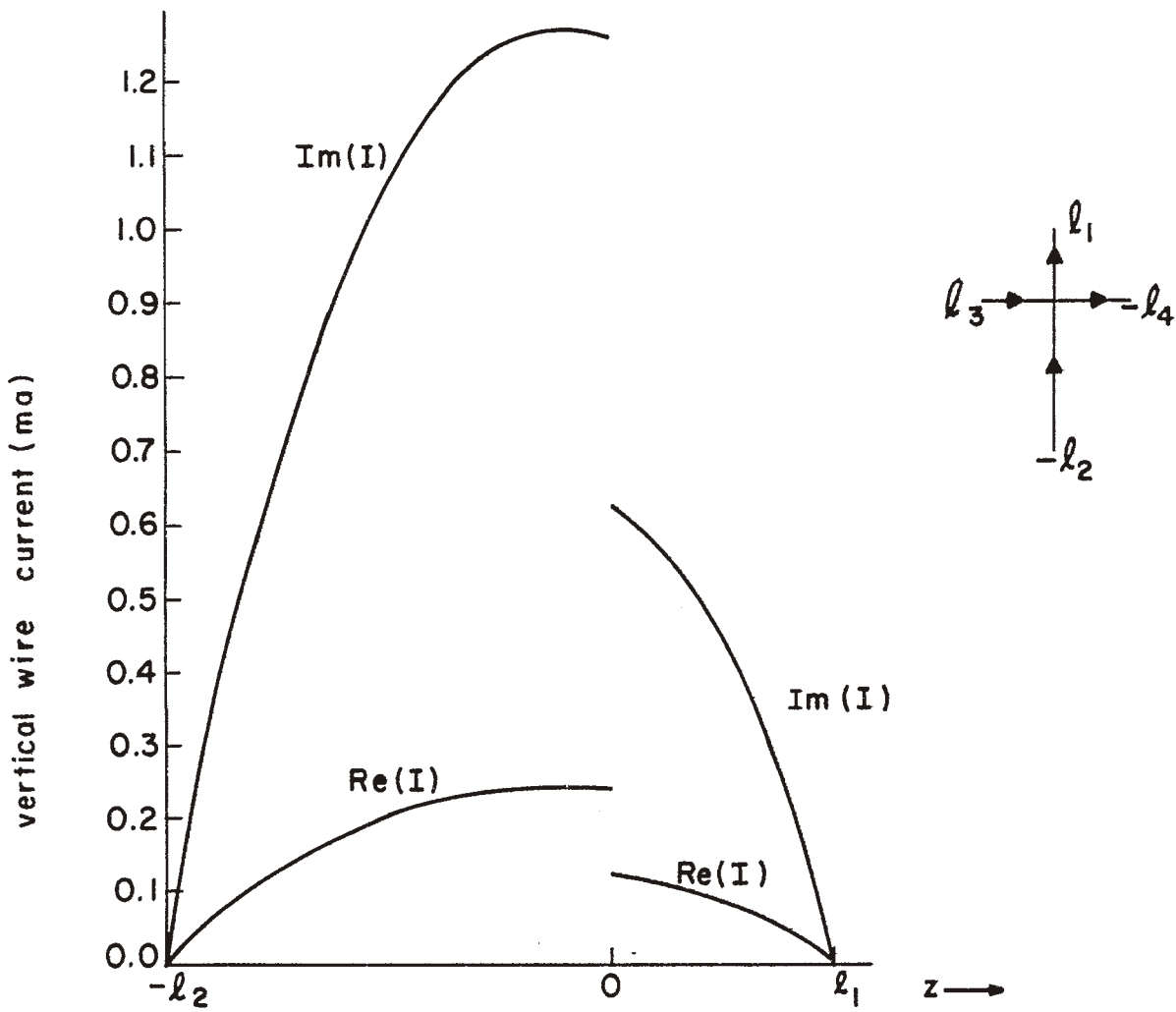


Fig. 4-29. Current on the wire cross scatterer. (example 11, see page 55)

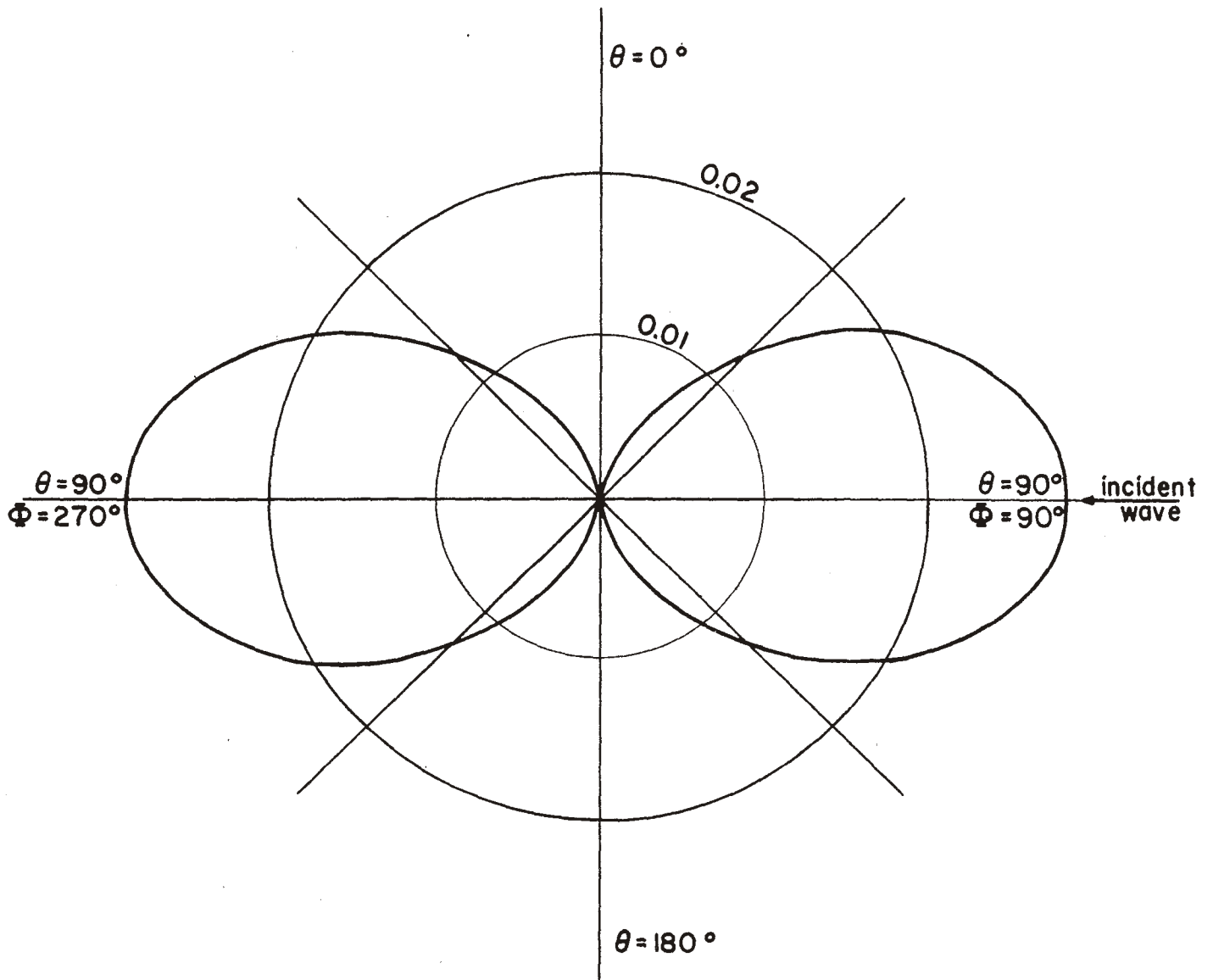


Fig. 4-30. Bistatic radar cross-section  $\sigma_{\theta\theta}/\lambda^2$  pattern in the plane  $\phi = 90^\circ, 270^\circ$  for the wire cross. (example 11, see page 55)

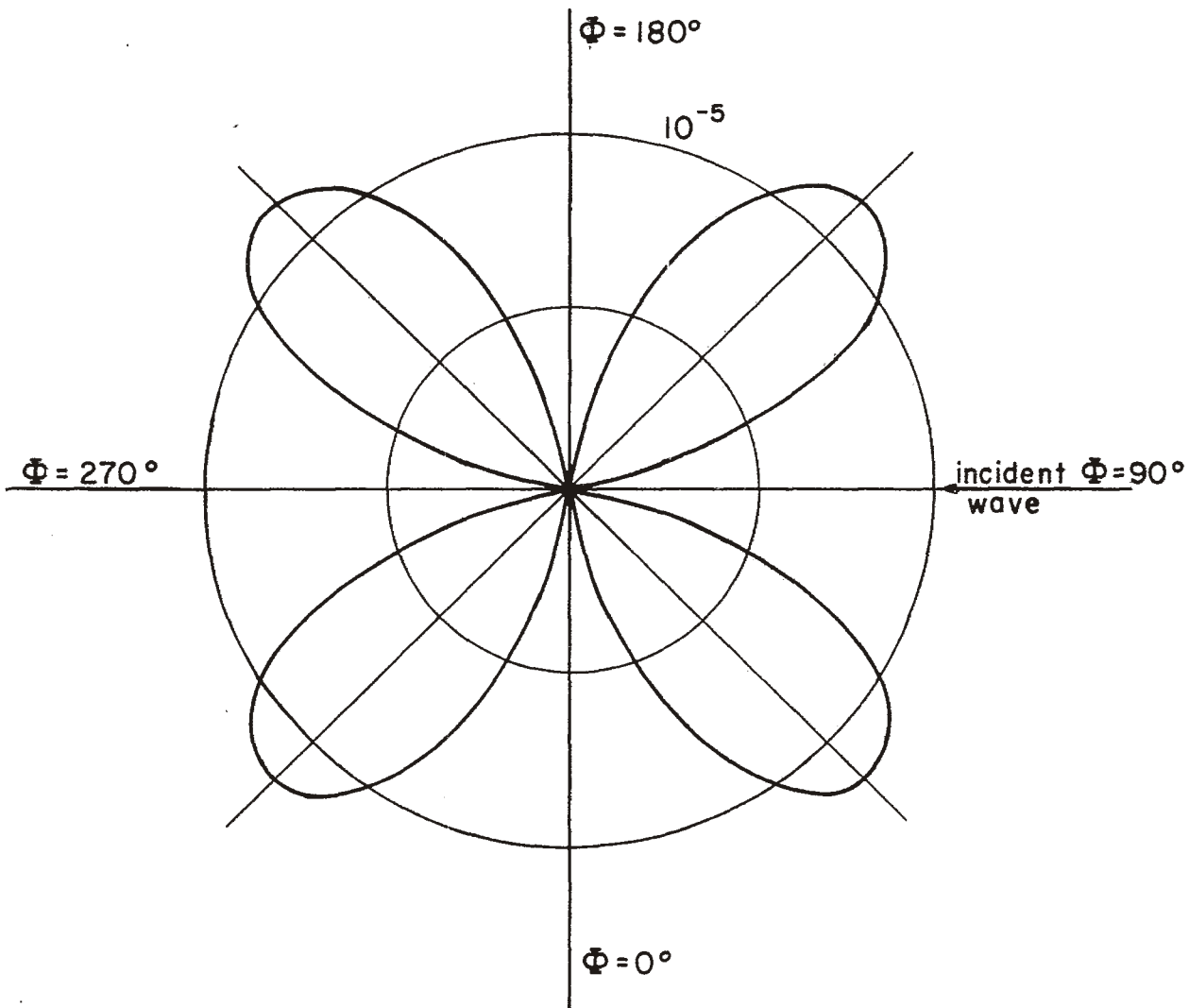


Fig. 4-31. Bistatic radar cross-section  $\sigma_{\phi\theta}/\lambda^2$  pattern in the plane  $\theta = 90^\circ$  for the wire cross. (example 11, see page 55)

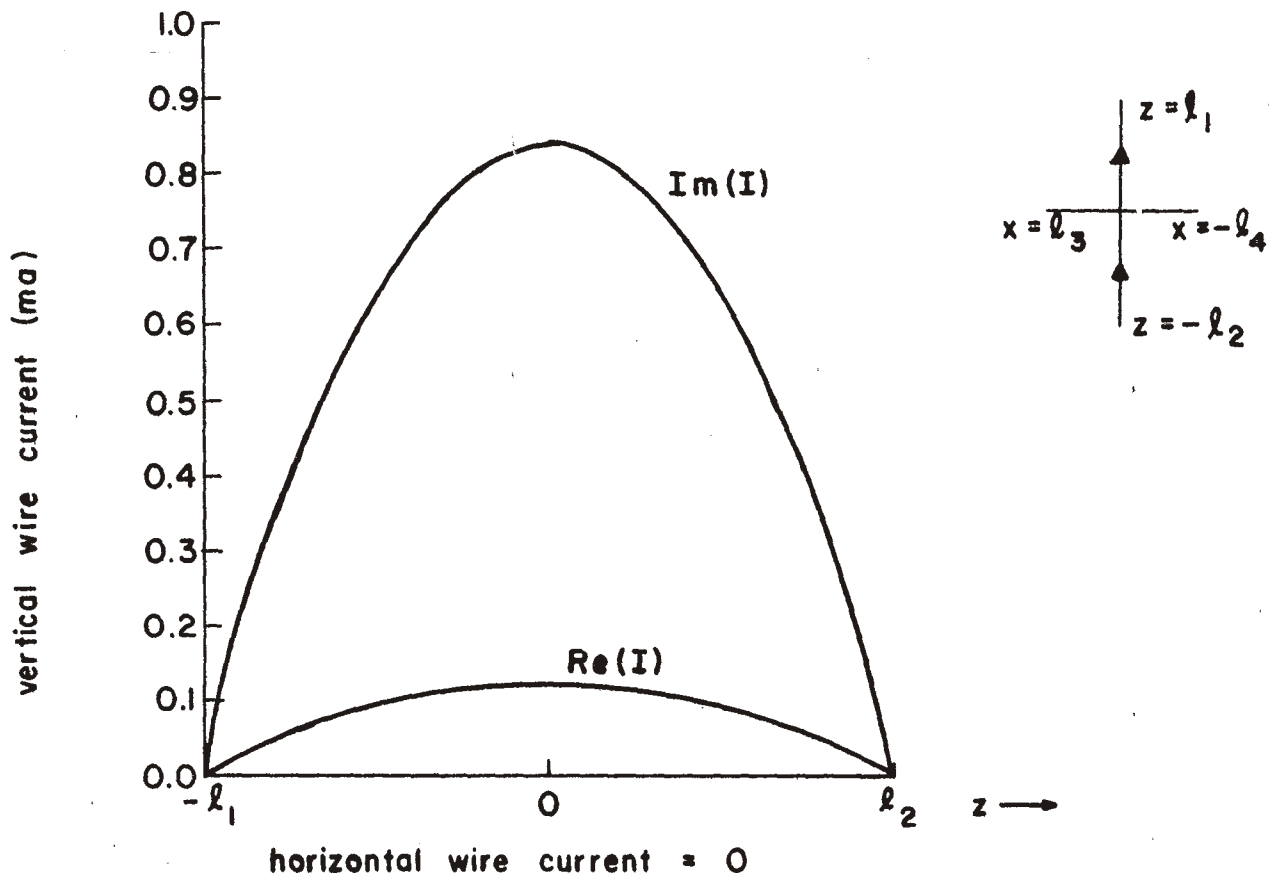


Fig. 4-32. Current on the wire cross scatterer. (example 12, see page 56)

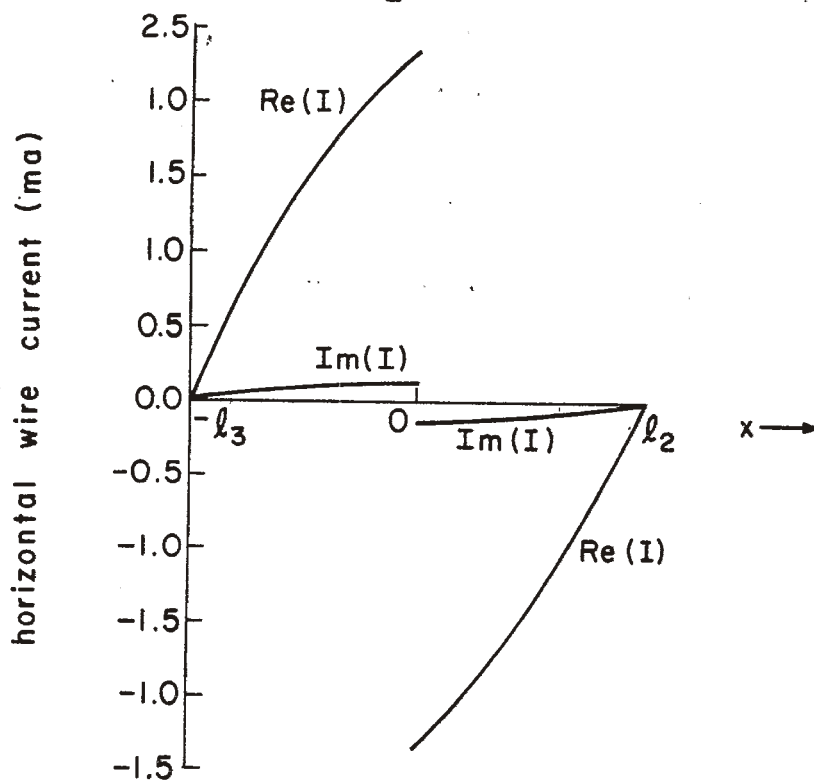
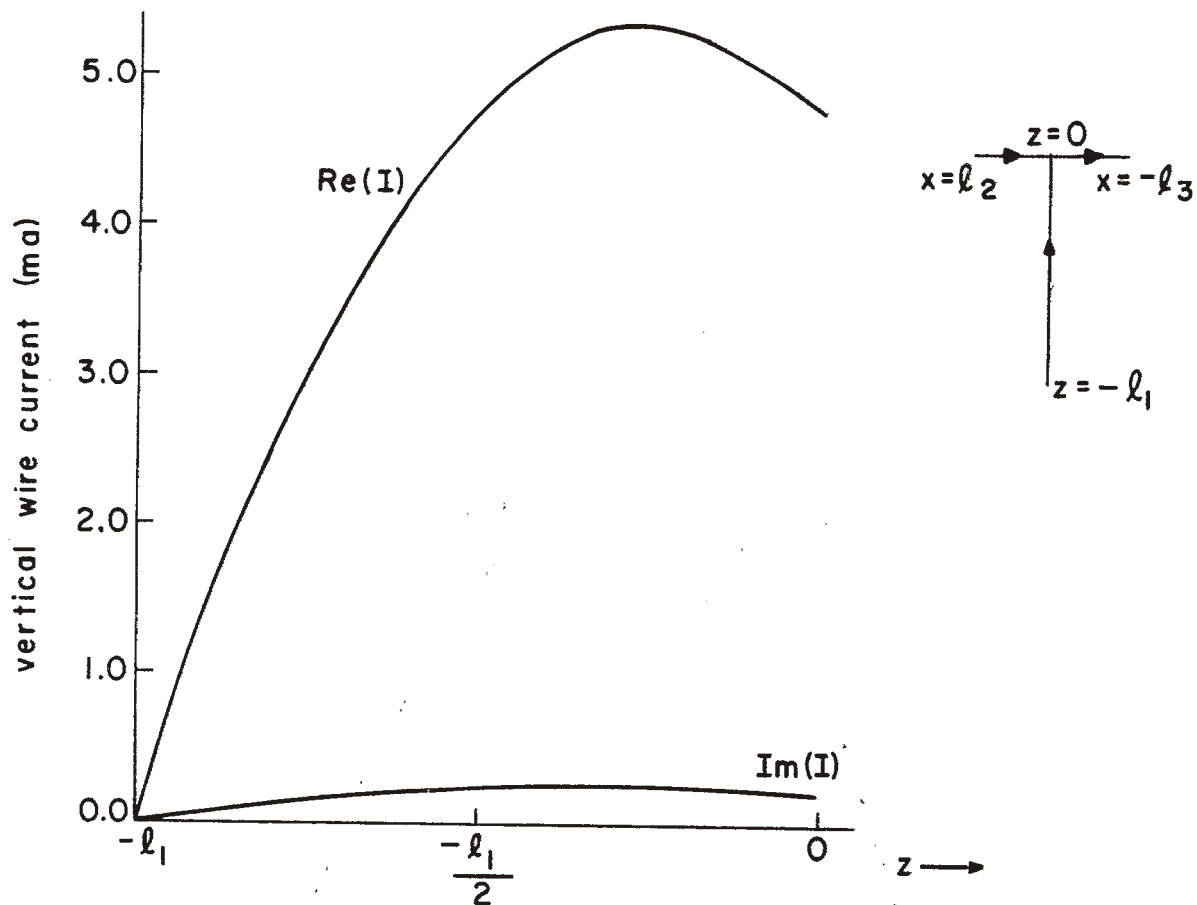


Fig. 4-33. Current on the wire cross scatterer. (example 13, see page 56)



```
DO 1519 J = 1,3
X(J,1,38) = X(J,3,12)
X(J,1,39) = X(J,3,11)
X(J,2,14) = X(J,1,36)
1519 X(J,2,15) = X(J,1,35)
```

Current reference in the program is as shown in Fig. 4-28. Current distributions are plotted in Fig. 4-33. The current reference in Fig. 4-33 is positive in the  $-x$  direction for the horizontal wire and in the  $+z$  direction for the vertical wire.

Scattering by a wire cross was also treated by Taylor and McAdams [12]. Their solution correctly regards both KCL (Kirchhoff's current law) and the continuity of potential condition at the wire junction as is true with the method presented here. However, they comment that these currents appear continuous from left to right and from top to bottom across the junction which is a condition not required by KCL. The results reported here show that these currents are indeed not continuous in this manner across the wire junction.

#### 4-4. Conclusion

In this chapter several examples were presented to illustrate certain applications of the programs described in Chapter 3 and presented in the Appendices. Numerical results compared favorably with experimental data and/or results computed by other investigators.

CONCLUSION

In this report computer programs were presented and described for handling analysis problems involving radiation and scattering by arbitrary configurations of straight and bent wires. The wires can be fed or loaded continuously or discretely at any point or points along their length, and the problem geometry can involve wire junctions.

The method of analysis used was originally presented by Harrington [1,2]. A piecewise linear approximation to the current was used in a Galerkin solution that provides rapid convergence for most problems of engineering interest. Results were obtained for several typical configurations and were compared with those of other investigators.

The treatment of wire junctions presented here has special significance. Only very limited results were heretofore available for radiation and scattering by configurations of this type, and these were somewhat misleading as discussed in this report with regard to the wire cross problem. The programs presented here are equipped to handle wire junctions in such a way that all appropriate boundary conditions are satisfied without requiring any additional or incorrect constraints.

Hence, the real significance of the programs presented in this report is that a wide variety of problems and wire configurations can be treated. And, although the programs as shown in the Appendices are limited to a total of four different wires, this limitation can be removed easily by simply changing appropriate dimension statements.

## REFERENCES

1. R. F. Harrington, "Matrix Methods for Field Problems," Proc. IEEE, Vol. 55, No. 2, pp. 136-149; February 1967.
2. R. F. Harrington, "Field Computation by Moment Methods," The Macmillan Company, New York; 1968.
3. R. F. Harrington and J. R. Mautz, "Straight Wires with Arbitrary Excitation and Loading," IEEE Trans. on Antennas and Propagation, Vol. AP-15, No. 4, pp. 502-515; July 1967.
4. B. J. Strait and K. Hirasawa, "Computer Programs for Radiation, Reception, and Scattering by Loaded Straight Wires," Scientific Report No. 3 on Contract No. F19628-68-C-0180, AFCRL-69-0440; Syracuse University, Syracuse, New York; October 1, 1969.
5. B. J. Strait and K. Hirasawa, "Array Design for a Specified Pattern by Matrix Methods," IEEE Transactions on Antennas and Propagation, Vol. AP-17, No. 2; March 1969.
6. B. J. Strait and K. Hirasawa, "Application of Matrix Methods to Array Antenna Problems," Scientific Report No. 2 on Contract No. F19628-68-C-0180, AFCRL-69-0158; Syracuse University, Syracuse, New York; April 1969.
7. J. A. Cummins, "Analysis of a Circular Array of Antennas by Matrix Methods," Ph.D. Dissertation, Syracuse University, Syracuse, New York; February 1969.
8. L. V. Kantorovich and V. I. Krylov, "Approximate Methods of Higher Analysis," 4th ed., translated by C. D. Benster, John Wiley and Sons, Inc., New York, 1959.
9. R. B. Mack, "A Study of Circular Arrays," Technical Reports No. 383, Cruft Laboratory, Harvard University, Cambridge, Mass.; May 1963.
10. Keigo Iizuka, "The Circular Loop Antenna Multiloaded with Positive and Negative Resistors," IEEE Transactions on Antennas and Propagation, Vol. AP-13, No. 1, pp. 7-20; January 1965.
11. R. F. Harrington and J. Mautz, "Electromagnetic Behavior of Circular Wire Loops with Arbitrary Excitation and Loading," Proc. IEE, Vol. 115, No. 1, pp. 68-77; January 1968.
12. C. D. Taylor, S. M. Lin, and H. V. McAdams, "Scattering from Crossed Wires," IEEE Transactions on Antennas and Propagation, Vol. AP-18, No. 1, pp. 133-136; January 1970.

13. B. J. Strait and K. Hirasawa, "Computer Programs for Analysis and Design of Linear Arrays of Loaded Wire Antennas," Scientific Report No. 5 on Contract No. F19628-68-C-0180, AFCRL-70-0108, Syracuse University, Syracuse, New York; February 1970.
14. R. H. Kyle, "Mutual Coupling Between Log-Periodic Antennas," IEEE Transactions on Antennas and Propagation, vol. AP-18, No. 1, pp. 15-22; January 1970.

## APPENDIX A

This program is suitable for radiation problems for thin wires with excitations represented by lumped voltage sources at the peaks of the triangle functions and loading represented by lumped loads, also at the peaks of the triangle functions. The maximum number of wires that can be handled here is four. The maximum number of expansion functions for any wire is fifteen. Subroutines are listed first. The sample input and output data listed here correspond to the analysis of example one. This program is described in Sec. 3-2.

```

SUBROUTINE CALZ( WAVE,NWIRE,A,NE,NN)
C THIS SUBROUTINE IS USED TO CALCULATE THE GENERALIZED IMPEDANCE
C MATRIX Z
COMPLEX Z( 60, 60), Z4(4,15,4,15),PSI(4,32,4)
1;RT, CFXP, CI, CMPLX, HOLD1, HOLD2
DIMENSION A(NWIRE),NE(NWIRE),NN(NWIRE),XX(3,4,32),
1XD(3,4,32), TLEN(4,32), R(4,32,4),RX(3,4,32,4),
2Z7(4,32,4), XDD(4,32,4),ALP(4),C(4),D(4),P(4),Q(4)
COMMON /COA/ XX,XD,TLEN /COB/ Z
CI=(0.0,1.0)
PI=3.14159265
BETA=2.0*PI/WAVE
EPSLN = 8.854E-12
OMEG = 2.0*PI*2.997928E8/WAVE
XMU=4.0E-7*PI
DO 10 NWS=1,NWIRE
NENWS=NE(NWS)
DO 10 NES=1,NENWS
IF(NES.EQ.1) GO TO 11
DO 17 NWF=1,NWIRE
NNNWF=NN(NWF)
DO 17 NSF=1,NNNWF
XDD(NWF,NSF,1) = XDD(NWF,NSF,3)
XDD(NWF,NSF,2) = XDD(NWF,NSF,4)
PSI(NWF,NSF,1) = PSI(NWF,NSF,3)
17 PSI(NWF,NSF,2) = PSI(NWF,NSF,4)
KK = 3
GO TO 18
11 KK=1
18 CONTINUE
DO 60 K =KK,4
NESK=2*NES-2+K
DO 60 NWF=1,NWIRE
NNNWF=NN(NWF)
DO 60 NSF=1,NNNWF

```

```

R(NWF,NSF,K) = 0.
DO 15 J=1,3
RX(J,NWF,NSF,K) = XX(J,NWF,NSF) - XX(J,NWS,NEK)
15 R(NWF,NSF,K) = R(NWF,NSF,K) + RX(J,NWF,NSF,K)**2
R(NWF,NSF,K) = SORT(R(NWF,NSF,K))
ALP(K) = TLEN(NWS,NEK)/2.
Z7(NWF,NSF,K) = 0.
DO 33 J=1,3
33 ZZ(NWF,NSF,K) = ZZ(NWF,NSF,K)+RX(J,NWF,NSF,K)*XD(J,NWS,NEK)/
1(2.*ALP(K))
Z7(NWF,NSF,K) = ABS(ZZ(NWF,NSF,K))
XED(NWF,NSF,K)=0.
DO 65 J=1,3
65 XDD(NWF,NSF,K) = XDD(NWF,NSF,K)+XD(J,NWS,NEK)*XD(J,NWF,NSF)
AL = SORT(ABS(R(NWF,NSF,K)**2-ZZ(NWF,NSF,K)**2))
AL=SORT(AL**2+A(NWF)**2)
IF (R(NWF,NSF,K).GE.10.*ALP(K)) GO TO 31
R(NWF,NSF,K) = SORT(R(NWF,NSF,K)**2+A(NWF)**2)
RI = COS(-BETA*R(NWF,NSF,K)) + CI*SIN(-BETA*R(NWF,NSF,K))
ZA = Z7(NWF,NSF,K) + ALP(K)
ZAM = Z7(NWF,NSF,K)-ALP(K)
SZA=SORT(AL**2+ZA**2)
SZAM=SORT(AL**2+ZAM**2)
IF (ZZ(NWF,NSF,K).GT.ALP(K)) GO TO 41
AI1=ALOG((ZA+SZA)*(-ZAM+SZAM)/AL**2)
GO TO 42
41 AI1=ALOG((ZA+SZA)/(ZAM+SZAM))
42 AI2=2.*ALP(K)
AI3=(7A*SZA-ZAM*SZAM+AL**2*AI1)/2
AI4=AI2*AL**2+(2.*ALP(K)**3+6.*ALP(K)*Z7(NWF,NSF,K)**2)/3.
PSI1=AI1-BETA**2/2.*(AI3-2.*R(NWF,NSF,K)*AI2+R(NWF,NSF,K)**2*AI1)
PSI2=-BETA*(AI2-R(NWF,NSF,K)*AI1)+BETA**3/6.*(AI4-3.*R(NWF,NSF,K)
1*AI3+3.*R(NWF,NSF,K)**2*AI2-R(NWF,NSF,K)**3*AI1)
PSI(NWF,NSF,K) = RT/(8*PI*ALP(K))*CMPLX(PSI1,PSI2)
GO TO 59
31 XKI=BETA*ALP(K)
RI = COS(-BETA*R(NWF,NSF,K)) + CI*SIN(-BETA*R(NWF,NSF,K))
ZR=Z7(NWF,NSF,K)/R(NWF,NSF,K)
DR=ALP(K)/R(NWF,NSF,K)
ZR2=ZR**2
ZR4=ZR2**2
DR2=DR**2
H=(-1.0+3.0*ZR2)/6.0
H1=(3.0-30.0*ZR2+35.0*ZR4)/40.0
A0=1.0+H*DR2+H1*DR2**2
A1=H*DR+H1*DR2*DR
A2=-ZR2/6.0-DR2/40.0*(1.0-12.0*ZR2+15.0*ZR4)

```

```

A3=DR/60.0*(3.0*ZR2-5.0*ZR4)
A4=ZR4/120.0
PSI1=A0+XKD**2*A2+XKD**4*A4
PSI2=XKD*A1+XKD**3*A3
PSI(NWF,NSF,K) = RT/(4*PI*R(NWF,NSF,K))*CMPLX(PSI1,PSI2)
59 CONTINUE
60 CONTINUE
ARCA=TLEN(NWS,2*NES-1)
ARCB=TLEN(NWS,2*NES)
ARCC=TLEN(NWS,2*NES+1)
ARCD=TLEN(NWS,2*NES+2)
C(1) = 1/2.*ARCA/(ARCA+ARCB)
C(2) = (ARCA+1/2.*ARCB)/(ARCA+ARCB)
C(3) = (1/2.*ARCC+ARCD)/(ARCC+ARCD)
C(4) =1/2.*ARCD/(ARCC+ARCD)
D(1) = 1./(ARCA+ARCB)
D(2) =D(1)
D(3) =-1./(ARCC+ARCD)
D(4) =D(3)
DO 10 NWF=1,NWIRE
NENWF=NE(NWF)
DO 10 NEF=1,NENWF
ARCA=TLEN(NWF,2*NEF-1)
ARCB=TLEN(NWF,2*NEF)
ARCC=TLEN(NWF,2*NEF+1)
ARCD=TLEN(NWF,2*NEF+2)
P(1) = 1/2.*ARCA/(ARCA+ARCB)
P(2) = (ARCA+1/2.*ARCB)/(ARCA+ARCB)
P(3) = (1/2.*ARCC+ARCD)/(ARCC+ARCD)
P(4) =1/2.*ARCD/(ARCC+ARCD)
Q(1) = 1./(ARCA+ARCB)
Q(2) = Q(1)
Q(3) =-1./(ARCC+ARCD)
Q(4) =Q(3)
Z4(NWF,NEF,NWS,NES) = (0.,0.)
DO 70 I=1,4
DO 70 K=1,4
L=2*NEF-2+I
70 Z4(NWF,NEF,NWS,NES) = Z4(NWF,NEF,NWS,NES) + CI*OMEG*XMU*C(K)*P(I)*
1XDD(NWF,L,K)*PSI(NWF,L,K)+1./(CI*OMEG*EPSLN)*D(K)*Q(I)*PSI(NWF,L,
2K)*TLEN(NWS,2*NES-2+K)*TLEN(NWF,L)
10 CONTINUE
NOF = 0
DO 90 NWF =1,NWIRE
NENWF=NE(NWF)
DO 90 NEF=1,NENWF
NOF = NOF +1
NOS = 0
DO 90 NWS=1,NWIRE

```

```

NENWS=NE(NWS)
DO 90 NES=1,NENWS
NJS = NOS+1
90 Z(NOF,NOS) = Z4(NWF,NFF,NWS,NES)
RETURN
END

```

C  
C  
C  
C  
C  
C

```

SUBROUTINE CALZL(NL,NE,NWIRE)
THIS SUBROUTINE IS USED TO MODIFY THE GENERALIZED IMPEDANCE
MATRIX Z TO INCLUDE THE EFFECTS OF LOADING ON THE WIRES
COMPLEX Z(60,60),ZL(4,32)
DIMENSION LP(4,32),NL(NWIRE),NE(NWIRE)
COMMON /COB/ Z /COC/ZL,LP

```

```

JJ=0
DO 20 K=1,NWIRE
IF (K.EQ.1) GO TO 11
JJ=JJ+NE(K-1)
11 CONTINUE
NLK=NL(K)
DO 20 I=1,NLK
J=JJ+LP(K,I)
20 Z(J,J)=Z(J,J)+ZL(K,I)
RETURN
END

```

C  
C  
C  
C  
C  
C

```

SUBROUTINE LINEQ(N, L,M)
THE STANDARD GAUSS-JORDAN METHOD IS USED TO INVERT A COMPLEX
MATRIX IN THIS SUBROUTINE
N=ORDER OF THE MATRIX
A=THE INPUT AND OUTPUT MATRIX
L,M=WORKING VECTOR
COMPLEX A(60,60),BIGA,HOLD
DIMENSION L(N),M(N)
COMMON /COB/ A
DO 80 K=1,N
L(K)=K
M(K)=K
BIGA=A(K,K)
DO 20 J=K,N
DO 20 I=K,N

```



```

10 IF (CABS(BIGA)-CABS(A(I,J))) 15,19,19
15 BIGA=A(I,J)
   L(K)=I
   M(K)=J
19 CONTINUE
20 CONTINUE
   J=L(K)
   IF(J-K) 35,35,25
25 CONTINUE
   DO 30 I=1,N
   HOLD=-A(K,I)
   A(K,I)=A(J,I)
30 A(J,I)=HOLD
35 I=M(K)
   IF(I-K) 45,45,38
38 CONTINUE
   DO 40 J=1,N
   HOLD=-A(J,K)
   A(J,K)=A(J,I)
40 A(J,I)=HOLD
45 CONTINUE
   DO 55 I=1,N
   IF(I-K) 50,55,50
50 A(I,K)=A(I,K)/(-BIGA)
55 CONTINUE
   DO 65 I=1,N
   DO 65 J=1,N
   IF(I-K) 60,64,60
60 IF(J-K) 62,64,62
62 A(I,J)=A(I,K)*A(K,J)+A(I,J)
64 CONTINUE
65 CONTINUE
   DO 75 J=1,N
   IF(J-K) 70,75,70
70 A(K,J)=A(K,J)/BIGA
75 CONTINUE
   A(K,K)=1./BIGA
80 CONTINUE
   K=N
100 K=K-1
   IF(K) 150,150,105
105 I=L(K)
   IF(I-K) 120,120,108
108 CONTINUE
   DO 110 J=1,N
   HOLD=A(J,K)
   A(J,K)=-A(J,I)
110 A(J,I)=HOLD

```

```

120 J=M(K)
    IF(J-K) 100,100,125
125 CONTINUE
    DO 130 I=1,N
        HOLD=A(K,I)
        A(K,I)=-A(J,I)
130 A(J,I)=HOLD
    GO TO 100
150 RETURN
    END

```

```

SUBROUTINE CRNT(U, C,NS)

```

THIS SUBROUTINE IS USED TO PERFORM THE PRODUCTION OF A MATRIX AND A VECTOR

U = THE INPUT VECTOR

Y = THE INPUT MATRIX

C = THE RESULT VECTOR

NS = ORDER OF MATRIX

```

COMPLEX U(NS),Y(60,60),C(NS)

```

```

COMMON /COR/ Y

```

```

DO 5 I=1,NS

```

```

C(I)=(0.,0.)

```

```

DO 5 L=1,NS

```

```

5 C(I)=C(I)+Y(I,L)*U(L)

```

```

RETURN

```

```

END

```

```

SUBROUTINE BIGV (U,NF,NWIRE,NE,NEP)

```

THIS SUBROUTINE IS USED TO CALCULATE THE GENERALIZED VOLTAGE MATRIX V

```

COMPLEX V(4,32) ,U(NEP)

```

```

DIMENSION IF(4,32) ,NF(NWIRE),NE(NWIRE)

```

```

COMMON /COD/V,IF

```

```

DO 5 I=1,NEP

```

```

5 U(I) = (0.,0. )

```

```

JJ=0

```

```

DO 10 K=1,NWIRE

```

```

IF (K.EQ.1) GO TO 11

```

```

JJ=JJ+NE(K-1)

```

```

11 CONTINUE

```

```

NFK=NF(K)
DO 10 I=1,NFK
  J = JJ + IF(K,I)
10 U(J) = V(K,I)
RETURN
END

```

C  
C  
C  
C  
C

```

SUBROUTINE ROW(RO,ATHE,APHI,NE,NN,BETA,NWIRE,NEP)
C THIS SUBROUTINE IS USED TO CALCULATE THE MEASUREMENT MATRIX RO
COMPLEX RO(2,NEP),CEXP,CI
DIMENSION NE(NWIRE),NN(NWIRE),TLEN(4,32) ,XX(3,4,32),
1 XD(3,4,32) ,U(2,3),TK(3),TKRPI(4),C(4),XDU(4)
COMMON /COA/XX,XD,TLEN
THE=ATHE/57.2958
PHI=APHI/57.2958
C U(1,I) = UNIT VECTOR OF THE THETA DIRECTION
U(1,1)=COS(THE)*COS(PHI)
U(1,2)=COS(THE)*SIN(PHI)
U(1,3)= -SIN(THE)
C U(2,I) = UNIT VECTOR OF THE PHI DIRECTION
U(2,1)=-SIN(PHI)
U(2,2)= COS(PHI)
U(2,3)=0.
C TK = -(WAVE NUMBER VECTOR)*(UNIT RADIUS VECTOR)
TK(1)=SIN(THE)*COS(PHI)*BETA
TK(2)=SIN(THE)*SIN(PHI)*BETA
TK(3)=COS(THE)*BETA
N=0
DO 20 NWS=1,NWIRE
  NENWS=NE(NWS)
  DO 20 NES=1,NENWS
    N=N+1
    ABCA=TLEN(NWS,2*NES-1)
    ARCB=TLEN(NWS,2*NES)
    ABCC=TLEN(NWS,2*NES+1)
    ABCD=TLEN(NWS,2*NES+2)
    C(1) = 1/2.*ABCA/(ABCA+ARCB)
    C(2) = (ABCA+1/2.*ARCB)/(ABCA+ARCB)
    C(3) = (1/2.*ABCC+ABCD)/(ABCC+ABCD)
    C(4) =1/2.*ABCD/(ABCC+ABCD)
    DO 30 M=1,4
      TKRPI(M)=0.
    DO 30 J=1,3
30 TKRPI(M)=TKRPI(M)+XX(J,NWS,2*NES-2+M)*TK(J)

```



```

PI = 3.14159265
C XMU = THE PERMEABILITY OF FREE SPACE
XMU = 4.0E-7*PI
C EPSLN = THE PERMITTIVITY OF FREE SPACE
EPSLN = 8.854E-12
CI = (0.,1.)
C WAVE = THE WAVELENGTH
100 READ (1,2, END=500) WAVE
WRITE (3,11) WAVE
C OMEG = THE ANGLE FREQUENCY
OMEG = 2.997928E8/WAVE*2.*PI
C KFTA = THE WAVE NUMBER OF FREE SPACE
KFIA = 2.*PI/WAVE
C NWIRE = THE TOTAL NUMBER OF WIRES IN THE PROBLEM GEOMETRY
READ (1,3) NWIRE
WRITE (3,12) NWIRE
WRITE (3,151)
DO 550 NW=1,NWIRE
WRITE (3,13) NW
C RA(NW) = THE WIRE RADIUS OF THE NW'ITH WIRE ( IN WAVELENGTH)
C NS(NW) = THE NUMBER OF SEGMENTS MAKING UP THE NW'ITH WIRE
C NF(NW) = THE NUMBER OF EXCITATIONS ON THE NW'ITH WIRE
C NL(NW) = NUMBER OF LOADS ON THE NW'ITH WIRE
READ(1,1) RA(NW), NS(NW), NF(NW), NL(NW)
WRITE (3,5) RA(NW),NS(NW),NF(NW),NL(NW)
C IF(NW,I) SPECIFIED THE POSITION OF THE EXCITATIONS ON THE WIRE
NFNW = NF(NW)
READ(1,3) (IF(NW,I),I=1,NFNW )
WRITE(3,6) (IF(NW,I),I=1,NFNW )
C V(NW,I) IS THE VOLTAGE OF THE SOURCE AT THE PEAK OF THE I'ITH
C EXPANSION FUNCTIONS ON THE NW'ITH WIRE
READ (1,4) (V(NW,I),I=1,NFNW )
WRITE(3,7) (V(NW,I),I=1,NFNW )
C LP(NW,I) SPECIFIED THE POSITIONS OF THE LOADS ON THE WIRES
NLNW = NL(NW)
READ (1,3) (LP(NW,I),I=1,NLNW )
WRITE (3,8) (LP(NW,I),I=1,NLNW )
C ZL(NW,I) = LOAD IMPEDANCES AT THE POINTS SPECIFIED BY LP(NW,I)
READ (1,4) (ZL(NW,I),I=1,NLNW )
WRITE(3,9) (ZL(NW,I),I=1,NLNW )
WRITE (3,152)
C NE(NW) = THE NUMBER OF EXPANSION FUNCTIONS ON THE NW'ITH WIRE
C NP(NW) = THE NUMBER OF POINTS ON THE AXIS OF THE NW'ITH WIRE
C WHICH SHOULD BE SPECIFIED
NE(NW) = NS(NW)/2-1
NP(NW) = NS(NW) + 1
22 NN(NW) = 2*NF(NW)+2
C ( X(1,NW,I),X(2,NW,I),X(3,NW,I) ) IS THE CARTESIAN COORDINATE
C OF THE I'ITH POINT ON THE AXIS OF THE NW'ITH WIRE

```

```

HH = 0.25*WAVE
NPNW = NP(NW)
DO 1510 I=1,NPNW
X(1,NW,I) = 0.
X(2,NW,I) = 0.
1510 X(3,NW,I)=2*HH/NS(NW)*(I-1)-HH
WRITE (3,310)
NPNW = NP(NW)
WRITE(3,300) ((X(J,NW,I),J=1,3),I=1,NPNW)
WRITE (3,152)
550 CONTINUE
DO 560 NW=1,NWIRE
NNNW=NN(NW)
C ( XX(1,NW,I),XX(2,NW,I),XX(3,NW,I) ) IS THE COORDINATE OF THE
C CENTER POINT OF THE I' TH SEGMENT OF THE NW' TH WIRE
DO 15 I=1,NNNW
DO 15 J=1,3
XX(J,NW,I) = (X(J,NW,I)+X(J,NW,I+1))/2.
15 XD(J,NW,I) = X(J,NW,I+1)-X(J,NW,I)
C TLEN(NW,I) IS THE LENGTH OF THE I' TH SEGMENT OF THE NW' TH WIRE
DO 20 I=1,NNNW
20 TLEN(NW,I) = SORT(XD(1,NW,I)**2+XD(2,NW,I)**2+XD(3,NW,I)**2)
A(NW) = BA(NW)*WAVE
560 CONTINUE
WRITE(3,151)
NEP=0.
DO 28 NW=1,NWIRE
28 NEP =NEP+NE(NW)
C NEP = THE ORDER OF THE GENERALIZED IMPEDANCE MATRIX Z
CALL CALZ(WAVE,NWIRE,A,NE,NN)
CALL CALZL(NL,NE,NWIRE)
CALL LINEQ(NEP,LMNOP,MMNOP)
CALL RIGV(U,NF,NWIRE,NE,NEP)
C U IS THE GENERALIZED VOLTAGE MATRIX
C C IS THE GENERALIZED CURRENT MATRIX
CALL CRNT(U,C,NEP)
WRITE(3,200)
WRITE(3,205)
DO 30 I=1,NEP
CMAG=CABS(C(I))
CPHA=ATAN2(AIMAG(C(I)),REAL(C(I)))*180./3.1416
30 WRITE (3,50) I,C(I),CMAG,CPHA
WRITE(3,151)
POWER =0.
JJ=0
DO 55 K=1,NWIRE
IF(K.EQ.1) GO TO 37
JJ=JJ+NE(K-1)

```

```

37 CONTINUE
   NFK=NF(K)
   DO 55 J=1,NFK
     I=JJ+IF(K,J)
C     ZIN = INPUT IMPUDANCE
C     YIN = INPUT ADMITTANCE
     ZIN=U(I)/C(I)
     YIN = (0.,0.)
     ABSZIN = CABS(ZIN)
     IF (ABSZIN.GE.0.1E-6) YIN=1./ZIN
     POWER = POWER + 1./2.*REAL(U(I)*CONJG(C(I)))
     WRITE(3,53) J,K,ZIN
55  WRITE(3,54) J,K,YIN
     WRITE(3,201)
     WRITE (3,203)
     DO 35 IPHI = 1,1
     DO 35 ITHI = 1,181,20
     ATHE = ITHI - 1
     APHI=IPHI-1
C     RO IS THE MEASUREMENT MATRIX
     CALL ROW( RO,ATHE,APHI,NE,MN,BETA,NWIRE,NEP)
     CALL PATT(C,RO,E,OMEG,XMU,NEP)
C     E(1) IS THE THETA COMPONENT OF THE SCATTERED FIELD
C     F(2) IS THE PHI COMPONENT OF THE SCATTERED FIELD
     DO 40 K=1,2
     HH = CABS(E(K))
     IF(HH.EQ.0.) GO TO 32
     EPHA(K) = ATAN2(AMAG(F(K)),REAL(E(K)))
     GO TO 33
32  EPHA(K)=0.
33  GPHA(K)=EPHA(K)*180.0/3.1416
40  GMAG(K)=CABS(E(K))
     IF(IPHI.EQ.1) GMAGN=GMAG(1)
     WRITE(3,44) ATHE,APHI,E(1),GMAG(1),GPHA(1),F(2),GMAG(2),GPHA(2)
     GATHE = GMAG(1)**2/30./POWER/2.
     GAPHI = GMAG(2)**2/30./POWER/2.
     WRITE (3,206) GATHE,GAPHI
35  CONTINUE
     WRITE(3,151)
7941 CONTINUE
     GO TO 100
1   FORMAT ( F10.5,4I5)
2   FORMAT (3F10.5)
3   FORMAT(16I5)
4   FORMAT( 8F10.3)
5   FORMAT(' RA=',F10.5,'   NS=',I5,'   NF=',I5,'   NL=',I5)
6   FORMAT(' IF(I)=',16I5)

```

```

7 FORMAT(' V(I)=',8F10.3)
8 FORMAT(' LP(I)=',16I5)
9 FORMAT(' ZL(I)=',8F10.3)
10 FORMAT (' ',3F10.5)
11 FORMAT(' WAVE =',F20.5)
12 FORMAT(' NWIRE = ',I5)
13 FORMAT(' DATA FOR THE ',I5,'TH WIRE')
44 FORMAT(' ',2F5.0,8E13.5)
50 FORMAT(I5,3E12.4,F10.3)
53 FORMAT(' INPUT IMPEDANCE AT', I5,'TH FEEDING POINT OF ',I5,'TH
WIRE ZIN=',2E10.3)
54 FORMAT(' INPUT ADMITTANCE AT',I5,'TH FEEDING POINT OF ',I5,'TH
WIRE YIN=',2E10.3)
151 FORMAT(' *****')
152 FORMAT(' -----')
200 FORMAT(' CURRENT DISTRIBUTION')
201 FORMAT(' FIELD PATTERN')
203 FORMAT(' -ATHE ARHI E(THE) MAGNITUDE PHAS
IF E(PHI) MAGNITUDE PHASE')
205 FORMAT(' I C(I) MAGNITUDE PHASE')
206 FORMAT(' GAIN PATTERN GATHE =',E10.3,'
1 GAIN PATTERN GAPHI = ',E10.3,' LOGARITHMIC GAIN =',E10.3)
300 FORMAT(' ',12E10.2)
310 FORMAT(' THE COORDINATE OF THE WIRE')
500 STOP
END)
$DATA
1.0
1
0.007022 28 1 1
7
1. 0.
1
0. 0.
$STOP
/*

```



WAVE = 1.00000  
 NWIRE = 1  
 \*\*\*\*\*  
 DATA FOR THE 1TH WIRE  
 BA= 0.00702 NS= 28 NF= 1 JL= 1  
 IF(I)= 7  
 V(I)= 1.000 0.000  
 LP(I)= 1  
 ZL(I)= 0.000 0.000

-----  
 THE COORDINATE OF THE WIRE

0.00E 00	0.00E 00	-0.25E 00	0.00E 00	0.00E 00	-0.23E 00
0.00E 00	0.00E 00	-0.21E 00	0.00E 00	0.00E 00	-0.20E 00
0.00E 00	0.00E 00	-0.18E 00	0.00E 00	0.00E 00	-0.16E 00
0.00E 00	0.00E 00	-0.14E 00	0.00E 00	0.00E 00	-0.13E 00
0.00E 00	0.00E 00	-0.11E 00	0.00E 00	0.00E 00	-0.09E-01
0.00E 00	0.00E 00	-0.71E-01	0.00E 00	0.00E 00	-0.54E-01
0.00E 00	0.00E 00	-0.36E-01	0.00E 00	0.00E 00	-0.18E-01
0.00E 00	0.00E 00	-0.60E-07	0.00E 00	0.00E 00	0.18E-01
0.00E 00	0.00E 00	0.36E-01	0.00E 00	0.00E 00	0.54E-01
0.00E 00	0.00E 00	0.71E-01	0.00E 00	0.00E 00	0.89E-01
0.00E 00	0.00E 00	0.11E 00	0.00E 00	0.00E 00	0.12E 00
0.00E 00	0.00E 00	0.14E 00	0.00E 00	0.00E 00	0.15E 00
0.00E 00	0.00E 00	0.18E 00	0.00E 00	0.00E 00	0.20E 00
0.00E 00	0.00E 00	0.21E 00	0.00E 00	0.00E 00	0.23E 00
0.00E 00	0.00E 00	0.25E 00			

\*\*\*\*\*

CURRENT DISTRIBUTION

I	C(I)	MAGNITUDE	PHASE	
1	0.2814E-02	-0.2147E-02	0.3539E-02	-37.344
2	0.4580E-02	-0.3325E-02	0.5659E-02	-35.976
3	0.6161E-02	-0.4241E-02	0.7480E-02	-34.540
4	0.7435E-02	-0.4803E-02	0.8851E-02	-32.863
5	0.8378E-02	-0.4977E-02	0.9745E-02	-30.713
6	0.8959E-02	-0.4826E-02	0.1018E-01	-28.311
7	0.9155E-02	-0.3382E-02	0.9759E-02	-20.274
8	0.8959E-02	-0.4826E-02	0.1018E-01	-28.310
9	0.8378E-02	-0.4977E-02	0.9745E-02	-30.713
10	0.7434E-02	-0.4802E-02	0.8850E-02	-32.862
11	0.6161E-02	-0.4241E-02	0.7480E-02	-34.541
12	0.4580E-02	-0.3325E-02	0.5659E-02	-35.978
13	0.2814E-02	-0.2147E-02	0.3539E-02	-37.345

\*\*\*\*\*

INPUT IMPEDANCE AT 1TH FEEDING POINT OF 1TH WIRE  
 ZIN= 0.961E 02 0.355E 02  
 INPUT ADMITTANCE AT 1TH FEEDING POINT OF 1TH WIRE  
 YIN= 0.915E-02-0.338E-02

FIELD PATTERN

ATHE	APHI	E(THI)	MAGNITUDE	PHAS F	Gain
0.	0.	-0.00000E 00	-0.00000E 00	0.00000E 00	0.00000E 00
		GAIN PATTERN		GATHE = 0.000E 00	GAIN
20.	0.	0.91340E-01	0.15664E 00	0.18133E 00	0.59753E 02
		GAIN PATTERN		GATHE = 0.120E 00	GAIN
40.	0.	0.18853E 00	0.31873E 00	0.37031E 00	0.59395E 02
		GAIN PATTERN		GATHE = 0.499E 00	GAIN
60.	0.	0.28149E 00	0.46895E 00	0.54695E 00	0.59025E 02
		GAIN PATTERN		GATHE = 0.109E 01	GAIN
80.	0.	0.34161E 00	0.56415E 00	0.65952E 00	0.58804E 02
		GAIN PATTERN		GATHE = 0.158E 01	GAIN
100.	0.	0.34161E 00	0.56415E 00	0.65952E 00	0.58804E 02
		GAIN PATTERN		GATHE = 0.158E 01	GAIN
120.	0.	0.28149E 00	0.46896E 00	0.54695E 00	0.59025E 02
		GAIN PATTERN		GATHE = 0.109E 01	GAIN
140.	0.	0.18853E 00	0.31873E 00	0.37031E 00	0.59395E 02
		GAIN PATTERN		GATHE = 0.499E 00	GAIN
160.	0.	0.91338E-01	0.15664E 00	0.18133E 00	0.59754E 02
		GAIN PATTERN		GATHE = 0.120E 00	GAIN
180.	0.	0.40661E-06	0.70158E-06	0.81089E-06	0.59955E 02
		GAIN PATTERN		GATHE = 0.239E-11	GAIN

\*\*\*\*\*

## APPENDIX B

This program is suitable for scattering problems of thin wires with loading represented by lumped loads at the peaks of the triangle functions. The maximum number of wires that can be handled here is four and the maximum number of expansion functions for any wire is fifteen. All subroutines except subroutine BIGV are exactly the same as those in Appendix A, hence, are not repeated here. Subroutine BIGV is listed first. The sample input and output data correspond to the analysis of example 11. This program is described in Sec. 3-3.

```

SUBROUTINE BIGV(UV,NWIRE,NN,NF,NFP,ET,THEI,PHII,BETA)
C THIS SUBROUTINE IS USED TO CALCULATE THE GENERALIZED VOLTAGE MATRIX V
COMPLEX UV(NFP),V(4,32),EI(2),      CI
DIMENSION NN(NWIRE),NF(NWIRE),XX(3,4,32),XD(3,4,32),TLEN(4,32),
TK(3),P(4),U(2,3)
COMMON /C01A/XX,XD,TLEN
CI = (0.,1.)
PI=3.1415926
THE = PI*THEI/180.
PHI = PI*PHII/180.
DO 26 NW=1,NWIRE
NNNW = NN(NW)
DO 26 NSS=1,NNNW
V(NW,NSS) = (0.,0.)
U(1,1)=COS(THE)*COS(PHI)
U(1,2)=COS(THE)*SIN(PHI)
U(1,3)= -SIN(THE)
U(2,1)=-SIN(PHI)
U(2,2)= COS(PHI)
U(2,3)=0.
TK(1)=SIN(THE)*COS(PHI)*BETA
TK(2)=SIN(THE)*SIN(PHI)*BETA
TK(3)=COS(THE)*BETA
TKRPI=0.
DO 27 J=1,3
27 TKRPI=TKRPI+XX(J,NW,NSS)*TK(J)
DO 26 I=1,2
XDII=0.
DO 28 J=1,3
28 XDII=XDII+XD(J,NW,NSS)*U(I,J)
26 V(NW,NSS) = V(NW,NSS)+XDII*EI(I)*(COS(TKRPI)+CI*SIN(TKRPI))
JJ=0
DO 10 NWF=1,NWIRE
NFNWF = NF(NWF)

```

```

DO 10 NEF=1,NENWF
JJ=JJ+1
UV(JJ) = (0.,0.)
ABCA=TLEN(NWF,2*NEF-1)
ABCB=TLEN(NWF,2*NEF)
ABCC=TLEN(NWF,2*NEF+1)
ABCD=TLEN(NWF,2*NEF+2)
P(1) = 1/2.*ABCA/(ABCA+ARCB)
P(2) = (ABCA+1/2.*ARCB)/(ABCA+ARCB)
P(3) = (1/2.*ARCC+ABCD)/(ARCC+ABCD)
P(4) =1/2.*ABCD/(ARCC+ABCD)
DO 10 K=1,4
10 UV(JJ) = UV(JJ)+P(K)*V(NWF,2*NEF-2+K)
RETURN
END

```

C  
C  
C  
C  
C  
C

MAIN PROGRAM

COMPLEX ZL( 4,32) ,EI(2) ,Z( 60,60 ),U( 60),C(60),RO( 2,60),  
LE(2),ZIN,CONJG,CI,YIN

DIMENSION RA(12),A(12),NS(12), NF(12), NL(12),

1X(3, 4,33), NE(12), NP(12), NN(12), LP( 4,32),

2XX(3, 4,32), XD(3, 4,32), TLEN( 4,32), LMNOP(60),MMNOP(60),

3EPHA(2),GPHA(2),GMAG(2)

COMMON /COA/XX,XD,TLEN /COB/Z /COC/ZL,LP

PI =3.14159265

C XMU = THE PERMEABILITY OF FREE SPACE

XMU = 4.0E-7\*PI

C EPSLN = THE PERMITTIVITY OF FREE SPACE

EPSLN = 8.854E-12

CI = (0.,1.)

C WAVE = THE WAVELENGTH

100 READ (1,2, END=500) WAVE

WRITE (3,11) WAVE

C OMEG = THE ANGLE FREQUENCY

OMEG=2.997928E8/WAVE\*2.\*PI

C BETA = THE WAVE NUMBER OF FREE SPACE

BETA = 2.\*PI/WAVE

C NWIRE = THE TOTAL NUMBER OF WIRES IN THE PROBLEM GEOMETRY

READ (1,3) NWIRE

WRITE (3,12) NWIRE

WRITE (3,151)

DO 550 NW=1,NWIRE

WRITE (3,13) NW

C RA(NW) = THE WIRE RADIUS OF THE NW'TH WIRE ( IN WAVELENGTH)

```

C      NS(NW) = THE NUMBR OF SEGMENTS MAKING UP THE NW' TH WIRE
C      NL(NW) = NUMBER OF LOADS ON THE NW' TH WIRE
      READ(1,1) BA(NW), NS(NW), NL(NW)
      WRITE (3,5) BA(NW),NS(NW), NL(NW)
C      LP(NW,I) SPECIFIED THE POSITIONS OF THE LOADS ON THE WIRES
      NLNW =NL(NW)
      READ (1,3) (LP(NW,I),I=1,NLNW )
      WRITE (3,8) (LP(NW,I),I=1,NLNW )
C      ZL(NW,I) = LOAD IMPEDANCES AT THE POINTS SPECIFIED BY LP(NW,I)
      READ (1,4) (ZL(NW,I),I=1,NLNW )
      WRITE(3,9) (ZL(NW,I),I=1,NLNW )
      WRITE (3,152)
C      NE(NW) = THE NUMBER OF EXPANSION FUNCTIONS ON THE NW' TH WIRE
C      NP(NW) = THE NUMBER OF POINTS ON THE AXIS OF THE NW' TH WIRE
C      WHICH SHOULD BE SPECIFIED
      NE(NW) = NS(NW)/2-1
      NP(NW) =NS(NW) +1
22  NN(NW) = 2*NE(NW)+2
C      ( X(1,NW,I),X(2,NW,I),X(3,NW,I) ) IS THE CARTESIAN COORDINATE
C      OF THE I' TH POINT ON THE AXIS OF THE NW' TH WIRE
1501 AENOS = 0.22*WAVE/24.
      NPNW = NP(NW)
      DO 1512 I=1,NPNW
      IF (NW.LE.2) X(1,NW,I) = 0.
      IF (NW.EQ.3) X(1,NW,I) = 0.11*WAVE-AENOS*(I-1)
      IF (NW.EQ.4) X(1,NW,I) = -X(1,3,I)
      X(2,NW,I) = 0
      IF(NW.GE.3) X(3,NW,I) =0.
      IF (NW.EQ.2) X(3,NW,I) = AENOS*(I-1) - 0.22*WAVE
      IF (NW.EQ.1) X(3,NW,I) = 0.11*WAVE-AENOS*(I-1)
1512 CONTINUE
550  CONTINUE
      DO 1517 J= 1,3
      X(J,1,14) = X(J,3,12)
      X(J,1,15) = X(J,3,11)
      X(J,2,26) = X(J,4,12)
      X(J,2,27) = X(J,4,11)
      X(J,3,14) = X(J,2,24)
1517 X(J,3,15) = X(J,2,23)
      DO 560 NW=1,NWIRE
      WRITE (3,310)
      NPNW = NP(NW)
      WRITE(3,300) ((X(J,NW,I),J=1,3),I=1,NPNW)
      WRITE (3,152)
      NNW=NN(NW)
C      ( XX(1,NW,I),XX(2,NW,I),XX(3,NW,I) ) IS THE COORDINATE OF THE

```

```

C      CENTER POINT OF THE I' TH SEGMENT OF THE NW' TH WIRE
      DO 15 I=1,NNNW
      DO 15 J=1,3
      XX(J,NW,I) = (X(J,NW,I)+X(J,NW,I+1))/2.
15  XD(J,NW,I) = X(J,NW,I+1)-X(J,NW,I)
C      TLEN(NW,I) IS THE LENGTH OF THE I' TH SEGMENT OF THE NW' TH WIRE
      DO 20 I=1,NNNW
20  TLEN(NW,I) = SORT(XD(1,NW,I)**2+XD(2,NW,I)**2+XD(3,NW,I)**2)
      A(NW) = BA(NW)*WAVE
560  CONTINUE
      WRITE(3,151)
      NEP=0.
      DO 28 NW=1,NWIRE
28  NEP = NEP+NE(NW)
C      NEP = THE ORDER OF THE GENERALIZED IMPEDANCE MATRIX Z
      CALL CALZ(WAVE,NWIRE,A,NE,NN)
      CALL CALZL(NL,NE,NWIRE)
      CALL LINEQ(NEP ,LMNOP,MMNOP)
      READ (1,3) NOSET
      WRITE (3,3) NOSET
      DO 794 IKA=1,NOSET
      READ (1,4) THEI,PHII
      WRITE (3,6) THEI,PHII
C      THEI,PHII = THE ANGLES DESIGNATING THE DIRECTION OF PROPAGATION OF
C-     THE INCIDENT WAVE
      READ(1,4) EI(1),EI(2)
      WRITE (3,7) EI(1),EI(2)
C      EI(1) = THE THETA COMPONENT OF THE INCIDENT ELECTRIC FIELD
C      EI(2) = THE PHI COMPONENT OF THE INCIDENT ELECTRIC FIELD
      WRITE(3,151)
      CALL      RIGV( U,NWIRE,NN,NE,NEP,EI,THEI,PHII,BETA)
C      U IS THE GENERALIZED VOLTAGE MATRIX
C      C IS THE GENERALIZED CURRENT MATRIX
      CALL CRNT(U,C,NEP)
      WRITE(3,200)
      WRITE(3,205)
      DO 30 I=1,NEP
      CMAG=CABS(C(I))
      CPHA=ATAN2(AIMAG(C(I)),REAL(C(I)))*180./3.1416
30  WRITE (3,50) I,C(I),CMAG,CPHA
      WRITE(3,151)
      WRITE(3,201)
      WRITE (3,203)
      DO 35 ISTA =1,2
      IF (ISTA.EQ.1) IKPHI = 180
      IF (ISTA.EQ.1) IKTHE = 10
      IF (ISTA.EQ.2) IKTHE = 300
      IF (ISTA.EQ.2) IKPHI = 10

```

```

001 35 I PHI = 91.271, I K PHI
001 35 I THE = 1.181, I K THE
APHI = I PHI -1
ATHE = I THE -1
IF (I STA.EQ.2) ATHE = ATHE+90.
RU IS THE MEASUREMENT MATRIX
CALL ROW( RU, ATHE, A PHI, NE, NN, BETA, NWIRE, NEP)
F(1) IS THE THETA COMPONENT OF THE SCATTERED FIELD
F(2) IS THE PHI COMPONENT OF THE SCATTERED FIELD
CALL PAIT(C, RU, F, I MEG, X MU, NEP)
001 40 K=1,2
HH = CABS(F(K))
IF(HH.EQ.0.) GO TO 32
EPHA(K) = ATAN2(AIMAG(E(K)), REAL(E(K)))
GO TO 33
32 EPHA(K)=0.
33 GPHA(K)=EPHA(K)*180.0/3.1416
40 GMAG(K)=CABS(F(K))
WRITE(3,44) ATHE, A PHI, E(1), GMAG(1), GPHA(1), E(2), GMAG(2), GPHA(2)
SIGMA = THE ECHO AREA/WAVE**2
E02 = E(1)**2+E(2)**2
SIGMA1=4.*PI*GMAG(1)**2/(E02*WAVE**2)
SIGMA2=4.*PI*GMAG(2)**2/(E02*WAVE**2)
WRITE(3,206) SIGMA1, SIGMA2
35 CONTINUE
WRITE(3,151)
793 CONTINUE
794 CONTINUE
WRITE(3,151)
WRITE(3,152)
WRITE(3,151)
GO TO 100
1 FORMAT ( F10.5,4I5)
2 FORMAT (3F10.5)
3 F1FORMAT(16I5)
4 FORMAT( 8F10.3)
5 F1FORMAT(' RA=',F10.6,' NS=',I5,' NL=',I5)
6 FORMAT(' THEI=',F12.2,' PHII=',F12.2)
7 FORMAT(' EI(1) = ',2E12.4,' EI(2) = ',2F12.4)
8 FORMAT(' LP(I)=' , 16I5)
9 FORMAT(' 7L(I)=' ,8F10.3)
10 FORMAT (' ',3F10.5)
11 FORMAT(' WAVE =',F20.5)
12 FORMAT(' NWIRE = ',I5)
13 FORMAT(' DATA FOR THE ',I5,'TH WIRE')
44 FORMAT(' ',2F5.0,8F13.5)
50 FORMAT(I5,3E12.4,F10.3)
151 FORMAT(' *****')

```

```

152 FORMAT('-----')
200 FORMAT(' CURRENT DISTRIBUTION')
201 FORMAT(' FIELD PATTERN')
203 FORMAT(' -ATHE      APhi      E(THE)      MAGNITUDE      PHAS
      IF      E(PHI)      MAGNITUDE      PHASE')
205 FORMAT('      I      C(I)      MAGNITUDE      PHASE')
206 FORMAT('      SIGMA1 = ',E20.5,'      SIGMA2 = ',E20.5)
300 FORMAT(' ',12E10.2)
310 FORMAT(' THE COORDINATE OF THE WIRE')
500 STOP
      END

```

```

/*
//GO.SYSIN DD *
      4
0.00222      14      1
      1
      0.
0.00222      26      1
      1
      0.
0.00222      14      1
      1
      0.
0.00222      12      1
      1
      0.
      1
      90.      90.
      -1.      0.      0.      0.
/*

```



WAVE = 1.00000  
 NWIRE = 4  
 \*\*\*\*\*  
 DATA FOR THE 1TH WIRE  
 BA= 0.002220 NS= 14 NL= 1  
 LP(I)= 1  
 ZL(I)= 0.0 0.0

DATA FOR THE 2TH WIRE  
 BA= 0.002220 NS= 26 NL= 1  
 LP(I)= 1  
 ZL(I)= 0.0 0.0

DATA FOR THE 3TH WIRE  
 BA= 0.002220 NS= 14 NL= 1  
 LP(I)= 1  
 ZL(I)= 0.0 0.0

DATA FOR THE 4TH WIRE  
 BA= 0.002220 NS= 12 NL= 1  
 LP(I)= 1  
 ZL(I)= 0.0 0.0

THE COORDINATE OF THE WIRE  
 0.0 0.0 0.11E 00 0.0 0.0 0.10E 00  
 0.0 0.0 0.92E-01 0.0 0.0 0.82E-01  
 0.0 0.0 0.73E-01 0.0 0.0 0.64E-01  
 0.0 0.0 0.55E-01 0.0 0.0 0.46E-01  
 0.0 0.0 0.37E-01 0.0 0.0 0.27E-01  
 0.0 0.0 0.18E-01 0.0 0.0 0.92E-02  
 0.0 0.0 0.0 0.92E-02 0.0 0.0  
 0.18E-01 0.0 0.0

THE COORDINATE OF THE WIRE  
 0.0 0.0 -0.22E 00 0.0 0.0 -0.21E 00

THE COORDINATE OF THE WIRE  
 0.11E 00 0.0 0.0 0.10E 00 0.0 0.0

THE COORDINATE OF THE WIRE  
 -0.11E 00 0.0 0.0 -0.10E 00 0.0 0.0

\*\*\*\*\*

1  
 THEI= 90.00 PHII= 90.00  
 FI(1) = -0.1000E 01 0.0 FI(2) = 0.0 0.0  
 \*\*\*\*\*

CURRENT DISTRIBUTION

I	C(I)	MAGNITUDE	PHASE
1	-0.3919E-04	-0.2037E-03	0.2074E-03 -100.889
2	-0.6443E-04	-0.3340E-03	0.3401E-03 -100.919
3	-0.8577E-04	-0.4436E-03	0.4519E-03 -100.942
4	-0.1028E-03	-0.5310E-03	0.5408E-03 -100.961
5	-0.1156E-03	-0.5962E-03	0.6073E-03 -100.975
6	-0.1216E-03	-0.6266E-03	0.6383E-03 -100.982
7	0.5785E-04	0.2962E-03	0.3018E-03 78.949
8	0.7674E-04	0.4946E-03	0.5039E-03 78.932
9	0.1313E-03	0.6705E-03	0.6832E-03 78.918
10	0.1613E-03	0.8228E-03	0.8385E-03 78.907
11	0.1870E-03	0.9530E-03	0.9712E-03 78.899
12	0.2083E-03	0.1061E-02	0.1081E-02 78.892
13	0.2253E-03	0.1147E-02	0.1169E-02 78.887
14	0.2378E-03	0.1211E-02	0.1234E-02 78.885
15	0.2460E-03	0.1252E-02	0.1276E-02 78.883
16	0.2499E-03	0.1272E-02	0.1296E-02 78.883
17	0.2497E-03	0.1271E-02	0.1295E-02 78.884
18	0.6313E-04	0.3175E-03	0.3237E-03 78.753
19	-0.1741E-04	-0.8638E-04	0.8861E-04 -101.330
20	-0.2952E-04	-0.1477E-03	0.1506E-03 -101.304
21	-0.4055E-04	-0.2032E-03	0.2072E-03 -101.283
22	-0.5024E-04	-0.2522E-03	0.2572E-03 -101.266
23	-0.5853E-04	-0.2942E-03	0.2999E-03 -101.253
24	-0.1847E-03	-0.9441E-03	0.9620E-03 -101.071
25	-0.1741E-04	-0.8638E-04	0.8861E-04 -101.330
26	-0.2952E-04	-0.1477E-03	0.1506E-03 -101.304
27	-0.4055E-04	-0.2032E-03	0.2072E-03 -101.284
28	-0.5025E-04	-0.2522E-03	0.2572E-03 -101.266
29	-0.5853E-04	-0.2942E-03	0.2999E-03 -101.253

\*\*\*\*\*

FIELD PATTERN

ATHE	APHI	E(THF)	MAGNITUDE	PHASE
0.	90.	-0.23640E-12	0.19320E-13	0.33696E-12 0.17671E 03 0.2670 . .
		SIGMA1 = 0.14268E-23	SIGMA2 =	0.89940E-12
10.	90.	-0.62333E-02	0.41524E-02	0.74897E-02 0.14633E 03 0.2670 . .
		SIGMA1 = 0.70493E-03	SIGMA2 =	0.89969E-12
20.	90.	-0.12533E-01	0.80242E-02	0.14381E-01 0.14737E 03 0.2664 . .
		SIGMA1 = 0.27829E-02	SIGMA2 =	0.89532E-12
30.	90.	-0.18912E-01	0.11333E-01	0.22048E-01 0.14907E 03 0.2662 . .
		SIGMA1 = 0.61084E-02	SIGMA2 =	0.89426E-12
.	.	.	.	.
.	.	.	.	.
.	.	.	.	.

170.	90.	-0.73432E-02	-0.14944E-02	0.74937E-02	-0.16850E 03	0.267	..
	SIGMA1 =	0.70567E-03		SIGMA2 =	0.89969E-12		
180.	90.	-0.66595E-07	-0.13977E-07	0.68046E-07	-0.16815E 03	0.267	..
	SIGMA1 =	0.58185E-13		SIGMA2 =	0.89940E-12		
0.	270.	0.50338E-12	-0.29032E-13	0.50422E-12	-0.33065E 01	-0.267	..
	SIGMA1 =	0.31948E-23		SIGMA2 =	0.89940E-12		
10.	270.	-0.62333E-02	0.41524E-02	0.74897E-02	0.14633E 03	-0.267	..
	SIGMA1 =	0.70493E-03		SIGMA2 =	0.89912E-12		
:	:	:	:	:	:	:	:
:	:	:	:	:	:	:	:
:	:	:	:	:	:	:	:

180.	270.	-0.66595E-07	-0.13977E-07	0.68046E-07	-0.16815E 03	-0.267	..
	SIGMA1 =	0.58186E-13		SIGMA2 =	0.89940E-12		
90.	90.	-0.46629E-01	0.91300E-02	0.47514E-01	0.16892E 03	0.267	..
	SIGMA1 =	0.28370E-01		SIGMA2 =	0.87652E-12		
90.	100.	-0.46629E-01	0.91300E-02	0.47514E-01	0.16892E 03	0.679	..
	SIGMA1 =	0.28370E-01		SIGMA2 =	0.15011E-05		
90.	110.	-0.46629E-01	0.91300E-02	0.47514E-01	0.16892E 03	0.127	..
	SIGMA1 =	0.28370E-01		SIGMA2 =	0.52775E-05		
:	:	:	:	:	:	:	:
:	:	:	:	:	:	:	:
:	:	:	:	:	:	:	:

90.	250.	-0.46629E-01	0.91300E-02	0.47514E-01	0.16892E 03	-0.127	..
	SIGMA1 =	0.28370E-01		SIGMA2 =	0.52776E-05		
90.	260.	-0.46629E-01	0.91300E-02	0.47514E-01	0.16892E 03	-0.679	..
	SIGMA1 =	0.28370E-01		SIGMA2 =	0.15012E-05		
90.	270.	-0.46629E-01	0.91300E-02	0.47514E-01	0.16892E 03	-0.267	..
	SIGMA1 =	0.28370E-01		SIGMA2 =	0.89902E-12		

\*\*\*\*\*  
 \*\*\*\*\*

APPENDIX C

The following modifications to the radiation program listed in Appendix A are sufficient to make the program suitable for problems of thin wires with excitations represented by distributed voltage sources as described in Sec. 2-6. In the main program the statement

CALL BIGV(U,NF,NWIRE,NE,NEP)

is replaced by the statement

CALL BIGV(U,NWIRE,NN,NE,NEP,NF)

and DO LOOP 55 is replaced by

```

DO 55 K=1,NWIRE
  IF(K.EQ.1) GO TO 37
  JJ=JJ+NE(K-1)
37 CONTINUE
  NFK=NF(K)
  DO 55 J=1,NFK
    IFKJ = IF(K,J)
    IFA = IF(K,J)/2.
    IFR = IF(K,J)/2
    IF(IFA.EQ.IFR) GO TO 818
    CAI = (0.,0.)
    IF ( IFR.GT.0) CAI = C(JJ+IFR)
    CBI = (0.,0.)
    IF (IFR.LE.NE(K)-1) CBI = C(JJ+IFR+1)
    CC = CAI + (CBI-CAI)*1./2.*TLEN(K,IFKJ)/(TLEN(K,IFKJ)+TLEN(K,
1IFKJ+1))
    GO TO 819
818 CAI = (0.,0.)
    IF (IFR.GT.1) CAI=C(JJ+IFR-1)
    CBI = (0.,0.)
    IF (IFR.LE.NE(K)) CBI = C(JJ+IFR)
    CC = CAI + (CBI-CAI)* ( TLEN(K,IFKJ-1)+1./2.*TLEN(K,IFKJ  )
1/(TLEN(K,IFKJ-1)+TLEN(K,IFKJ  ))
819 ZIN = V(K,J)/CC
C   ZIN = INPUT IMPUDANCE
C   YIN = INPUT ADMITTANCE
    YIN = (0.,0.)
    ABSZIN = CABS(ZIN)
    IF (ABSZIN.GE.0.1E-6) YIN=1./ZIN
    POWER = POWER+1./2.*REAL(V(K,J)*CONJG(CC))
    WRITE(3,53) J,K,ZIN
55 WRITE(3,54) J,K,YIN

```

The subroutine BIGV is replaced by

```
SUBROUTINE BIGV(UV,NWIRE,NN,NE,NEF,NF)
  COMPLEX UV(NEF),V(4,32),U(4,32)
  DIMENSION NN(NWIRE),NF(NWIRE),XX(3,4,32),XD(3,4,32),TLEN(4,32),
  IP(4),IF(4,32),NF(NWIRE)
  COMMON /COA/XX,XD,TLEN /COU/ V,IF
  DO 6 NW=1,NWIRE
    NNNW = NN(NW)
    DO 5 I=1,NNNW
      U(NW,I) = (0.,0.)
      NFNW = NF(NW)
      DO 6 K=1,NFNW
        J = IF(NW,K)
      6 U(NW,J) = V(NW,K)
        JJ=0
        DO 10 NWF=1,NWIRE
          NENWF = NE(NWF)
          DO 10 NEF=1,NENWF
            JJ=JJ+1
            UV(JJ) = (0.,0.)
            ARCA=TLEN(NWF,2*NEF-1)
            ARCB=TLEN(NWF,2*NEF)
            ARCC=TLEN(NWF,2*NEF+1)
            ARCD=TLEN(NWF,2*NEF+2)
            P(1) = 1/2.*ARCA/(ARCA+ARCB)
            P(2) = (ARCA+1/2.*ARCB)/(ARCA+ARCB)
            P(3) = (1/2.*ARCC+ARCD)/(ARCC+ARCD)
            P(4) =1/2.*ARCD/(ARCC+ARCD)
            DO 10 K=1,4
          10 UV(JJ) = UV(JJ)+P(K)*U(NWF,2*NEF-2+K)
        RETURN
      END
```

APPENDIX D

The following modifications to the programs listed in Appendix A and Appendix B are sufficient to make the programs suitable for problems of thin wires with loading represented by distributed loads as described in Sec. 2-8. In the main program the statement

```
CALL CALZL(NL,NE,NWIRE)
```

is replaced by the statement

```
CALL CALZL(NL,NE,NWIRE,NN)
```

and the subroutine CALZL is replaced by

```
SUBROUTINE CALZL(NL,NE,NWIRE,NN)
COMPLEX Z(60,60),ZL(4,32),ZLL(4,32)
DIMENSION LP(4,32),NL(NWIRE),NE(NWIRE),XX(3,4,32),
1 XI(3,4,32),TLEN(4,32),NN(NWIRE),P(4),PP(2),PM(2)
COMMON /COA/XX,XI,TLEN /COB/ Z /COC/ ZL,LP
DO 6 NW = 1,NWIRE
NNNW = NN(NW)
DO 5 I=1,NNNW
5 ZLL(NW,I) = (0.,0.)
NL(NW) = NL(NW)
DO 6 K=1,NLNW
J = LP(NW,K)
6 ZLL(NW,J) = ZL(NW,K)
JJ=0
DO 10 NWF=1,NWIRE
NEFWF = NE(NWF)
DO 10 NEF=1,NEFWF
JJ=JJ+1
ARCA=TLEN(NWF,2*NEF-1)
ARCB=TLEN(NWF,2*NEF)
ARCC=TLEN(NWF,2*NEF+1)
ARCD=TLEN(NWF,2*NEF+2)
P(1) = 1/2.*ARCA/(ARCA+ARCB)
P(2) = (ARCA+1/2.*ARCB)/(ARCA+ARCB)
P(3) = (1/2.*ARCC+ARCD)/(ARCC+ARCD)
P(4) = 1/2.*ARCD/(ARCC+ARCD)
PP(1) = 1./2.*ARCC/(ARCC+ARCD)
PP(2) = (ARCC+1./2.*ARCD)/(ARCC+ARCD)
PM(1) = -(1./2.*ARCA+ARCB)/(ARCA+ARCB)
PM(2) = 1./2.*ARCB/(ARCA+ARCB)
DO 15 K=1,4
15 Z(JJ,JJ) = Z(JJ,JJ) + P(K)**2*ZLL(NWF,2*NEF-2+K)
```

```
IF (NEF.EQ.NENWF) GO TO 16
DO 20 K=3,4
20 Z(JJ, JJ+1) = Z(JJ, JJ+1) + P(K)*PP(K-2)*ZLL(NWF, 2*NEF-2+K)
16 CONTINUE
IF (NEF.EQ.1) GO TO 21
DO 35 K=1,2
35 Z(JJ, JJ-1) = Z(JJ, JJ-1) + P(K)*PM(K)*ZLL(NWF, 2*NEF-2+K)
21 CONTINUE
10 CONTINUE
RETURN
END
```